SUSTAINABLE STRUCTURAL SYSTEMS COLLECTION

Mohammad Noori, *Editor*

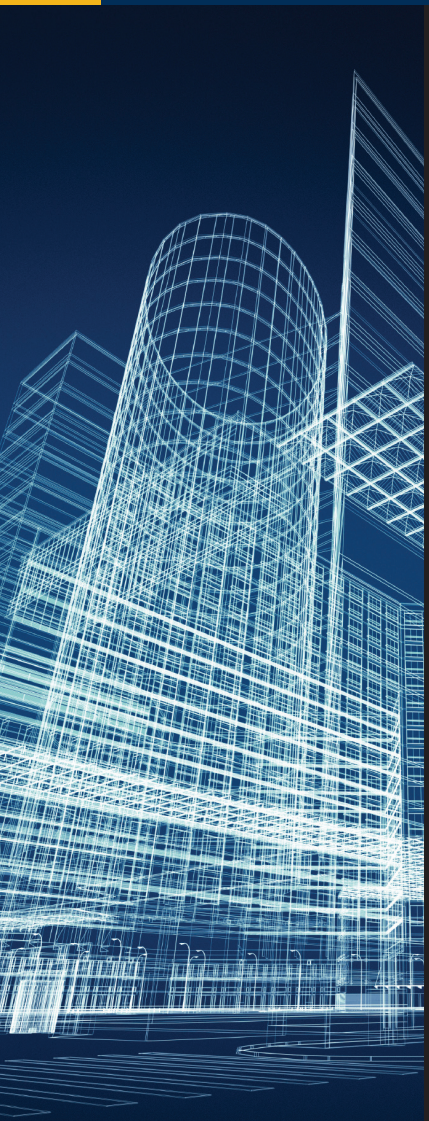

Seismic Analysis and Design Using the Endurance Time Method

Volume II

Advanced Topics and Application

H.E. Estekanchi
H.A. Vafai

MOMENTUM PRESS
ENGINEERING

SEISMIC ANALYSIS AND DESIGN USING THE ENDURANCE TIME METHOD

SEISMIC ANALYSIS AND DESIGN USING THE ENDURANCE TIME METHOD

VOLUME II

ADVANCED TOPICS AND APPLICATION

H.E. ESTEKANCHI AND H.A. VAFAI

MOMENTUM PRESS
ENGINEERING

MOMENTUM PRESS, LLC, NEW YORK

Seismic Analysis and Design Using the Endurance Time Method, Volume II: Advanced Topics and Application

First published by Momentum Press®, LLC
222 East 46th Street, New York, NY 10017
www.momentumpress.net

ISBN-13: 978-1-94708-326-4 (print)
ISBN-13: 978-1-94708-327-1 (e-book)

Momentum Press Sustainable Structural Systems Collection

Collection ISSN: 2376-5119 (print)
Collection ISSN: 2376-5127 (electronic)

Cover and interior design by Exeter Premedia Services Private Ltd., Chennai, India

10 9 8 7 6 5 4 3 2 1

Printed in the United States of America

Abstract

A new approach to seismic assessment of structures called endurance time method (ETM) is developed. ETM is a dynamic analysis procedure in which intensifying dynamic excitations are used as the loading function. ETM provides many unique benefits in seismic assessment and design of structures. ETM is a response history-based procedure. ETM considerably reduces the computational effort needed in typical response history analyses. Conceptual simplicity makes ETM a great tool for preliminary response history analysis of almost any dynamic structural system. Most important areas of application of ETM are in the fields of seismic design optimization, value-based seismic design, and experimental studies. This book is aimed to serve as a coherent source of information for students, engineers, and researchers who want to familiarize themselves with the concepts and put the concepts into practice.

KEYWORDS

endurance time method, dynamic structural analysis, earthquake engineering, seismic assessment, seismic design, structural design optimization, value-based seismic design

Contents

List of Figures

List of Tables

CHAPTER 7

MULTICOMPONENT ENDURANCE TIME ANALYSIS

7.1 INTRODUCTION

Earthquake-induced ground motions have three translational components that are directly recorded by accelerographs.[1] There are some codified provisions that require consideration of the effects of ground-motion components in the seismic analysis of sensitive structures. In this respect, three-dimensional analysis is obligatory for asymmetric, tall buildings or important structures such as dams, bridges, and power plants (Wilson 2002). In these circumstances, the most appropriate analysis procedure is time-history analysis, including components of consistent ground motions.

With the development of new computational tools, the capability of realistic dynamic modeling and complex analysis of structures has been increased and in this situation, using improved and more complicated methods for seismic evaluation of structures has become a reasonable choice. Therefore, traditional two-dimensional static and response spectrum methods are gradually being replaced by nonlinear three-dimensional time-history analysis. In response to this increasing demand for application of these complex methods, it is necessary to develop procedures for clear and logical use of these new approaches.

Three-dimensional analysis under actual records has two major issues. First, for a particular site specification, the number of available recorded earthquakes might not be sufficient and the selection of

[1] Chapter Source: Valamanesh, V., and H.E. Estekanchi. 2011. "Endurance Time Method for Multi-Component Analysis of Steel Elastic Moment Frames." *Scientia Iranica* 18, no. 2, pp. 139–42.

consistent accelerograms complicates the situation. Second, analysis of structures under these ground motions is time consuming, especially when considering critical orientation is necessary. Moreover, interpretation of results for complex structures is quite difficult. Therefore, it is advantageous to use simpler methods that can estimate structural behavior under multidirectional excitation with satisfactory approximation and with less-computational operations.

The Endurance Time (ET) method is a new method that is capable of being used in both the linear and nonlinear seismic analysis of structures (Estekanchi, Vafai, and Sadeghazar 2004). One of the advantages of this method over other time-history analysis procedures is in reducing the required computational effort and relative simplicity. In the ET method, the response of a structure is monitored against the intensity of excitation from beginning to collapse (somewhat similar to the Incremental Dynamic Analysis method [Vamvatsikos and Cornell 2002]). The structure is then assessed based on its response at various equivalent excitation levels.

In this paper, application of the ET method in linear seismic analysis of structures is investigated. ET method is evaluated by comparing results of the ET analysis with results of time-history analysis using horizontal components of real ground motions according to seismic analysis regulations such as the Iranian National Building Code (INBC) (Iranian Code of Practice for Seismic Resistant Design of Buildings) and ASCE 7-05 (ASCE 2006).

The first part of this paper is devoted to a brief review of code regulations and some investigations on the three-dimensional analysis of buildings. In the next section, various structures, which are designed according to the INBC code are analyzed by both ET and time-history analysis under real earthquakes. Finally, by comparing results of these two methods, an algorithm for code compliant ET analysis is proposed for simultaneous excitation in perpendicular directions of structures. Even though time-history analyses are seldom required in linear elastic analysis of structures, the current research is aimed at laying the foundations for extension of application of ET method to seismic assessment using three-dimensional dynamic models subjected to realistic multicomponent ground motions. Obviously, major benefits of the procedure can only be realized when dealing with complicated nonlinear models. Even though nonlinear two-dimensional analysis results using currently available ET records indicate that reasonable estimates can also be obtained in nonlinear range, nonlinear multicomponent ET analysis is beyond the scope of current research.

7.2 REVIEW OF CODE PROVISIONS AND RELATED RESEARCH

Although there are some guidelines in seismic codes for multidirectional analysis under real ground motions, these methods are not routinely applied in the seismic analysis and design of common buildings (Beyer and Bommer 2007). Considerable research has been conducted in the past to clarify and simplify three-dimensional analysis. Naeim, Alimoradi, and Pezeshk (2004) proposed the use of a genetic algorithm for selecting and scaling records. Many investigations have been performed to find characteristics of components of an earthquake (López 2006; Baker and Cornell 2006; Penzien and Watabe 1975) [8–10] and the structural response due to two or three components of ground motions (Hernández and López 2002). These efforts lead, not only to suggestions for the time-history analysis of structures, but also to recommendations for the application of components in static and response spectrum analysis (López, Chopra, and Hernández 2001; Zovani and Barrionuevo 2004).

Nearly all structural codes have essentially the same recommendations for the selection of earthquake records for the purpose of three-dimensional analysis; however, they are somewhat different in the scaling method and application of components of records. For example, INBC, ASCE4-98, and EC8 recommend that analysis should be performed under components in principal directions of buildings (ASCE 2000; CEN 2003), but, for columns or walls intersecting seismic force-resistant systems of a building located in Categories E and F, as defined in the code, ASCE7-05, necessitate application of ground-motions components in critical direction in addition to analysis under horizontal components along principal directions. FEMA (2001) recommends that each pair of time histories be applied at the same time to the model, considering the most disadvantageous location of mass eccentricity.

One of the ways for considering critical directions is rotating the angle of induced excitation. By this procedure, an analysis requires a great deal of effort and time that might not be justified for typical structures. To avoid such problems, simplified methods have been proposed to estimate the critical response of structures due to an earthquake without rotating the angle of excitation (Athanatopoulou 2005). However, rotating the angle of excitation is still more practical for considering the critical response of structures. The huge amount of computational effort required in three-dimensional response history analysis using bidirectional excitation at multilevels can be prohibitive in many analysis and design situations. ET method can considerably reduce the number

of required analyses and, with appropriate approximation, provides a simple method for the three-dimensional analysis of structures. It should be noted again that in this paper only the linear behavior is investigated where results at various excitation levels can be obtained by applying a scale factor, However, it should be obvious that this does not hold in general nonlinear cases.

7.3 ENDURANCE TIME METHOD

7.3.1 THE BASIC CONCEPTS OF ET METHOD

The ET method has been introduced as a new seismic analysis method (Estekanchi, Vafai, and Sadeghazar 2004) and application of this method in two-dimensional linear and nonlinear analyses of steel frames has been reported in literature (Estekanchi, Valamanesh, and Vafai 2007; Riahi and Estekanchi 2010). In the ET method, structures are subjected to a set of specially designed intensifying accelerograms, called "ET acceleration functions" and their seismic performance is judged based on their response at various equivalent dynamic excitation intensities.

In ET analysis, ET is considered to be the time when the maximum value of the specified design parameter exceeds its allowable limit. In order to decide on whether the achieved performance can be considered as adequate or not, the structural response at equivalent intensity of imposed dynamic action should be considered. Spectral acceleration is the most popular intensity measure used in practice and has been considered for calibrating the ET acceleration functions used in this study.

The acceleration functions are linearly intensifying by time. In this approach, if the target time is set to t = 10 sec, that is, ET acceleration functions are calibrated in such a way that their response spectra in a window from t = 0 to 10 sec match the design spectrum with a scale of unity. When the window of an acceleration function is taken from t = 0 sec to t = 5 sec, its response spectrum corresponds to half the template spectra at all periods and if interval of t = 0 sec to t = 15 sec is taken, its response spectrum matches with 1.5 times the template spectrum, and so on. Therefore, for a certain structure, which is designed according to a design spectrum that matches the template spectrum with a scale factor of unity at $t = t_{Target}$ (10 seconds in this research), if, for example, the drift ratio exceeds its limit at t = 15 sec, it can be concluded that the structure satisfies drift criteria, since its ET is more than that is required by the code, that

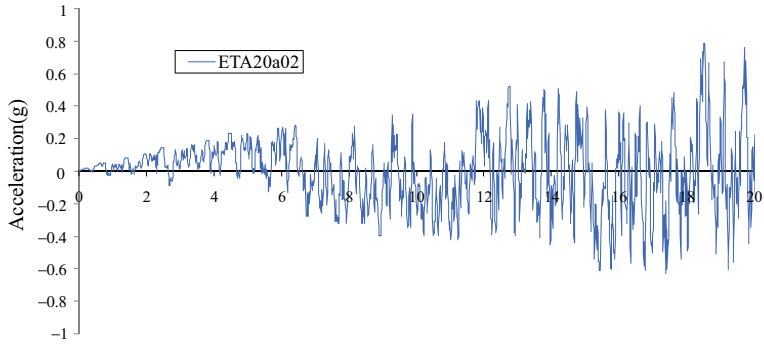

Figure 7.1. A typical ET acceleration function.

is, a minimum ET of 10 seconds, in this case. A typical ET acceleration function is depicted in Figure 7.1.

For generation of ET acceleration functions used in this study, the concept of the response spectrum has been directly applied. By scaling the ET acceleration functions using a simple linear scale factor, spectral acceleration and spectral displacement (Sa and Sd) can be set to reach the required target level at any desired time. By applying this method, we define the target response of ET acceleration functions as in Equations (1) and (2):

$$S_{aT}(T,t) = \frac{t}{t_{T\,\mathrm{arg}\,et}} S_{aC}(T) \tag{1}$$

$$S_{uT}(T,t) = \frac{t}{t_{T\,\mathrm{arg}\,et}} S_{aC}(T) \times \frac{T^2}{4\pi^2} \tag{2}$$

where $S_{aT}(T,t)$ is the target acceleration response at time t, T is the period of free vibration, $S_{aC}(T)$ is the codified design acceleration spectrum, and $S_{uT}(T,t)$ is the target displacement response at time t. The problem of generating accelerograms with such characteristics was approached by formulating it as an unconstrained optimization problem in the time domain as follows:

$$Minimize\ F(a_g) = \int_0^{T_{max}} \int_0^{t_{max}} \left\{ \left[S_a(T,t) - S_{aT}(T,t) \right]^2 + a \left[\left[S_u(T,t) - S_{uT}(T,t) \right]^2 \right\} dt\, dT \tag{3}$$

where a_g is the ET accelerogram being sought and a is an optimization weighting parameter set to 1.0 in this study (Estekanchi, Vafai, and Sadeghazar 2004).

7.4 CHARACTERISTICS OF ET ACCELERATION FUNCTIONS USED IN THIS STUDY

Various sets of ET acceleration functions have been developed based on intended application. In general, these fall into two major categories of code compliant and ground-motions compliant. Code compliant ET acceleration functions are based on a template spectrum that matches that of a particular design spectrum of a specified seismic code. These acceleration functions are mostly interesting from the design application perspective. On the other hand, ground-motions compliant ET records, are based on the average response spectrum of a set of ground motions pertaining to specific soil conditions without any modifications to provide a safety margin. These records are more suitable when for comparative studies to analyze some inherent sources of inconsistency and scatter of the estimations obtained by ET method. Major characteristics of ET acceleration functions which have greatest influence on structural response match well with the ground motions (Valamanesh, Estekanchi, and Vafai 2010). This is mostly due to the fact that ET acceleration functions are designed in such a way as to produce response spectrums matching those of ground motions. In the present article, ETA20f01-03 acceleration functions, who's template spectrum matches with the average response spectrum of major components from seven real accelerograms, (listed in FEMA 440 for soil type C), at the target time of 10th second are used. Similar to other sets of ET acceleration functions, in this set the response spectra of these acceleration functions increase with time. In Figure 7.2, the response spectra of the ETA20f acceleration functions are compared at different times. As it is shown in Figure 7.2, linear intensification of response spectra at different times is apparent.

7.5 COMPARISON OF ET METHOD WITH CONVENTIONAL APPROACHES

In static analysis, by applying an equivalent load based only on a first mode shape, the effect of higher vibration modes of the structure is mostly excluded. By increasing the irregularities and complexities in buildings, the effects of dynamic specifications become remarkable and static analysis will not be reliable (Iranian Code of Practice for Seismic Resistant Design of Buildings). The ET method is based on time-history analysis and intrinsically includes all significant dynamic properties of the structure into account. Moreover, due to the fact that ET acceleration functions

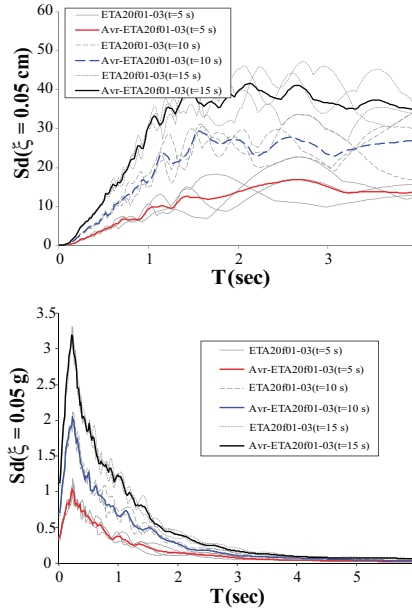

Figure 7.2. Response spectra of ETA20f01-03 at different times.

are intensifying with time, in each ET analysis, the strength of the structure can be predicted at different levels of intensity; while, the analysis of a building with real accelerograms at different levels needs Incremental Dynamic Analysis (IDA) (Vamvatsikos and Cornell 2002), which requires a considerable computational effort. This advantage of ET method cannot be realized in linear analysis that is the subject of this research. While some particular problems, such as optimal damper placement in linear systems, still requires response history-based analysis procedure, the major goal of this research should be considered as laying the necessary foundations in order to extend the application of ET into multicomponent seismic analysis.

7.6 STRUCTURAL MODELS

In the studied models, the endeavor is to focus on those parameters which have the most influence on three-dimensional analysis. Several steel moment resistant frames with one, three, four, five, and seven stories in three states of regular, irregular in one direction and irregular in two directions, for considering effects of torsion, are designed and investigated. It should be noted that for all frames, the story height is 3.2 m and all

spans are equally 6 m. Box sections were assigned to columns and HE-A (European wide flange I section) profiles were assigned to beams.

Models are named based on their lateral load resisting system, the number of stories, spans in both directions and irregularities in each direction as follows: All frame names begin with F3DMM signifying that all of them are 3D moment frames in both directions. This is followed by letter S and a number that shows the number of stories. Then the number of bays in X and Y directions is specified as XnYm meaning n bays in X and m bays in Y direction. Irregularity of the frame in X or Y or both directions in indicated next, for example, IRX means irregular in X direction and so on. For example, as shown in Figure 7.3b, F3DS3X3Y3IRXY represents a three-story moment resistant building, with three spans in X, Y directions, and irregularities in both directions.

The equivalent static lateral force procedure, based on provisions of INBC (INBC 2005) for soil type 2 has been used for the design of frames. Dead and live loads are assumed 7,500 and 2,500 N/m2, respectively, and an accidental eccentricity of 0.05L (where L is dimension of buildings plan in each direction) is considered for the design per code's requirements. The damping ratio for all frames is assumed to be 0.05, a typical value for this type of structure. Beam and column profiles are HEA and Box profiles, respectively. The importance factor is assigned to be 1 and the R factor is considered to be 7 in both directions due to the moment resistant frame in both directions. Properties of frames and design assumptions are listed in Table 7.1. These buildings have predominant periods between 0.1 and 1.5 seconds. It seems that by covering a reasonable range of model variety, results of ET analysis can be extended for three-dimensional analysis of low-rise steel moment frames.

7.7 SELECTION OF RECORDS

To verify results of the ET method with real earthquakes, seven real accelerograms are selected from 20 records listed in FEMA 440 for Soil Condition C. These records and their components are listed in Table 7.2. In this chapter, the effect of a vertical component is not included. The average response spectra of these real accelerograms, which are scaled according to code requirements, are illustrated in Figure 7.4.

One important issue in Figure 7.4 is in the difference between the response spectra of horizontal components of each ground motion. Although the spectrum of each component is not the same at different periods, especially between 0.5 and 3 seconds, for the general purpose of

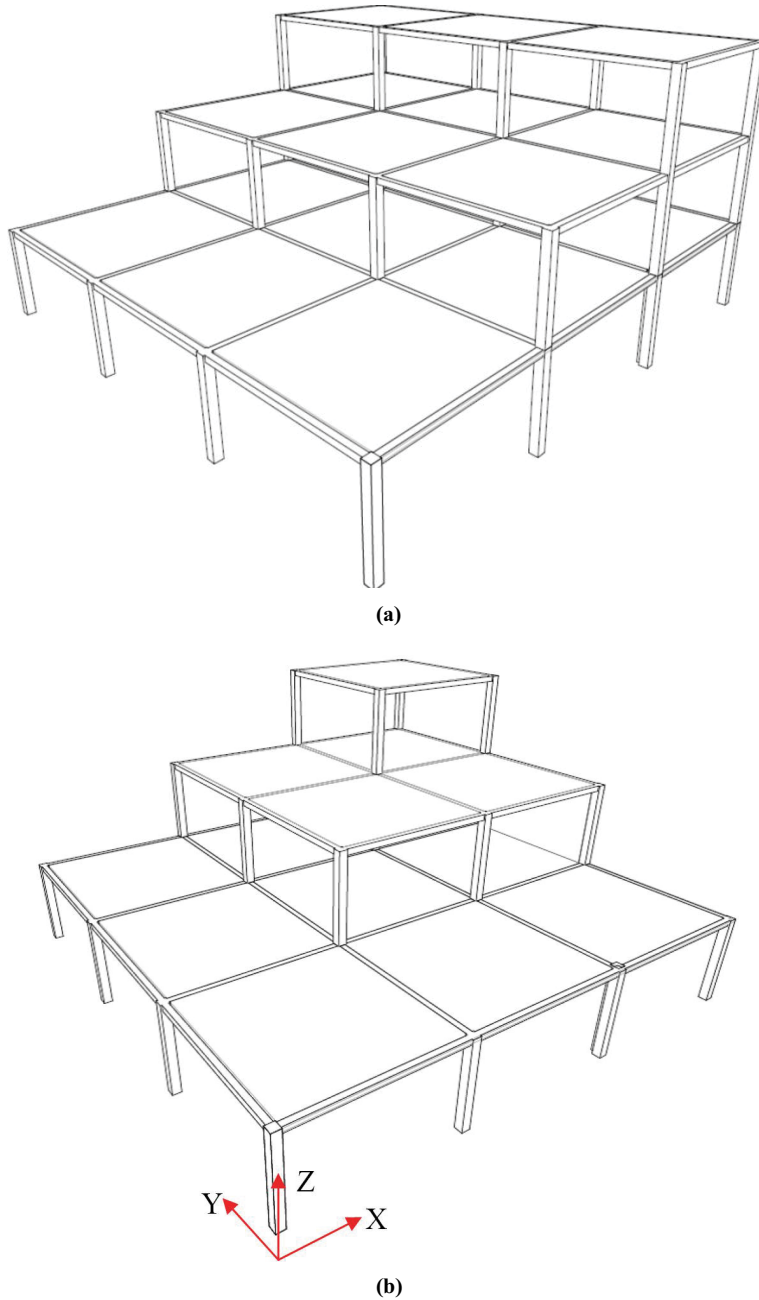

Figure 7.3. Investigated three-storey models, (a) F3DMMS3X3Y3IRX, (b) F3DMMS3X3Y3IRXY.

Table 7.1. Investigated frames, properties and design assumptions

Name	No. stories	No. span X	No. span Y	Seismic coefficient	T(sec)	Base shear (KN)
F3DMMS3X3Y3IRX	3	3	3	0.125	0.722	735.004
F3DMMS3X3Y3IRXY	3	3	3	0.125	0.627	601.069
F3DMMS4X3Y3	4	3	3	0.119	0.93	1411.33
F3DMMS4X3Y3IRX	4	3	3	0.119	0.913	1269.93
F3DMMS4X3Y3IRXY	4	3	3	0.119	0.875	810.326
F3DMMS5X4Y4	5	4	4	0.106	1.08	2826.04
F3DMMS5X4Y4IRX	5	4	4	0.106	0.996	2209.49
F3DMMS5X4Y4IRXY	5	4	4	0.106	0.976	2142.8
F3DMMS7X3Y5	7	3	5	0.091	1.505	3159.01

Table 7.2. Properties of real accelerograms and their components

Name	Ms	Station name	Abbreviation	Component (deg)	PGA (cm/s^2)
Landers	7.5	Yermo, Fire Station	LADSP000	0	167.80
			LADSP090	90	151.05
Loma Prieta	7.1	Saratoga, Aloha Ave.	LPSTG000	0	494.50
			LPSTG090	90	317.90
Loma Prieta	7.1	Gilroy, Gavilon College Phys Sch Bldg	LPGIL067	67	349.10
			LPGIL337	337	318.80
Loma Prieta	7.1	Santa Cruz, University of California	LPLOB000	0	433.10
			LPLOB090	90	387.00
Loma Prieta	7.1	Anderson Dam, Downstream	LPAND270	270	239.40
			LPAND360	360	235.10
Morgan Hill	6.1	Gilroy #6, San Ysidro Microwave Site	MHG06090	90	280.40
			MHG06000	0	217.87
Northridge	6.8	Castaic, Old Ridge Route	NRORR360	360	504.20
			NRORR090	90	557.30

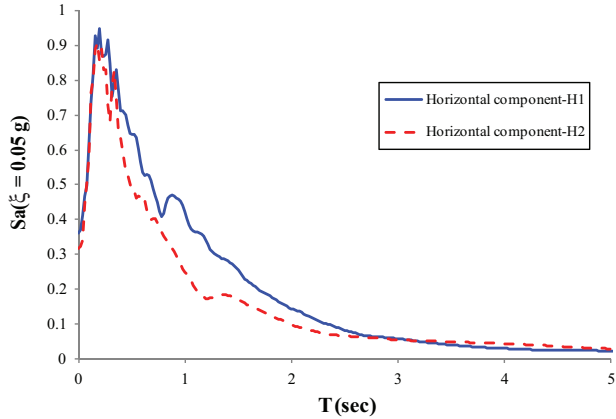

Figure 7.4. Average response spectra of horizontal components of selected accelerograms.

seismic analysis in this study, this difference is assumed to be insignificant due to the fact that each record is applied in orthogonal directions, thus maximum response is the significant parameter anyway. In all ET analyses in this study, ET acceleration functions with the same intensity and spectral shape are used in the bidirectional analysis of studied frames.

7.8 MULTICOMPONENT ANALYSIS

7.8.1 SCALING PROCEDURE

There are different approaches for scaling earthquake records, such as the square root of the sum of the squares (SRSS), arithmetic and geometric mean and the maximum spectral response. All types of averaging were primarily evaluated in this research, then, among scaling methods, SRSS was selected because of a better fitness with the target spectrum. According to ASCE 7-05 horizontal components of ground motions shall be scaled in such a way that the average SRSS spectrum from all horizontal component pairs, in range of 0.2T to 1.5T, where T is predominant period of vibration for studied structure, doesn't fall below 1.3 times of corresponding ordinate of design spectrum by more than 10 percent. This approach is used for scaling the components of ground motions. These scaling values for used ground motions are illustrated in Table 7.3.

The scaling procedure for applying ET acceleration functions resembles scaling of actual records, that is, mentioned methods are used to obtain the scale factor for ET acceleration functions considering their

Table 7.3. Scaling value of records components used in analysis of frames

	LADSP	LPSTG	LPGIL	LPLOB	LPAND	MHG06	NRORR
F3DMMS3X3Y3IRXY	1.805	0.988	1.042	1.017	1.158	1.078	0.533
F3DMMS3X3Y3IRX	1.734	0.986	1.097	1.082	1.203	1.062	0.527
F3DMMS4X3Y3	1.678	0.954	1.192	1.246	1.276	1.024	0.526
F3DMMS4X3Y3IRX	1.678	0.954	1.192	1.246	1.276	1.024	0.526
F3DMMS4X3Y3IRXY	1.678	0.954	1.192	1.246	1.276	1.024	0.526
F3DMMS5X4Y4	1.655	0.925	1.228	1.329	1.292	1.036	0.523
F3DMMS5X4Y4IRX	1.655	0.925	1.228	1.329	1.292	1.036	0.523
F3DMMS5X4Y4IRXY	1.655	0.925	1.228	1.329	1.292	1.036	0.523
F3DMMS7X3Y5	1.555	0.842	1.314	1.599	1.304	1.121	0.515

response spectrum at target time. For example, for a pair of ET acceleration functions which consist of ETA20f01 and ETA20f02, the acceleration response spectrum for each ETAF (Endurance Time Excitation Function) is calculated at target time. Then using SRSS method, mentioned earlier, these response spectra are combined and comparing to amplified design spectrum (1.3 time of design spectrum), the scaling factor could be calculated which should be applied for both used ET acceleration functions. In this way, not only did the results from all scaling approaches lead to almost the same factor for ET acceleration functions; this scaling factor did not change significantly from one frame to another; while these scale factors were considerably different in different ground motions due to their specific response spectrum. The major reason for such consistency of scaling methods in ET acceleration functions is that they inherently comply with the design response spectrum and, so, the shape of the response spectrum will be almost the same in different accelerations functions belonging to the same set of records. The scale factors for pairs of ET acceleration functions are shown in Table 7.4. As shown in Table 7.4, the average scale factor of three pairs of ET acceleration function is used for all individual pairs, in the analysis of each model.

7.8.2 MULTICOMPONENT ANALYSIS BY ET METHOD

ET acceleration functions used in this study are designed in such a way that their response spectra increase by time. When used for response history analysis, most of the regulations set forth in design codes, regarding the general three-dimensional time-history analysis, are also applicable for ET analysis. However, some special characteristics of ET acceleration functions require particular consideration. Although ET acceleration functions are statistically independent, all ET acceleration functions are produced in the same manner and use the same assumptions; thus, statistically, the intensity and response spectrum at each time are, theoretically, the same for all ET acceleration functions in a set of ET acceleration functions. Therefore, definition of a major or a minor component in the ET method is not relevant. Second, as the ET acceleration functions are produced synthetically, critical angle or principal direction of excitation is also of little significance. Finally, because all ET acceleration functions in each set are statistically alike, in this study, pairs of ET acceleration functions can be considered by swapping ET acceleration functions alternatively with each other; that is, the first pair of ET excitations include ETA20f01 in X direction and ETA20f02 in Y direction, the second pair is

Table 7.4. Scaling value for pairs of ET acceleration function

	ETA20f01,02	ETA20f02,03	ETA20f03,01	Average ET
F3DMMS3X3Y3IRXY	0.473	0.475	0.478	0.475
F3DMMS3X3Y3IRX	0.482	0.482	0.483	0.482
F3DMMS4X3Y3	0.480	0.483	0.483	0.482
F3DMMS4X3Y3IRX	0.480	0.483	0.483	0.482
F3DMMS4X3Y3IRXY	0.480	0.483	0.483	0.482
F3DMMS5X4Y4	0.485	0.488	0.484	0.486
F3DMMS5X4Y4IRX	0.485	0.488	0.484	0.486
F3DMMS5X4Y4IRXY	0.485	0.488	0.484	0.486
F3DMMS7X3Y5	0.495	0.499	0.497	0.497

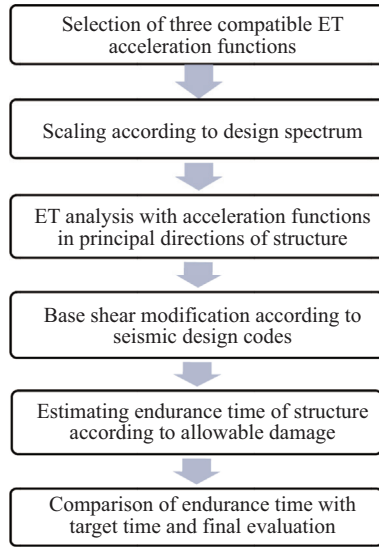

Figure 7.5. Proposed flowchart for bidirectional analysis of structures by ET method.

a combination of ETA20f02 in X direction and ETA20f03 in Y direction and the third pair is made up of ETA20f03 and ETA20f01 in X and Y directions, respectively. These pairs are applied to the structure alternatively and results are averaged for final evaluation. A proposed algorithm for three-dimensional ET analysis is illustrated in Figure 7.5.

Following the flowchart in Figure 7.5, the designed frames were analyzed and compared with results from time-history analysis under previously mentioned real accelerograms in a situation where components of records are applied in principal directions of structures. For instance, displacements in X and Y directions of a three-story building, obtained from two methods are compared.

As in ET analysis, time is a representative of intensity; it is obvious that results from the ET method are plotted over the time, while responses of real accelerograms appear as points with +/− one standard deviation marks and are extended by a line (representing the linear analysis) for comparison. These values are compared with the ET method at target time, that is, t = 10 sec in this study (Figure 7.6). In this figure, Uxsti and Uysti determine ith story displacement in X and Y directions, respectively. As shown, the results of ET analysis at t = 10 sec are close to the results obtained from analysis under real accelerograms in principal directions. It should be noticed that the curve is an average of results from ET analysis and points are the average of results from real accelerograms. Further

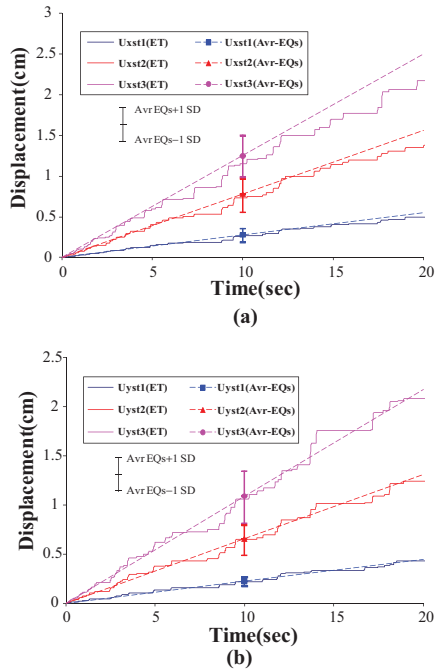

Figure 7.6. Displacement responses at any time in ET analysis and comparison with real earthquakes, F3DMMS3X3Y3IRX, (a) displacement in X direction, (b) displacement in Y direction.

investigations show that other frames had similar results. For example, drifts of a seven-story building in X direction obtained from ET analysis at t = 10 sec are compared with results from real accelerograms (Figure 7.7).

In addition to displacement and drifts, internal forces of all members, for example, moments in beams and columns, and axial force in columns, are studied. In Figure 7.8, for a three-story building, moments and axial forces in some random beams and columns are sketched by time for ET analysis and compared with real accelerograms. In this figure, M_Bi and P_Cj refer to maximum moment in beam number i, and maximum axial force in Column Number j, respectively. These elements are specified in Figure 7.3b. It is obvious from Figure 7.8 that the response of all studied structural indices in studied frames are approximately the same as in the ET method at target time (t = 10 sec) and horizontal components of real ground motions in principal directions. Obviously, there are some discrepancies that will be discussed later in this chapter.

In addition to some random members, all members, including all beams and columns, were investigated to specify any member which

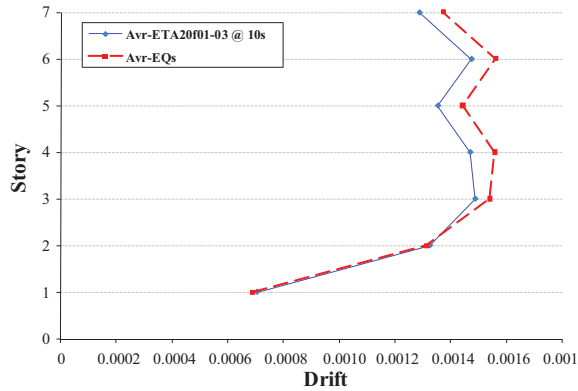

Figure 7.7. Comparison of drifts from ET analysis at t = 10 sec and actual records, F3DMMS7X5Y3.

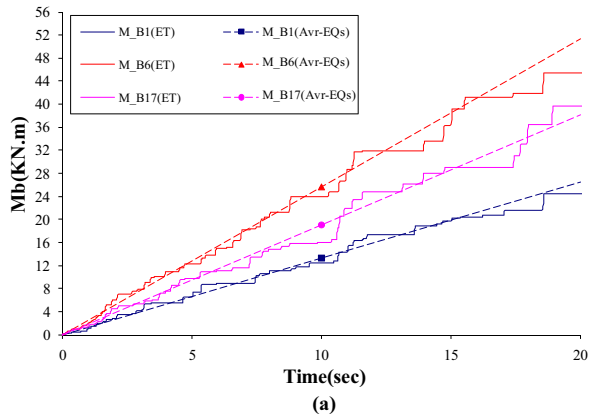

Figure 7.8. Internal force in members of F3DMMS3X3Y-3IRXY in ET method and real earthquakes, (a) moment in beams, (b) axial force in columns.

might behave differently from others. Furthermore, in this step the correlation of results between the ET method and real earthquakes is derived. In Figure 7.9, drifts and displacements of stories in both directions for the average of real earthquakes are drawn versus the average of ET analysis at the target time for the regular five-story frame. In addition, in Figure 7.10, the same figures are shown for the maximum moment in beams and axial force in all columns of the five-story building which is irregular in both directions.

It is essential to note that the response of these structures is compared only under lateral loads and, in this state, the effect of vertical loads, such as gravity load and the effect of vertical acceleration, is ignored. Of course, considering gravitational loads doesn't affect the conclusions obtained in this chapter, which are based on lateral load response.

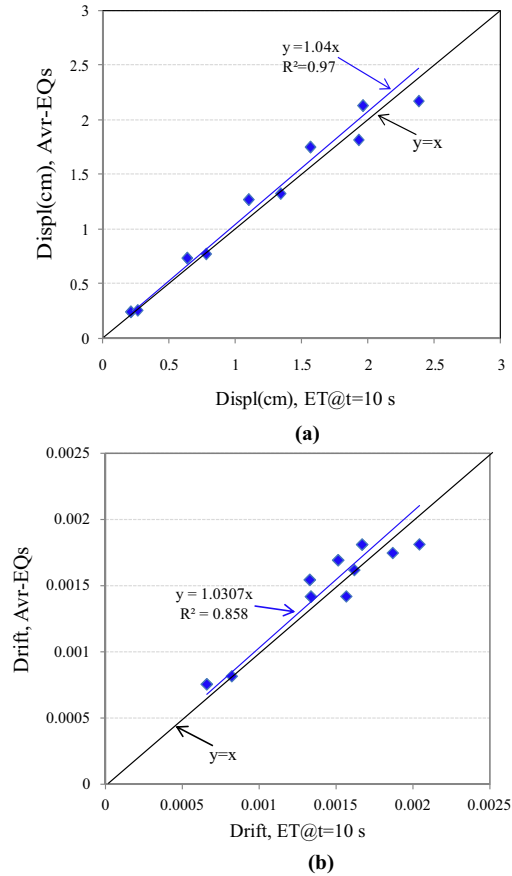

Figure 7.9. Drifts and displacement values from earthquakes vs. ET results at t = 10 sec for, F3DMMS5X4Y4, (a) displacement, (b) drift.

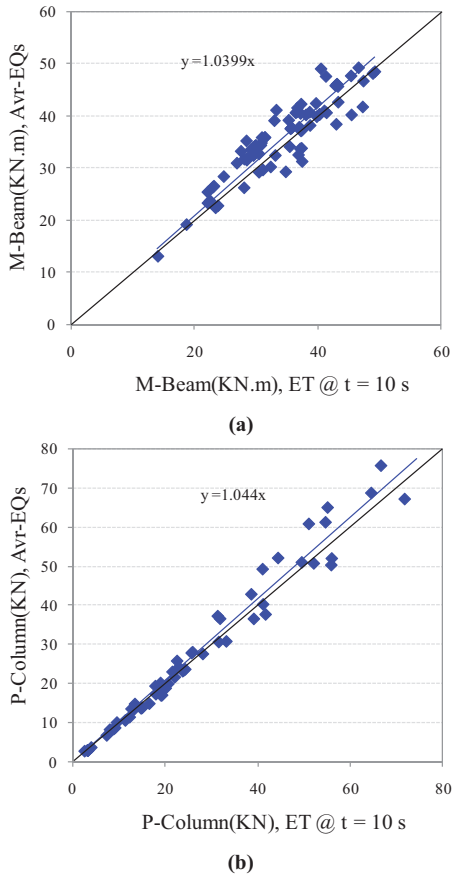

Figure 7.10. Internal forces from earthquakes vs. ET results at t = 10 sec for, F3DMMS5X4Y4IRXY, (a) Moment in beams, (b) Axial force in columns.

As indicated from the figures, for studied damage criteria, the correlation of results from the ET method and real earthquakes is close to 1 and results from the average of earthquakes in principal directions can be estimated by a unique correction factor for each frame.

The correction factor is defined as the relation between results from real earthquakes and ET analysis at target time (t = 10 sec), that is,

$$CF = \frac{DI_{Avr-EQs}}{DI_{ET@t=10}} \tag{4}$$

Correction factors and correlation coefficients of all studied frames and most damage criteria for each frame are shown in Table 7.5.

Table 7.5. Correction factor and correlation coefficient of structural responses in ET method and real earthquake

	Displ		Drift		Mb		Pc		MxC		MyC	
	CF	r	CF	r	CF	r	CF	r	CF	r	CF	r
F3DMMS3X3Y3IRX	1.039	1.000	1.026	0.989	1.021	0.948	1.017	0.985	1.033	0.902	0.974	0.990
F3DMMS3X3Y3IRXY	0.997	0.997	0.949	0.985	0.990	0.959	0.961	0.992	0.969	0.932	0.992	0.835
F3DMMS4X3Y3	1.041	0.994	1.029	0.977	1.080	0.994	1.092	0.997	1.077	0.977	1.090	0.973
F3DMMS4X3Y3IRX	1.055	0.990	1.059	0.963	1.122	0.995	1.113	0.994	1.156	0.998	1.153	0.997
F3DMMS4X3Y3IRXY	1.049	0.993	1.053	0.976	1.120	1.000	1.108	0.990	1.115	0.998	1.114	0.998
F3DMMS5X4Y4	1.040	0.986	1.031	0.942	1.125	0.994	0.987	0.977	1.158	0.999	1.148	0.991
F3DMMS5X4Y4IRX	0.988	0.998	0.978	0.987	1.000	0.987	0.969	0.996	0.985	0.992	1.078	0.995
F3DMMS5X4Y4IRXY	1.009	0.984	0.991	0.959	1.040	0.907	1.044	0.988	0.978	0.989	1.154	0.997
F3DMMS7X5Y3	1.089	0.978	1.068	0.923	1.153	0.991	1.134	0.985	1.155	0.999	1.106	0.999

As can be seen in Table 7.5, the correlation coefficient between the ET method and real accelerograms for various responses of studied frames is near 1. This means that all members conform to one correction factor (CF) and with application of this factor, the average response of real ground motions in principal directions can be estimated by the ET method. The next point in this table is that the correction factors are nearly the same for various response parameters in each frame; thus, there is no need to apply different CF for different parameters. It is also found that discussed CFs for all frames are about unity, (with maximum 15 percent tolerance), meaning that results from the ET method at target time is the same as results from the average of real accelerograms in principal directions of the structure.

As can be seen, there are some differences between results of ET acceleration functions and real earthquakes, these differences occur due to the incompatibility of response spectra of ET acceleration functions and actual ground motions. As can be seen in Figure 7.11 the average response spectrum obtained from the maximum response of two horizontal components for seven selected earthquake ground motions is not exactly the same and at the most periods of vibrations is a bit greater than average response spectrum of three ET acceleration functions This inconsistency happens when at some periods of vibrations the response spectrum of the second component of each ground motion is greater than the first component which the ET acceleration functions produced to be compatible with. Also, the discrepancy is caused by the roughness of the target spectrum and optimization problems in generating ET acceleration functions.

To reduce these discrepancies, the compatibility between two spectra should be improved. This goal can be achieved by producing more

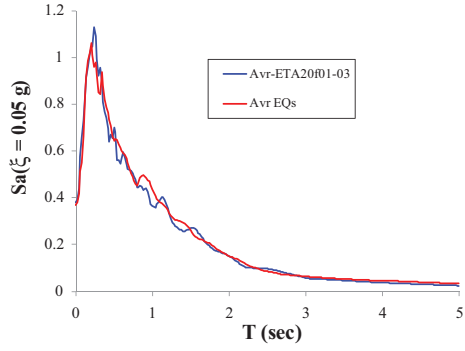

Figure 7.11. Average response spectrum of ETA20f01-03 at t = 10 sec and average of maximum response of two horizontal components of real earthquakes.

optimized ET acceleration functions or using more than three acceleration functions in ET analysis. Also, instead of considering the first component of earthquake ground motions, the maximum response of two horizontal components should be considered for generating or scaling of ET acceleration functions. However, due to the fact that the ratio of intensities for two horizontal components is not determined and there is no unique value for such parameter, it could be assumed that the ET acceleration functions are produced to be compatible with the component which has greater intensity. Because of this assumption, depending on structural period, the results from ET method may involve a slight underestimation as compared to those obtained from actual ground motions. Due to the fact that this incompatibility can be ignored in current study considering the insignificance of the differences, (maximum difference is 20 percent), these set of ET acceleration functions can be regarded as acceptable for a reasonable response estimation.

As stated at the beginning of this paper, most seismic codes accept the application of seismic excitation only in principal directions; however, some structural codes, such as ASCE7-05, impose more stringent requirement, such as obligating that the analysis of members in intersections of two lateral resistant systems of buildings which are located in E and F seismic category, be performed at critical direction. According to this requirement, engineers should analyze the structure under components of each earthquake at its critical direction. Then, maximum values obtained from each record are averaged from seven accelerograms. Although it is not likely that all members reach their maximum value simultaneously in the critical direction, and this approach seems to be conservative, it is necessary that this type of analysis be performed for vital structures. In the next step of current paper the average of maximum structural response in the most adverse direction will be evaluated. However more investigation is required in order to draw general conclusions in this regard. In Figure 7.12, internal forces of all members for irregular three-storey frame are compared between average of maximum results of each earthquake at their critical direction and ET method at target time.

It is apparent that correlations of results from two methods are high and a correction factor can be applied to estimate the average of maximum results of earthquakes by the ET method. For studied frames, these correction factors are obtained and shown in Table 7.6. It should be noted that while strong correlation exists in each case, the correction factor varies based on the model and no clear trend can be observed in order to propose a general correction factor.

Obviously, from Table 7.6, correlations of all frames and all damage criteria are significantly high and, for each frame, results from the ET

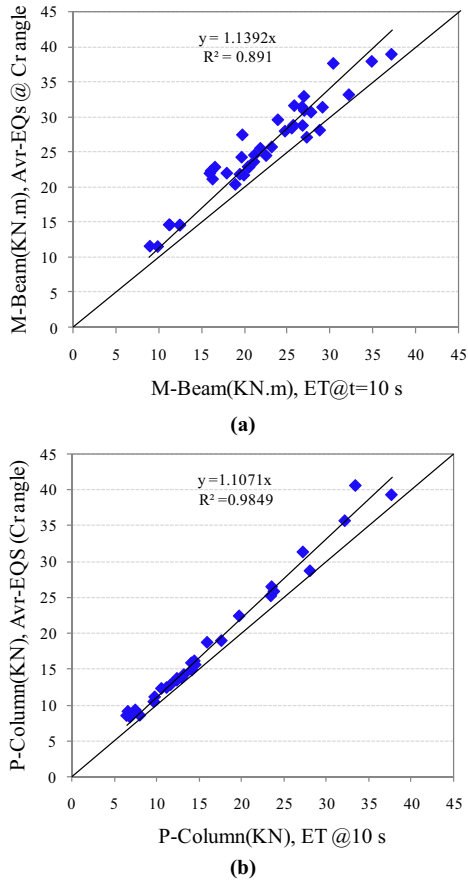

Figure 7.12. Internal forces obtained for earthquakes at critical angle vs. ET method at target time F3DMMS3X3Y-3IRXY, (a) moment in beams, (b) axial force in columns.

method could be scaled up to results from the average of real accelerograms at their critical angles. One reason for this is that, when maximum responses of earthquakes at critical angle for each ground motion are averaged, the effective level of response spectrum as an index of intensity increases as a result of the statistical process of maximizing between more analysis cases. On the other hand, the probability of exceedance of seismic hazard is reduced (Bazzurro et al. 1998). For example, the average of the maximum response in x direction of a 2DOF system under components of used earthquakes at their critical directions were computed and compared with that of ET acceleration functions at target time (t = 10 sec) in Figure 7.13. It is obvious that ET acceleration functions are applied just

Table 7.6. Correction factor and correlation coefficient of structural responses in ET method and real earthquake at their critical directions

	Displ		Drift		Mb		Pc		MxC		MyC	
	CF	r	CF	r	CF	r	CF	r	CF	r	CF	r
F3DMMS3X3Y3IRX	1.16	0.999	1.15	0.986	1.16	0.953	1.16	0.986	1.18	0.928	1.09	0.987
F3DMMS3X3Y3IRXY	1.12	0.996	1.07	0.99	1.14	0.961	1.11	0.993	1.12	0.919	1.14	0.764
F3DMMS4X3Y3	1.16	0.99	1.15	0.956	1.22	0.995	1.17	0.994	1.21	0.98	1.22	0.971
F3DMMS4X3Y3IRX	1.16	0.984	1.16	0.946	1.14	0.997	1.20	0.993	1.17	0.998	1.17	0.997
F3DMMS4X3Y3IRXY	1.19	0.983	1.19	0.941	1.27	1	1.20	0.989	1.17	0.999	1.17	0.999
F3DMMS5X4Y4	1.09	0.98	1.08	0.919	1.20	0.989	1.08	0.992	1.16	0.999	1.14	0.99
F3DMMS5X4Y4IRX	1.18	0.997	1.18	0.986	1.21	0.989	1.22	0.993	1.19	0.993	1.23	0.996
F3DMMS5X4Y4IRXY	1.16	0.983	1.12	0.959	1.18	0.904	1.23	0.989	1.17	0.991	1.22	0.997
F3DMMS7X5Y3	1.01	0.976	1.00	0.904	1.09	0.99	1.08	0.986	1.10	0.999	1.05	0.999

at two orthogonal directions and will not be rotated and critical angle for ET analysis is meaningless. It is seen that the response spectrum of ET acceleration functions is less than the response of the 2DOF system under horizontal components of real earthquakes at their critical angles at most periods of vibration. More studies are required in order to obtain effective response spectra pertaining to ground motions applied at all directions. In this way, ET acceleration functions can be developed based on these critical direction spectra and improved estimates can be made. However, it is also possible to improve the estimation by upscaling current ET records so that their response in Figure 7.13 matched those of ground motions at their critical angle. The spectral ratio of horizontal components of earthquakes at critical direction and those at principal direction and ET acceleration functions are depicted in Figure 7.14.

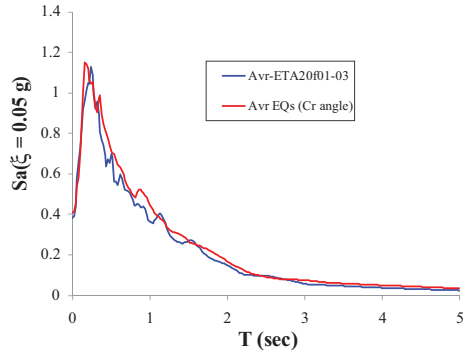

Figure 7.13. Average acceleration response of 2DOF system in x-direction under components of real earthquakes at their critical orientation and ETAf01-03 at t = 10 sec.

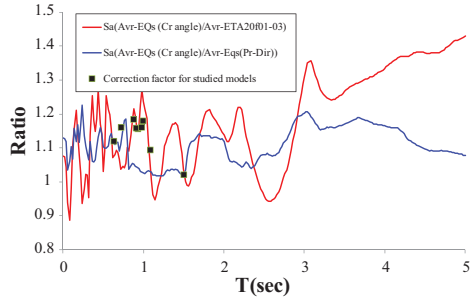

Figure 7.14. The comparison of spectral ratio of horizontal components of earthquakes at critical direction and principal direction and ET acceleration functions.

As can be seen in Figure 7.14, the spectral ratio of horizontal components for actual ground motions vary between 1 and 1.2 and for ETAFs are between 0.9 and 1.4. Furthermore, it is seen that at the periods T>3 sec, the ratio of spectrum from earthquakes at critical angle and ET acceleration functions increase. This matter can be expected from Figure 7.4. The response spectrum from second component of earthquakes at higher periods, after T = 3 sec, is greater than that of first component which ET acceleration functions are consistent with. Thus, at higher periods, especial consideration should be made for determining design spectrum which based on it, the ET acceleration functions are selected or produced. Also, it is seen that the curve obtained for actual ground motions is smoother than that of ETAFs. It is due to the fact that the response spectra of ETAFs and used records are not exactly the same and there are always minor differences between ETAFs and target spectrum. By the way, this figure is consistent with results obtained from Table 7.6, where the scale factor varies between 1 and 1.23. Comparing the CF obtained from Table 7.6 with Figure 7.14, it is concluded that the differences from ET analysis and results of time-history analysis at critical angle can be interpreted by their response spectra, It seems that an appropriate scale factor, estimated from Figure 7.14, can be applied to studied frames, to estimate the average response of real earthquakes at their critical angle. It should also be noted that this required statistical correction factor is conceptually the same considering either ground motions or ET analysis results. On the other hand, in ET analysis, this scale factor, can be converted into its equivalent extra time thus, the average response of earthquakes at a critical angle can be estimated in the ET method by reading the response at a higher time, provided that this observation can be verified considering more elaborate studies. Anyways, it should be noted that the response at critical direction can be quite different from that obtained from analysis based on orthogonal direction excitation and further research in this area is required if any general conclusion is to be achieved.

7.9 SUMMARY AND CONCLUSIONS

In this chapter, application of the ET method in the analysis of buildings under bidirectional excitation was investigated and a procedure for three-dimensional analysis by the ET method was proposed. Following seismic code recommendations, results of the time-history analysis of buildings under horizontal components of earthquakes at principal directions and critical directions, were compared with the results of ET analysis

under pairs of ET acceleration functions applied in principal directions of the studied buildings. The following conclusions can be drawn:

1. Response of structures estimated by proposed bidirectional ET analysis procedure matches well with results from time-history analysis using real earthquakes components in principal directions of structures.
2. The average and minimum correlation coefficient for analysis results obtained from ET method and time-history analysis using real earthquakes for investigated frames are 0.97 and 0.80, respectively. Considering this strong correlation between the results, it can be concluded that the average response to seismic excitation in linear range can be predicted by the ET method with reasonable accuracy.
3. Response of structures studied in this chapter at critical directions of each earthquake can be correlated to their response using orthogonal direction analysis by applying a correction factor of about 1.05 to 1.2 in studied models. In these cases, results from ET analysis, at t = 10 sec, can be multiplied by a correction factor or, alternatively, damage values should be read as a higher target time on the ET response curve for critical direction estimations. However, this observation cannot be extended to general cases and more investigation is required before a reasonable conclusion can be made in this regard.
4. Based on the results from the studied models in this chapter, response of steel moment frames subjected to multicomponent seismic excitation can be predicted with reasonable accuracy by using the proposed procedure. This procedure can reduce the required computational effort when time-history analysis is required, such as the analysis of the effect of damping devices. However, in order to take advantage of the full potential of ET method in multicomponent seismic analysis, its application should be extended to nonlinear analysis in future.

NOMENCLATURE

$a_g(t)$	Ground acceleration
ET	Endurance Time
ETacc	Endurance Time acceleration function
T Free	vibration period (s)
S_a	Acceleration response

$S_a(T, t)$	Acceleration response for period T at time t
$S_{aC}(T)$	Codified design acceleration spectrum for period T
$S_{aT}(T, t)$	Target acceleration response for period T at time t
$S_u(T, t)$	Displacement response for period T at time t
$S_{uT}(T, t)$	Target displacement response value for period T at time t
t	Time
t_{max}	Time corresponding to the end of accelerogram
T_{max}	Maximum free vibration period (s) to be considered in the optimization
t_{Target}	Target time
α	Weighing factor in optimization target function
MMF	Moment resistant frame in both directions
CF	Correction Factor
$DI_{Avr-EQs}$	Damage Index obtained from averaging the response of earthquakes
$DI_{ET@t=10}$	Damage Index obtained under ET acceleration functions at t = 10 sec
r	Correlation Coefficient
Mb	Moment in Beams
Pc	Axial Force in Columns
MxC	Moment at the End of Column in X direction
MyC	Moment at the End of Column in Y direction
2DOF	Two Degree of Freedom system

REFERENCES

ASCE. 2000. *Seismic Analysis of Safety-Related Nuclear Structures and Commentary*. ASCE Standard No. 004-98, American Society of Civil Engineers.

ASCE. 2006. *Minimum Design Loads for Buildings and other Structures*. ASCE Standard No. 007–05, American Society of Civil Engineers.

Athanatopoulou, A.M. 2005. "Critical Orientation of Three Correlated Seismic Components." *Engineering Structures* 27, pp. 301–12.

Baker, J.W., and C.A. Cornell. 2006. "Correlation of Response Spectral Values for Multicomponent Ground Motions." *Bulletin of the Seismological Society of Americ* 96, no. 1, pp. 215–27.

Bazzurro, P., C.A. Cornell, N. Shome, and J.E. Carballo. 1998. "Three Proposals for Characterizing MDoF Non-Linear Seismic Response." *Journal of Structural Engineering* 124, no. 11, pp. 1281–89.

Beyer, K., and J.J. Bommer. 2007. "Selection and Scaling of Real Accelerograms for Bi-Directional Loading: A Review of Current Practice and Code Provisions." *Journal of Earthquake Engineering* 11, no. 1, pp. 13–45.

CEN. 2003. *Eurocode 8: Design of Structures for Earthquake Resistance. Part 1: General Rules, Seismic Actions and Rules for Buildings*. Brussels: European Committee for Standardization.

Estekanchi, H.E., A. Vafai, and M. Sadeghazar. 2004. "Endurance Time Method for Seismic Analysis and Design of Structures." *Scientia Iranica* 11, no. 4, pp. 361–70.

Estekanchi, H.E., V. Valamanesh, and A. Vafai. 2007. "Application of Endurance Time Method in Linear Seismic Analysis." *Engineering Structures* 29, no. 10, pp. 2551–62.

FEMA. 2001. *NEHRP Recommended Provisions for Seismic Regulations for New Buildings and other Structures*, *2000 Edition, Part 1: Provisions*. FEMA 368, Washington, DC: Building Seismic Safety Council for the Federal Emergency Management Agency.

Hernández, J.J., and O.A. López. 2002. "Response to Three-Component Seismic Motion of Arbitrary Direction." *Earthquake Engineering and Structural Dynamics* 31, no. 1, pp. 55–77.

INBC. 2005. *Iranian Code of Practice for Seismic Resistant Design of Buildings (Standard No. 2800-05)*, 3rd ed, Building and Housing Research Center, Tehran.

López, O.A. 2006. "Response Spectra for Multicomponent Structural Analysis." *Earthquake spectra* 22, no. 1, pp. 85–113.

López, O.A., A.K. Chopra, and J.J. Hernández. 2001. "Evaluation of Combination Rules for Maximum Response Calculation in Multicomponent Seismic Analysis." *Earthquake Engineering and Structural Dynamics* 30, no. 9, pp. 1379–98.

Naeim, F., A. Alimoradi, and S. Pezeshk. 2004. "Selection and Scaling of Ground Motion Time Histories for Structural Design Using Genetic Algorithms." *Earthquake Spectra* 20, no. 2, pp. 413–26.

Penzien, J., and M. Watabe. 1975. "Characteristics of 3-Dimensional Earthquake Ground Motion." *Earthquake Engineering and Structural Dynamics* 3, no. 4, pp. 365–73.

Riahi, H.T., and H.E. Estekanchi. 2010. "Seismic Assessment of Steel Frames with Endurance Time Method." *Journal of Constructional Steel Research* 66, no. 6, pp. 780–92.

Valamanesh, V., H.E. Estekanchi, and A. Vafai. 2010. "Characteristics of Second Generation Endurance Time Accelerograms." *Scientia Iranica* 17, no. 1, pp. 53–61.

Vamvatsikos, D., and C.A. Cornell. 2002. "Incremental Dynamic Analysis." *Earthquake Engineering and Structural Dynamics* 31, no. 3, pp. 491–514.

Wilson, E.L. 2002. *Three-Dimensional Static and Dynamic Analysis of Structures*, 3rd ed. Berkeley, CA: Computer and Structures, Inc.

Zovani, E.H., and R.M. Barrionuevo. 2004. "Response to Orthogonal Components of Ground Motion and Assessment of Percentage Combination Rules." *Earthquake Engineering and Structural Dynamics* 33, no. 2, pp. 271–84.

CHAPTER 8

PERFORMANCE-BASED DESIGN WITH ENDURANCE TIME

8.1 INTRODUCTION

Seismic performance of structures during strong earthquakes is one of the most sensitive considerations regarding their safety and economic requirements to be set as their design criteria.[1] Nowadays, usually, the owners like to know the performance of their structures during an earthquake in order to make relevant economic decisions with a reasonable level of confidence. This interest has led engineers to develop methods for designing structures such that they are capable of delivering a predictable performance during an earthquake. Performance-based earthquake engineering, essentially, consists of various procedures whereby the structure is ensured for an acceptable seismic performance. The procedure involves identification of the hazard level for the site; development of conceptual, preliminary, and final structural designs; construction; and the maintenance of a building during lifetime (Krawinkler and Miranda 2004).

As per FEMA-302 NEHRP Recommended Provisions for the Seismic Regulations for New Buildings and Other Structures (BSSC 1998a) (FEMA-302 1997) and FEMA 273 NEHRP Guidelines for the Seismic Rehabilitation of Buildings (BSSC 1997) (FEMA 1997), three performance levels (PLs) are considered. These are termed Immediate Occupancy (IO), Life Safety (LS), and Collapse Prevention (CP). In the first damage state, IO, only minor structural damages are visible and no substantial reduction in building gravity or lateral resistance has occurred.

[1] Chapter Source: Mirzai, A., H.E. Estekanchi, and A. Vafai. 2010. "Application of Endurance Time Method in Performance Based Design of Steel Moment Frames," *Scientia Iranica* 17, no. 6, pp. 482–92.

In the LS level, although significant damage to the structure has occurred, structural elements have enough capability of preventing collapse. The CP level is defined as the postearthquake damage state, in which critical damages are occurred and the structure is on the verge of experiencing collapse (FEMA 1997). Another practical notion is "Performance Objective (PO)" which consists of the specification of a structural PL (e.g., *CP, LS*, or *IO*) for a given level of seismic hazard. For example, in accordance with SAC 2000, ordinary buildings are expected to provide less than a 2 percent chance, over 50 years, of damage exceeding CP performance (Krawinkler and Miranda 2004).

Evaluating the performance of existing structures under an earthquake is another important task, through which the operational situation of a structure during and after the event can be predicted. The performance evaluation consists of structural analysis with computed demands on structural elements compared against specific acceptance criteria provided for each of the various PLs (Humberger 1997). These acceptance criteria are really some limitations that are specified for various structural parameters (such as interstory drift and plastic rotation at joints) at different PLs.

The performance evaluation might sound a straightforward process, but, in reality, it is not a simple undertaking. The erratic nature of earthquakes, uncertainties in the existent analysis methods and lack of enough information about the current strength of the structures are some factors that make the procedure intricate.

In this paper, a new methodology for extending the application of Endurance Time (ET) method into the area of performance-based design is introduced (Estekanchi, Vafai, and Sadeghazar 2004). In the ET method, the structural responses at different excitation levels are obtained in a single time-history analysis, thus, significantly reducing the computational demand. So, using the ET method and regarding the concepts of performance-based design, the performance of a structure at various levels of seismic hazard can be predicted in a single time-history analysis. In other words, one can estimate if the structure satisfies its POs only by one time-history analysis. This characteristic of ET method can best be utilized by extending the concepts of ET method to incorporate the basic concepts from performance-based design, which is the main purpose of this paper.

As will be explained in detail, in this proposed methodology, two new concepts of continuous Performance Curves (PCs) and generalized Damage Levels (DLs) are incorporated. Utilizing some equations such as Gutenberg–Richter equations, the equivalent ETs corresponding to each PL are obtained. A newly introduced Target Performance Curve or Target

Curve representing the required performance as a continuous function of the excitation level is drawn. The definition of the mentioned curve is accomplished assuming that the PLs are continuous and, theoretically, it is possible to consider an unlimited number of PLs between these three previously said levels in the form of a continuous curve. Then, in order to have a more versatile numerical presentation of the PLs, an index is introduced called "Damage Level" (or "DL"), which is defined as a numerical index in the arbitrary range of (0, 4) for the purpose of this study. Integer numbers in this interval are representatives of codified PLs, thus, a convenient numerical equivalent is created for each PL. As will be explained, this index is used in order to draw a continuous target curve as the indicator of PLs.

The actual performance is then plotted against this target performance based on the results of ET analysis. The overall performance of the structure can be anticipated by comparing the target to the actual performance and the design can be improved based on the observed performance.

Finally, the performance of three steel moment frames is evaluated using the target curve and the advantages and limitations of this procedure are explained. As will be explained, by providing a good estimate of structural performance at different excitation levels in each response-history analysis, the ET method can considerably reduce the huge computational effort required for the practical performance design of structures. Also, the concepts of PC and DL provide a simplified presentation of performance analysis results that can be used as a tool in practical design cases.

8.2 THE ENDURANCE TIME CONCEPT

ET is a new dynamic pushover procedure that predicts the seismic performance of structures by subjecting them to a gradually intensifying dynamic action and monitoring their performance at different excitation levels. Structures that can endure the imposed intensifying acceleration function for longer are expected to be capable of sustaining stronger seismic excitation. In fact, since intensifying acceleration functions are used, the time axis in ET analysis can be correlated to the intensity of excitation (Riahi and Estekanchi 2010).

The concept of ET method can be physically presented by a hypothetical shaking table experiment. Three different frames with unknown seismic properties are fixed on the table and the table is subjected to an intensifying shaking. After a short time, one of the frames (assume Frame 1) fails. The second model will also fail as the amplitude of the vibration is increased.

Assume that this happens to Frame Number 3. Considering the times at which the models have been failed and regarding that the lateral loads induced by the shaking table somehow correspond with earthquake loads, one can rank the three frames according to their seismic resistance. Hence, here the ET of each structure against intensifying shaking can be considered as the seismic resistance criterion. In this hypothetical analysis, the second frame is the strongest or the best performer, the first frame is the worst and the third's performance is somewhere in between (Estekanchi, Valamanesh, and Vafai 2007).

In Figure 8.1, the schematic result of the previous hypothetical analysis is presented. The demand and capacity ratio has been calculated for these frames as the maximum absolute value of the endurance index during the time interval from 0.0 to *t*. Since a structure collapses when its demand and capacity ratio exceeds unity, the ET for each frame can be easily derived from this figure.

To start an ET time-history analysis, after a representative model has been constructed, one should set a suitable damage measure and an appropriate ET accelerogram (Figure 8.2). The analysis results are usually presented by a curve, in which the maximum absolute value of the damage measure in the time interval (0, *t*) (as given in Equation [1]) corresponds to time.

$$\Omega(f(t)) \equiv Max\left(Abs(f(\tau) : \tau \in [0, t]\right) \tag{1}$$

In the previous equation, Ω is a Max-Abs operator and *f(t)* is the desired structural response history such as interstory drift ratio, base shear or damage index. For application of the ET method, intensifying accelerograms are generated in such a way as to produce dynamic responses equal to the desired response spectrum (such as code's design spectrum)

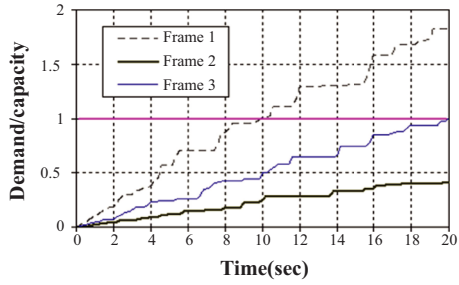

Figure 8.1. Demand/capacity of frames under acceleration function action (Riahi and Estekanchi 2010).

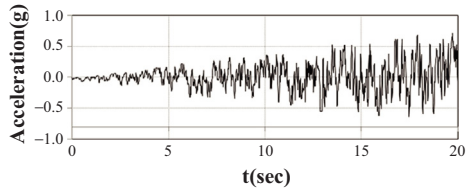

Figure 8.2. Typical ET accelerogram.

at a predefined time, t (Estekanchi et al. 2007). If such an accelerogram were designed and used, it would be possible to compare the results of the ET time history analysis with those obtained from other analysis methods and, moreover, to compare the performance of different structures with different periods of free vibration. The first suggested intensifying accelerograms for ET had a linear intensification scheme, that is, the response spectrum of an ET accelerogram should intensify proportionally with time. Hence, the target acceleration response of an ET accelerogram can be related to the codified design acceleration spectrum as:

$$S_{aT}(T,t) \equiv S_{aC}(T) \times \frac{t}{t_{\text{Target}}} \tag{2}$$

where $S_{aT}(T,t)$ is the target acceleration response at time t, T is the period of free vibration, and $S_{aC}(T)$ is the codified design acceleration spectrum.

Using unconstrained optimization in the time domain, the problem was formulated as follows:

$$Find\ a_g(t) \mid \forall\ T \in [0,\infty], t \in [0,\infty] \rightarrow \Omega(\ddot{u}(t)) = S_{aT}(T,t) \tag{3}$$

or

$$Minimize\ F(a_g(t)) = \int_0^{T_{\max}} \int_0^{t_{\max}} \Big\{ Abs\big[S_a(T,t) - S_{aT}(T,t)\big] + \alpha \times Abs\big[S_d(T,t) - S_{dT}(T,t)\big] \Big\} dt\ dT \tag{4}$$

Where a_g is the ET accelerogram being sought, $S_{aT}(T, t)$ and $S_{dT}(T, t)$ are the target acceleration response and displacement response at time t, respectively, $S_a(T, t)$ and $S_d(T, t)$ are the acceleration response and displacement response of acceleration function at time t, respectively, α is a weight parameter set to 1, and T is the period of free vibration (Riahi and Estekanchi 2010).

It should be noted that based on the mentioned linear scheme, different sets of ET accelerograms can be generated according to their

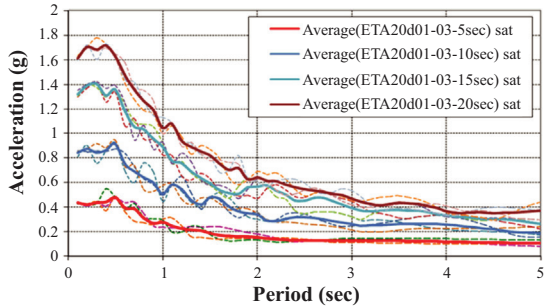

Figure 8.3. Acceleration response generated by ET accelerograms at various times.

compatibility with different spectrums and in different ranges (linear range or nonlinear range). Each set consists of a group of intensifying acceleration functions (usually three). For example, three acceleration functions named "ETA20d01-03" or briefly "d series" in this study are created in such a way that its response spectrum at t = 10 sec would be compatible with INBC 2800 design spectrum and supports nonlinear ranges.

Sample response spectra generated using various time windows of ET accelerograms are shown in Figure 8.3. In this figure, the curves are taken as average values between the results of three accelerograms of the d series. As can be seen in this figure, the response spectra produced by the ET acceleration function proportionally grows with time.

8.3 PERFORMANCE LEVELS

PLs are structural damage states that must be clearly defined as one of the first steps in a performance-based design procedure. These levels are usually expressed as some distinct bands in the damage spectrum of a structure, and divide damage status of structures according to the amount of damage to structural and nonstructural components. Moreover, some other concepts, such as cost, repair time, and injury, can also be related to PLs (Grecea, Dinu, and Dubina 2004).

Noting that the PLs are usually investigated at some specific levels of design earthquake motion, they can be thought of as a criterion for limiting values of measurable structural response parameters (such as interstory drift and absolute acceleration and displacement), under each mentioned level of earthquake motion.

There are three well-known PLs considered by FEMA-273 (NEHRP Commentary on the Guidelines for the Seismic Rehabilitation of Buildings

Table 8.1. Selected performance objective for a residential building

Earthquake having probability of exceedance	Mean return periods (years)	Performance level
50% per 50 year	75	IO
10% per 50 year	475	LS
2% per 50 year	2475	CP

1997): IO, LS, and CP, which were determined according to structural damages observed in earthquakes. For example, at the IO level, the building has experienced limited damage, since at the CP level, damage is relatively extreme.

On the other hand, in FEMA-356 Prestandard and Commentary for the Seismic Rehabilitation of Buildings, four levels of probabilistic earthquake hazard are defined. Combining these levels with the PLs, a table of POs can be created (FEMA-356 2000). These objectives are different according to the type of structure that is to be built. For example, if a hospital is planned to be built, an appropriate PO might be that it is capable of meeting the LS PL in an earthquake with a mean return period of 2,475 years, and the IO PL in an earthquake with a mean return period of 475 years. So, if one wants to evaluate the performance of a specific model of a hospital, he or she should first analyze the model under two sets of considered earthquakes with the defined mean return periods separately and, then, see if the model satisfies the related code criteria for each PL.

Since the descriptions of the POs are mostly qualitative, some performance criteria have been defined to bind these descriptions to engineering demand parameters so the POs can be predicted in analysis and design process (Krawinkler and Miranda 2004). In fact, these criteria are the rules and guidelines that must be met to ensure that the designed structure satisfies the POs. In this research, the PO shown in Table 8.1 is considered for a residential building.

8.4 TARGET AND PERFORMANCE CURVES

As previously mentioned, the target curve is a concept by means of which the specific properties of ET method can be readily put into use in the performance-based design procedure. Using the target curve is an

appropriate way to evaluate the performance of structures in ET method. In fact, the target curve will be used as the criteria curve for the ET response curve and the performance of a structure at different excitation levels can be evaluated by comparing the ET response curve with the target curve.

Since in the target response curve (or simply target curve), the target and the ET response curves will be compared in a single chart, the horizontal and the vertical axes of the target curve should be defined such as to match with the corresponded axes in the ET response curve; that is, the time in seconds on the horizontal axis and a damage index on the vertical axis. On the other hand, the target curve should be inclusive of a relation between the PLs and the corresponding performance criteria. The performance criteria are conceptually similar to the damage indices. Thus, the challenge is to correlate the PLs to the ETs. In other words, the first step in the process of creating the target curve is to identify the respective ET of each PL. To do so, the procedure shown in Figure 8.4 should be followed step by step. It is noticeable that this procedure is not an exact one. To have an exact calculation, it is needed to obtain the hazard curve for a special site and the PGA should be acquired according to that curve, but, since the main purpose of this research is to illustrate the basic concepts of the proposed procedure, the following approximate procedure can be considered as appropriate. The corresponding magnitude of each earthquake hazard has been

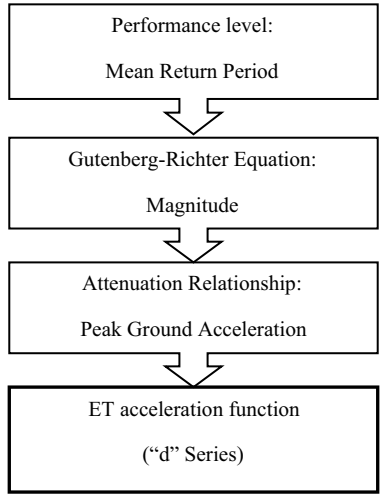

Figure 8.4. Target curve construction procedure.

obtained first using the Gutenberg-Richter relation, as follows (Mohraz and Sadek 2003):

$$LogN = a - bM \tag{5}$$

where
N is the return period of earthquake (years);
M is the magnitude of earthquake in Richter;
b is called the "*b*-value," and is typically in the range of 0.8–1.2;
and a is called the "productivity."

"*a*" and "*b*" are some parameters that severely depend on the properties of the region in which the earthquake had occurred. For Iran, the following form is recommended by Kaila and Narian (1971):

$$LogN = 6.02 - 1.18M \tag{6}$$

After that, the peak ground acceleration (*PGA*) must be acquired from magnitude. The following formula is suggested for Iran (Amiri, Mahdavian, and Manouchehri Dana 2007):

$$Ln(PGA) = 3.65 + 0.678M - 0.95\ \mathrm{In}(R) \tag{7}$$

where "*PGA*" is peak ground acceleration in cm/sec^2, "*M*" is magnitude in Richter and "*R*" is the distance to the fault in km, which is to be considered as 18 in this research.

This acceleration can be easily related to the ET. For this purpose, it is needed to specify which series of accelerograms are to be used. According to its conformability with the Iranian code 2800 standard (BHRC 2005), the "d" series of accelerograms (i.e., ETA20d01-03) has been chosen. Considering this series, the equivalent ETs in ET records corresponding to the three mentioned PGAs can be identified. To do so, it's enough to trace the times in the ET acceleration function at which the PGAs exceed the values of the PGAs corresponding to each PL.

The results of the previous procedure are shown in Table 8.2. In this table, the relevant interstory drift for each PL is indicated. These quantities are for steel moment frames and based on the FEMA-356 standard. Although these values are not intended in FEMA-356 to be used as acceptance criteria for evaluating the performance of structures and they are just some quantities which qualitatively indicate the behavior of structures at each level of performance, in this research, these values will be used as an index to show the limits of each PL. Plastic rotation in beams is the other index, which is used here to evaluate the performance of structures. To accurately evaluate the performance, one should obtain the values of plastic deformations in all elements (including beams, columns, panel

Table 8.2. Endurance times related to each PL

Performance level	Mean return periods (years)	Magnitude (richter)	PGA(g)	Endurance time (sec)	Interstory drift (%)
IO	75	6.7	0.22	5.16	0.7
LS	475	7.3	0.35	10.16	3.5
CP	2475	7.9	0.53	15.46	5

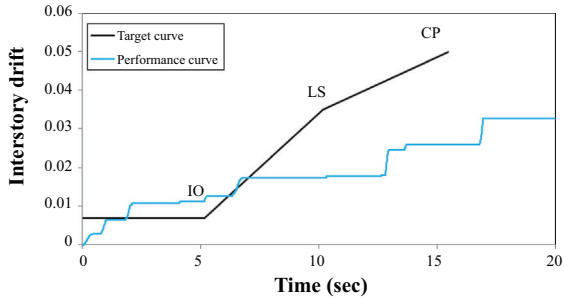

Figure 8.5. Target and existing performance curves.

zones, braces, etc.) and compare them to the acceptance criteria given in the FEMA-356 standard.

This means that the design of a typical structure should be such that if the "d" series of accelerograms were applied to the structure, it would be capable of meeting the IO PL up to 4.14 sec, the LS PL up to 10.21 sec and the CP PL up to 19.11 sec.

Based on the earlier discussion, the target curve has been drawn and compared with a three-story frame performance curve in Figure 8.5. In this figure, the limit of each PLs has been specified on the target curve. This frame is subjected to the "d" series of ET accelerograms and its interstory drift response is considered as the damage index. It should be noted that, while there is no criteria for damages below the IO level, this area is restricted by a horizontal line in the target curve.

8.5 DAMAGE LEVEL

The previous target curve has some ambiguities and incompetencies. One is that to evaluate the performance of structures, the performance of all elements should be checked by observing their plastic deformations and

comparing the values with the acceptance criteria. Since different limits are set on these parameters for various elements in each PL, it is difficult to compare the performance of different elements and clearly define the critical one. Thus, to accurately evaluate the performance of a structure, one should create a target curve for each mentioned index and element, and compare the related response curve with that target curve. In this way, even though the performance can be identified, the specification of the critical index is not a simple matter. A combined damage indicator has been defined for the purpose of this study that simplifies the compilation of DLs indicated by various indexes into one normalized numerical value. This index is named "Damage Level" or DL in this study. Another property of the DL is that this dimensionless index creates a numerical presentation for PLs, that is, one could distinguish and compare the performance of different structures with only one number. Moreover, if two structures lie within a same PL, their performance can be still comparable with this index.

To specify such an index, five PLs are considered as OP (fully operational), IO, LS, CP, and CC (complete collapse, an arbitrary point to extend the target performance curve beyond CP), which is a rather arbitrary level to simplify formulation. It should be noticed that OP and CC levels are just used as the limits of the performance and also the limits of the DL. Until more research is available to define the CC point based on more rational criteria, it will be considered arbitrarily in such a way that the slope of the target performance curve before the CP level, is maintained. This additional point is required in order to theoretically extend the performance curve beyond CP and has no practical significance in this study. The formulation proposed for the DL has been arranged is such a way as to assign an explicit number (preferably an integer) to each PL and use the determining parameters (such as interstory drift and plastic rotation) to compute the DL in a clear and understandable way.

An appropriate formulation, which satisfies the earlier-mentioned considerations, can be expressed as follows:

$$DL = \sum_{i=1}^{n} \frac{\max\left[\theta_{i-1}, \min\left(\theta, \theta_i\right)\right] - \theta_{i-1}}{\theta_i - \theta_{i-1}} \tag{8}$$

where θ is the related parameter-like drift, which should be computed from analysis and θ_i is the FEMA-356 Prestandard boundary of that parameter for each PL. The values of θ_i for interstory drift and plastic rotation for each PL and the corresponding DL's are given in Table 8.3.

As can be seen in Table 8.3, the obtained DL will satisfy its purpose satisfactorily. Because, first, it denotes the PL of the structure, second,

Table 8.3. Assigning damage levels to performance levels

Performance level	Damage level	(Drift) θ_i	θ_i* (Plastic rotation)		
			Case (a)	Case (b)	Case (c)
IO	1	0.7	1	0.25	Interpolation required
LS	2	3.5	6	2	
CP	3	5	8	3	
CC**	4	7	11	6	

* Case (a): $b_f/2t_f < 52/\sqrt{F_{ye}}$ and $h/t_w < 418/\sqrt{F_{ye}}$,
Case (b): $b_f/2t_f > 65/\sqrt{F_{ye}}$ or $h/t_w > 640/\sqrt{F_{ye}}$,
Case (c): Other.
** CC is an auxiliary point included so that the performance curve can be theoretically extended beyond CP

since it is a number, it will satisfy the need to create a numerical presentation for PLs, third, it can present all parameters in a normalized form and this will ease future computations.

In light of the earlier discussion, the determining parameter, like interstory drift (or plastic rotations) can be replaced by DL in the target curve. Likewise, the structure performance or response curve should be drawn according to this new index to comply with the target curve.

8.6 MODEL DESIGN

In order to demonstrate how the target curve can ease the visualization of the performance of structures, a set of 2D steel moment-resisting frames with a different number of stories and spans were selected and used in this research. These models consist of 3-story, 1-bay and 7-story, 3-bay frames that are designed in 3 alternatives (standard, weak, and strong frames) and a 12-story, 3-bay frame that is designed in 2 standard and strong alternatives. These frames are designed according to the AISC-ASD89 design code. To compare the performance of the frames with varying seismic resistance, the standard, weak and strong frames have been designed using base shears equal to 1, 0.5, and 1.5 times the codified base shear, respectively. As an example, the geometry and section properties of the seven-story, three bay frames is shown in Figure 8.6. In this figure, the black circles stand for the plastic hinges and show that the failure mechanism follows the strong column-weak beam concept. As can be seen in Figure 8.7, these hinges have been modeled as a rotational

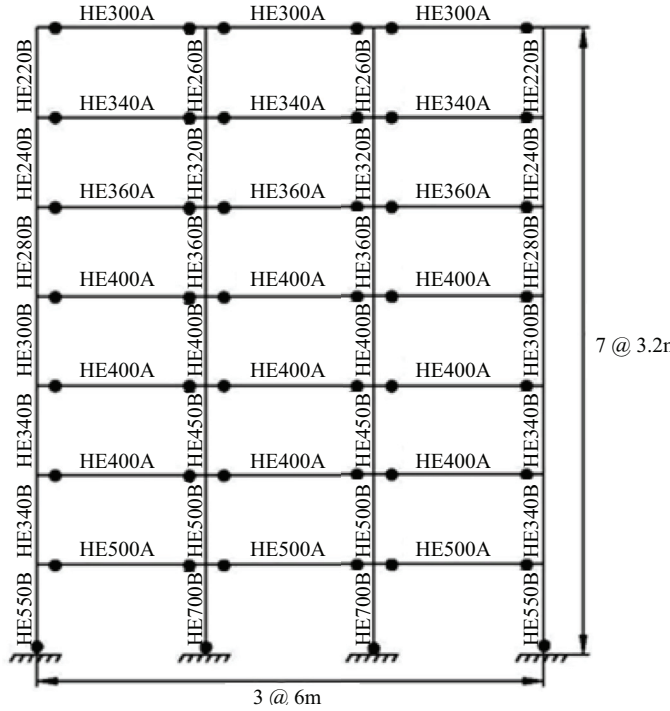

Figure 8.6. Standard seven story frame geometry and sections.

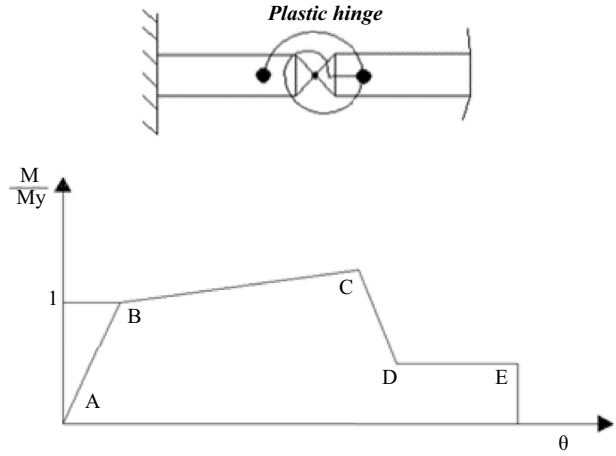

Figure 8.7. Plastic hinge model and its generalized force-deformation curve.

spring, with a moment-rotation curve shown in this figure. The capital letters in this figure (A to E) determine the boundaries of various behaviors of the hinge model.

8.7 ANALYSIS RESULTS

The modeling and nonlinear analysis were done with Opensees software (PEERC 2004) [14]. Nonlinear models of the frames are prepared by using the beam element with nonlinear distributed plasticity. In this research, the damping ratio is assumed to be 0.05 of the critical value and P-Δ effects have been included in the nonlinear analysis. Applicability of ET method in nonlinear analysis and acceptability of its approximation in estimating various damage indexes has already been studied (Riahi and Estekanchi 2010; Riahi, Estekanchi, and Vafai 2009; Estekanchi, Arjomandi, and Vafai 2008). Similar level of approximation is considered to be adequate for the purpose of this study.

The drift and plastic rotation responses of frames were obtained and converted to the DL index, according to Equation 8. Then, the ET response curve (performance curve) of each frame is plotted for each aforementioned parameter's related DL, separately. In Figure 8.8, the response curve for the plastic rotation and drift in a three-story standard frame is depicted. As illustrated in this figure, using the concepts of ET and DL, it is possible to compare the situation of various parameters, such as plastic rotation and drift, and identify the critical parameter in any seismic intensity. For example, in a three-story standard frame, as can be seen in Figure 8.8, drift is the critical parameter in low-intensity ground motions, but plastic rotation is critical at high-intensities. Note that the final performance curve for each frame should be created considering the maximum value of DL considering both the drift and rotation (or any other

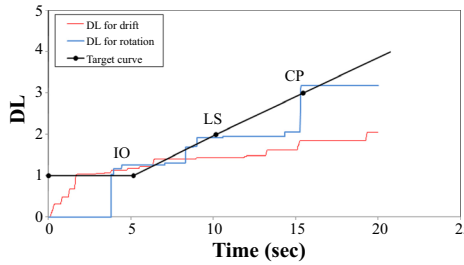

Figure 8.8. Performance curves for plastic rotation and drift in frame F3s1b.

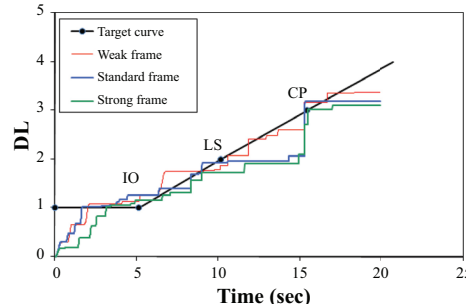

Figure 8.9. Performance curves for three-story frames.

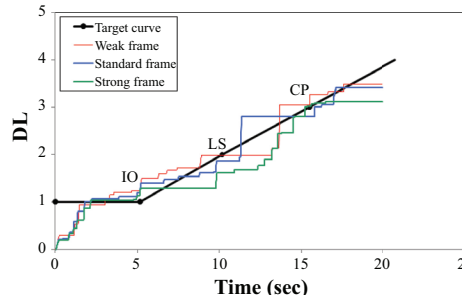

Figure 8.10. Performance curves for seven-story frames.

parameters that need to be considered based on the design criteria). The final DL response curve (or performance curve) for three alternatives of a three-story frame is shown in Figure 8.9. Using this figure, one can easily study and compare the performance of these three alternatives in various seismic intensities. For example, according to Figure 8.9, it can be concluded that all three alternatives fail the criteria of the IO PL, but remain in the safe region of LS and CP PLs; the standard frame performs similar to the weak frame at low intensities, but its performance resembles the strong frame performance as seismic intensity increases.

Figure 8.10 shows the performance curves of three types of seven-story frame. A good performance of the strong frame in comparison with two other frames can be easily observed in this figure. Moreover, it can be seen that the weak frame lies above the target curve almost at all times. The behavior of 12-story frames can be evaluated with a similar procedure.

Using the target curve, the performances of strong frames with various numbers of stories and bays can also be compared with each other. Such a comparison has been done for three strong frames with 3, 7, and

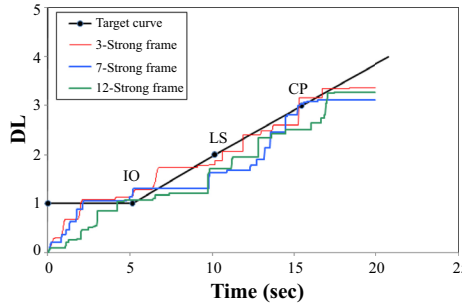

Figure 8.11. Performance curves for strong frames.

12 stories (Figure 8.11). Although all these three frames were designed on the basis of 1.5 times the codified base shear, their performance is not similar. The 12-story frame is the best performer and the 3-story frame is the worst one in this study.

To show and verify the versatility of the target curve, the three-story standard frame has been subjected to some earthquake records and its performance is evaluated by the target curve. To have a good evaluation, 7 earthquake records have been selected from the FEMA-440 recommended records and scaled in such a way as to create 7 modified records at each PL (i.e., 21 records). To do so, some correction factors are required to be computed and applied to each record. The correction factors for each PL and each record are the ratio of PL related PGA (see Table 8.2) to record's PGA. In Table 8.4, the properties of used records and the mentioned correction factors for each PL are indicated.

Thus, 21-time history analyses have been performed and responses of the frame are calculated in the form of the DL index. To provide a logical overview of the performance of standard frame, it is recommended that the maximum and average of the DL indices in each PL be considered and compared to those related to ET analysis results. Figure 8.12 shows the aforementioned comparison. In this figure, the crosses stand for the results of 21-time history analyses. As can be seen in this figure, the average values are compatible with ET analysis results, that is, the performance estimated by ET method is consistent with those from time history analysis using ground motions. Now it seems that if a line connects the average (or maximum) values, the performance of the frame will be coincident with this line at various seismic intensities. In fact, this line is similar to the familiar performance curve. However, it should be mentioned that selecting the optimal form of the connecting curve requires further research in this area.

Table 8.4. Properties of used records and the correction factors

No	Record	HP	LP	DT	Name	CF for CP	CF for LS	CF for IO	PGA
1	Northridge 24278	0.12	23	0.02	NRORR360	4.035	2.222	1.053	0.171g
2	Landers 12149	0.07	23	0.02	LADSP000	2.664	1.467	0.695	0.259g
3	Loma Preita 1652	0.2	41	0.005	LPAND270	1.575	0.868	0.411	0.438g
4	Loma Preita 47006	0.2	45	0.005	LPGIL067	2.255	1.242	0.588	0.306g
5	Morgan Hill 57383	0.1	27	0.005	MHG06090	1.933	0.504	0.504	0.357g
6	Loma Preita 58065	0.1	38	0.005	LPSTG000	2.828	1.577	0.615	0.244g
7	Loma Preita 58135	0.2	40	0.005	LPLOB000	1.342	0.739	0.35	0.514g

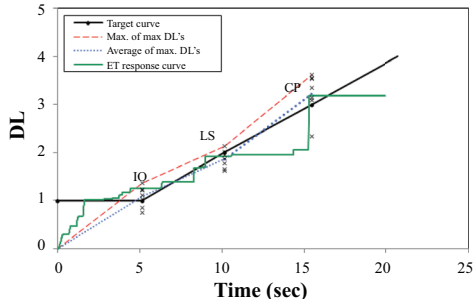

Figure 8.12. Comparison of ET and earthquakes results at equal PGA for three-story standard frame.

8.8 SUMMARY AND CONCLUSIONS

In this chapter, a methodology is proposed in order to extend the application of ET method to performance-based design of structures. Application of the ET method in performance-based design of steel frames is investigated from a conceptual viewpoint. In the ET method, structures are subjected to an intensifying acceleration function, thus, an estimate of the structural response at different levels of excitation is obtained in a single response history analysis, thus, considerably reducing the required computational effort. The concept of PLs has been extended from discrete presentation to a continuous target performance curve. This target performance curve, while theoretically more attractive, turns out to be quite versatile when investigating the ET analysis results, as shown in the paper. In order to be able to combine several different performance criteria into a single numerical performance index, a generalized DL index has been proposed. The DL index proposed in this chapter creates a versatile numerical representation of PLs and, also, provides a uniform index to express a performance of structures that incorporates various parameters (such as drift, plastic rotation, etc.). Furthermore, the target curve is an effective tool for estimating the performance of structures under various seismic intensities by the ET response curve. This curve can be used to anticipate the seismic performance of structures subjected to earthquakes. The target performance curve has a good potential to be used in the performance-based design of structures. The concepts of Performance Curve and DL introduced in this paper lay the necessary foundation for a more versatile application of the ET method in the practical performance-based design of structures. The analysis results are shown to be consistent with those obtained using ground motions scaled to represent particular excitation levels. It should be noted that extensive research in this area is

required in order to assess the precision and level of confidence that can be expected from proposed methodology.

NOMENCLATURE

Abs	Absolute value function
$a_g(t)$	ET acceleration function
b_f	Flange width
CC	Complete collapse
CP	Collapse prevention performance level
DL	Damage level
$F(a_g)$	Optimization target function
F_{ye}	Yield strength
IO	Immediate occupancy performance level
LS	Life safety performance level
M	Earthquake magnitude
Max	Maximum of the values
N	Earthquake mean return period
PGA	Peak ground acceleration
PL	Performance level
R	Distance to the fault
S_a	Spectral acceleration
$S_a(T, t)$	Acceleration response for period T at time t
$S_a(T)$	Acceleration response as a function of period T
$S_{aC}(T)$	Codified design acceleration spectrum
$S_{aT}(T, t)$	Target acceleration response for period T at time t
$S_d(T, t)$	Displacement response value for period T at time t
$S_{dT}(T, t)$	Target displacement response value for period T at time t
T	Free vibration period (sec)
t	Time
t_f	Flange thickness
t_{Target}	Target time (=10 sec in this paper)
T_{max}	Maximum free vibration period (sec) to be considered in the optimization
t_{max}	Time corresponding to the end of acceleration function
α	Weighting factor in optimization target function (=1.0 in this study)
θ_i	Determinant parameter (drift ratio or plastic rotation)
$\Omega(f(t))$	ET analysis result equal to Max(Abs(f(t1))): $t1 \in [0,t]$
|	Such that
$\forall$	For all values

REFERENCES

Amiri, G.G., A. Mahdavian, and F. Manouchehri Dana. 2007. "Attenuation Relationships for Iran." *Journal of Earthquake Engineering* 11, no. 4, pp. 469–92.

Estekanchi, H.E., A. Vafai, and M. Sadeghazar. 2004. "Endurance Time Method for Seismic Analysis and Design of Structures." *Scientia Iranica* 11, no. 4, pp. 361–70.

Estekanchi, H.E., K. Arjomandi, and A. Vafai. 2008. "Estimating Structural Damage of Steel Moment Frames by Endurance Time Method." *Journal of Constructional Steel Research* 64, no. 2, pp. 145–55.

Estekanchi, H.E., V. Valamanesh, and A. Vafai. 2007. "Application of Endurance Time Method in Linear Seismic Analysis." *Engineering Structures* 29, no. 10, pp. 2551–62.

FEMA (Federal Emergency Management Agency). 1997. *NEHRP Guidelines for the Seismic Rehabilitation of Buildings*, FEMA-273. Washington, DC: Federal Emergency Management Agency.

FEMA-302. 1997. *NEHRP Recommended Provisions for Seismic Regulations for New Buildings and Other Structures, Part 1: Provisions.* Washington, DC: Prepared by the Building Seismic Safety Council for the Federal Emergency Management Agency.

FEMA-356. 2000. *Prestandard and Commentary for the Seismic Rehabilitation of Buildings*. Washington, DC: Federal Emergency Management Agency.

Grecea, D., F. Dinu, and D. Dubina. 2004. "Performance Criteria for MR Steel Frames in Seismic Zones." *Journal of Constructional Steel Research* 60, no. 3, pp. 739–49.

Humberger, R.O. 1997. "A Framework for Performance-Based Earthquake Resistive Design." *EERC-CUREe Symposium in Honor of Vitelmo V. Bertero*, Berkeley, California.

Iranian Code of Practice for Seismic Resistance Design of Buildings 2005. BHRC. Standard No. 2800, 3rd ed. In *Permanent Committee for Revising the Iranian Code of Practice for Seismic Resistant Design of Buildings*. Tehran, Iran: Building and Housing Research Center.

Kaila, K.L., and H. Narian. 1971. "A New Approach for the Preparation of Quantitative Seismicity Maps." *Bulletin of the Seismological Society of America* 61, no. 5, pp. 1275–91.

Krawinkler, H., and E. Miranda. 2004. "Performance-Based Earthquake Engineering." In *Earthquake Engineering: from Engineering Seismology to Performance-Based Engineering*, eds. Y. Bozorgnia and V.V. Bertero. Boca Raton, FL: CRC Press.

Mohraz, B., and F. Sadek. 2003. "Earthquake Ground Motion and Response Spectra." In *Earthquake Engineering Handbook*, eds. W.F. Chen and C. Scawthorn. Boca Raton, Florida: CRC Press.

PEERC (Pacific Earthquake Engineering Research Center). 2004. *Open System for Earthquake Engineering Simulation (OpenSees)*. Berkeley, CA: Pacific Earthquake Engineering Research Center (http://opensees.berkeley.edu/).

Riahi, H.T., and H.E. Estekanchi. 2010. "Seismic Assessment of Steel Frames with Endurance Time Method." *Journal of Constructional Steel Research* 66, no. 6, pp. 780–92.

Riahi, H.T., H.E. Estekanchi, and A. Vafai. 2009. "Application of Endurance Time Method in Nonlinear Seismic Analysis of SDOF Systems." *Journal of Applied Sciences* 9, no. 10, pp. 1817–32.

CHAPTER 9

VALUE-BASED SEISMIC DESIGN WITH ET

9.1 INTRODUCTION

In recent decades, large economic losses following earthquakes and hurricanes have shown the need for improved design criteria and procedures that provide the necessities to reduce damage and economic impacts to an acceptable level along with life protection.[1] The prescriptive and also performance-based approaches of seismic design try to find a structure to satisfy minimal requirements under seismic actions in a number of levels of intensity and a design with lower initial cost is normally preferred. These approaches will not necessarily result in an economical design with lower total cost in life time of the structure. Thus, to incorporate directly the economic concerns in design or decision-making procedure Life-Cycle Cost Analysis (LCCA) has been applied in construction industry. LCCA has provided a reliable tool for estimating costs due to future earthquakes during the design life of a structure. This analysis in companion with an optimization algorithm can result in a design with the least total cost. The LCCA principles are based on economic theories and it was mainly implemented to introduce financial concerns in structural design area. However, this analysis can provide a baseline to incorporate technical, economic, and social or any other intended measures thought to be impressive in design procedure. Considering economic and also technical issues in design and construction field will lead to optimum allocation of the public resources. Although in construction industry LCCA was first introduced in economical investment

[1] Chapter Source: Basim, M.C., H.E. Estekanchi, and A. Vafai. 2016. "A Methodology for Value Based Seismic Design of Structures by the Endurance Time Method." *Scientica Iranica, Transaction A, Civil Engineering* 23, no. 6, p. 2514.

assessment of infrastructures, nowadays, LCCA becomes an essential component of the design process used to control the initial and the future cost of buildings in seismically active regions and is widely used in risk assessment and decision analysis. By the use of this method the expected total cost of a structure including the initial cost and also losses resulting from earthquakes during its life span can be considered as the main indicator of the priority of design alternatives. In this paper, LCCA is used to determine the total value of a structure as an investment appraisal tool to be incorporated in design procedure. Readily introduced value-based design can provide a wider description of design target by defining the earthquake consequences such as structural damages, loss of contents, losses due to downtime, human injuries and fatalities in the form of quantifiable parameters. In this way, it is expected that the resultant design will perform with desired postearthquake capabilities with manageable disruption.

LCCA demands the calculation of the cost components related to the performance of the structure in multiple hazard levels (Mitropoulou, Lagaros, and Papadrakakis 2011). In order to have a reasonably reliable performance assessment and estimate, the seismic capacity of a structural system to be incorporated into the LCCA methodology, response-history-based incremental analyses, and considering a realistic numerical model of the structure are inevitable. However, these procedures require repetitive and massive analyses and their huge computational demand and sophistications involved may make optimization algorithms impractical or the simplifications used decrease the reliability of the outcome. In this chapter, Endurance Time (ET) method, as a dynamic procedure requiring reasonably reduced computational effort, is applied to estimate the performance of the structure in various hazard levels (Estekanchi, Vafai, and Sadeghazar 2004). In the ET method, structures are subjected to specially designed intensifying acceleration functions instead of a set of progressively scaled up ground motions in incremental dynamic analysis (IDA) and their performance is assessed based on their response at different excitation levels correlated to specific ground motion intensities by each single response-history analysis. Thus, the required huge computational demand of a complete response history analysis is considerably reduced while maintaining the major benefits of it, that is, accuracy and insensitivity to model complexity (Estekanchi and Basim 2011). Application of ET method in combination with the concept of LCCA can pave the way for practical Value Based Seismic Design of Structures (VBSD).

The ET method introduced by Estekanchi, Vafai, and Sadeghazar (2004) as an analysis method, can be utilized to assess seismic performance of the structures in a continuous range of seismic hazard intensities.

In this method, structures are subjected to a predesigned gradually intensifying accelerogram and the seismic performance of the structure can be monitored while the seismic demand is increasing. Application of the ET method in performance assessment of structures has been studied by Mirzaee, Estekanchi, and Vafai (2010) and Hariri-Ardebili, Sattar, and Estekanchi (2014). Reasonably accurate estimates of expected seismic response at various excitation intensities of interest have been obtained through ET analysis by correlating the dynamic characteristics of intensifying excitations with those of ground motions at various hazard levels (Mirzaee and Estekanchi 2013).

In order to demonstrate the method, a five-story and three-bay steel special moment frame is optimally designed according to Iranian National Building Code (INBC), which is almost identical to the ANSI/AISC360 (2010) LRFD design recommendations. Also, the frame is designed optimally to conform to FEMA-350 (2000) limitations as performance-based design (PBD) criteria. The performance of the designed frames is investigated by the ET method and as a third step a new design section has been acquired through the introduced method to have the minimum total cost during its life time that is assumed 50 years. The resultant prescriptive, performance-based and value-based designs of the frame are different due to their distinct basic design philosophies. Seismic performance and cost components of these structures are investigated and discussed.

9.2 BACKGROUND

Although significant progress has been made in the last two decades in the area of seismic engineering, currently, most of the seismic design codes belong to the category of the prescriptive design codes, which consider a number of limit state checks to provide safety. The two common limit state checks are serviceability and ultimate strength. It is worthy of note that a design with a lower weight or initial material cost is commonly preferred. Prescriptive building codes do not provide acceptable levels of a building life-cycle performance, since they only include provisions aiming at ensuring adequate strength of structural members and overall structural strength (Mitropoulou, Lagaros, and Papadrakakis 2011). To fulfill the deficiencies of the primitive design procedures, design codes are migrating from prescriptive procedures intended to preserve life safety to reliability-based design and most of them have attempted to advance their design criteria toward PBD of structures. The report of the SEAOC committee in 1995 can be entitled as the start of this progress. Performance-based earthquake

engineering states the methodology in which structural design criteria are expressed in terms of achieving a set of different performance objectives defined for different levels of excitations where they can be related to the level of structural damage. In this methodology, the performance of the building after construction is inspected in order to ensure reliable and predictable seismic performance over its life. In PBD, more accurate and time-consuming analysis procedures are employed in order to estimate the entire nonlinear structural response. Various guidelines on PBD concept have been introduced over the last 10 years for assessment and rehabilitation of existing structures and the analysis and design of new ones. FEMA-350 (2000) supplies a probability-based guideline for PBD of new steel moment resisting frames considering uncertainties in seismic hazard and structural analyses. Design codes based on reliability of performance are useful in providing safety margins for the performance objectives with quantifiable confidence levels considering various sources of uncertainties.

In PBD after selecting the performance objectives and developing a preliminary design, seismic response of the design is evaluated. Afterwards, the design can be revised until the acceptance criteria for all intended performance objectives are satisfied. In order to achieve optimal structural designs with acceptable performance, optimization methods have been effectively used for PBD while the structural performances and also structural weight incorporated as objective functions or constraints to the optimization problem (Ganzerli, Pantelides, and Reaveley 2000). Among many others, Pan, Ohsaki, and Kinoshita (2007) incorporated multiple design requirements into a multiobjective programming problem using a new formulation based on the constraint approach and Liu et al. (2013) utilized a PBD approach for a multiobjective optimization using genetic algorithm subjected to uncertainties and provided a set of Pareto-optimal designs.

None of prescriptive and PBD of structures has the capability to incorporate the economic issues in design process and commonly in engineering practice a design alternative with lower initial cost is normally preferred. Large economic losses following recent earthquakes and hurricanes encouraged researchers to introduce financial concerns in structural design area. The LCCA principles are based on economic theories and it was mainly implemented to energy and water conservation projects as well as transportation projects. However, LCCA has become an important part of structural engineering to assess the structural comeback and evaluate the performance of the structure during its life span in economic terms and has gained considerable attention of decision making centers to decide on the most cost-effective solution related to the construction of building structures in seismic regions. First, LCCA was applied in the commercial area

and in particular in the design of products. Later in early 2000s, as one of the impressive works in this area, Wen and Kang (2001a) formulated long-term benefit versus cost considerations for evaluation of the expected life-cycle cost of an engineering system under multiple hazards. Many works has been accomplished later to take the advantages of economic accounts in structural engineering. Liu, Burns, and Wen (2003) defined a multiobjective optimization problem and an automated design procedure to find optimal design alternatives with respect to three objectives. Static pushover analyses were performed to verify the performance of steel frame design alternatives and genetic algorithm was used. Takahashi, Kiureghian, and Ang (2004) formulated the expected life-cycle cost of design alternatives using a renewal model for the occurrence of earthquakes in a seismic source, which accounts for the temporal dependence between the occurrence of characteristic earthquakes and applied the methodology to an actual office building as a decision problem. Liu, Burns, and Wen (2005) formulated performance-based seismic design of steel frame structures as a multi-objective optimization problem considering the seismic risk in terms of maximum interstory drift. Fragiadakis, Lagaros, and Papadrakakis (2006) used pushover analysis to compare single objective optimal design of minimizing the initial weight and a performance-based two objective designs of a steel moment resisting frame; in particular a framework to generate a Pareto front of the solutions were presented. Kappos and Dimitrakopoulos (2008) used cost benefit and life-cycle cost analyses as decision making tools to examine the feasibility of strengthening reinforced concrete buildings. Mitropoulou, Lagaros, and Papadrakakis (2010) probed the influence of the behavior factor in the final design of reinforced concrete buildings under earthquake loading in terms of safety and economy by demonstrating initial and damage cost components for each design. Mitropoulou, Lagaros, and Papadrakakis (2011) investigated the effect of the analysis procedure, the number of seismic records imposed, the performance criterion used, and the structural type on the life-cycle cost analysis of 3D reinforced concrete structures. Furthermore, the influence of uncertainties on the seismic response of structural systems and their impact on LCCA is examined using Latin hypercube sampling method.

9.3 ENDURANCE TIME METHOD

ET excitation functions are in the form of artificial accelerograms created in such a way that each time window of them from zero to a particular time produces a response spectrum that matches a template spectrum

with a scale factor which is an increasing function of time. This interesting characteristic has been achieved by resorting to numerical optimization procedures in producing ET accelerograms (Nozari and Estekanchi 2011). Various sets of ET acceleration functions have been produced with different template response spectra and are publicly available through the website of ET method (ET method website 2014). A typical ET accelerogram used in this work, ETA40h, is depicted in Figure 9.1. These records are optimized to fit average response spectrum of seven records (longitudinal accelerograms) used in FEMA-440 for soil type (C) as template spectrum.

As can be seen in Figure 9.2, the response spectrum of a window from $t_{ET} = 0$ to $t_{ET} = 10$ sec of used accelerogram matches with the template spectrum. Furthermore, the produced response spectra also match

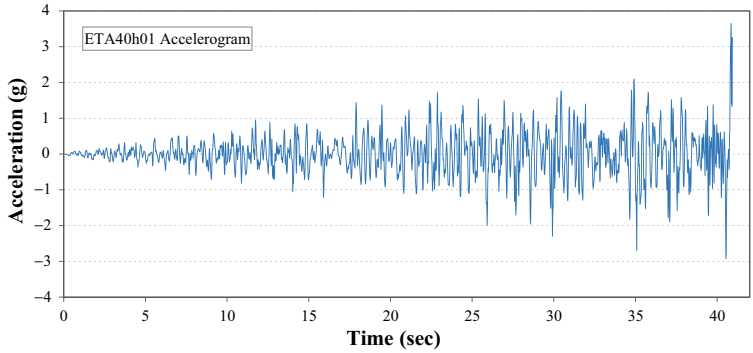

Figure 9.1. Acceleration function for ETA40h01.

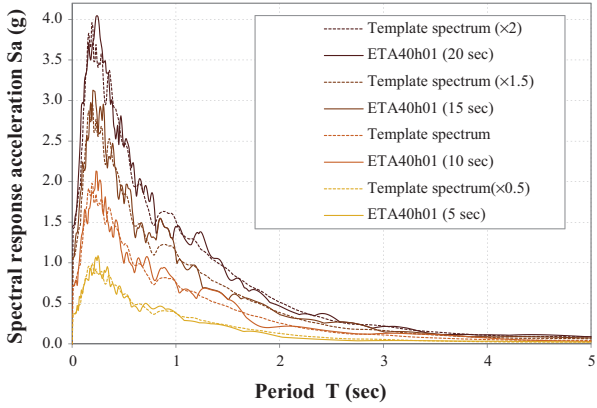

Figure 9.2. Acceleration response spectra for ETA40h01 at different times of excitation.

the template spectrum at all other times with a scale factor, thus producing a correlation between analysis time and induced spectral intensity. Hence, each ET analysis time is representative of a particular seismic intensity and results can be more effectively presented by considering a correlation between time in ET analysis and the equivalent hazard return period based on code recommendations considering the fact that hazard levels are well presented by acceleration response spectra in current codes. This can result in an appropriate baseline to calculate probabilistic damage and cost.

The application of the ET method in PBD was studied by Mirzaee et al. (2010) introducing "Performance Curve" and the "Target Curve," which expresses respectively the seismic performance of a structure along various seismic intensities and their limiting values according to code recommendations. Substituting return period or annual probability of exceedance for time in the expression of the performance will make the presentation of the results more explicit and their convenience for calculate probabilistic cost will be increased.

Hazard return period corresponding to a particular time in ET analysis can be calculated by matching the response spectra at effective periods, for example, from 0.2 to 1.5 times of structure's fundamental period of vibration. The procedure is based on the coincidence of response spectra obtained from the ET accelerogram at different times and response spectra defined for Tehran at different hazard levels. The results show that substitution of the return period for time in ET analysis and performance curves increases the usefulness of these curves and can simplify application of the ET method in value-based design. Figures 9.3 and 9.4 illustrate the

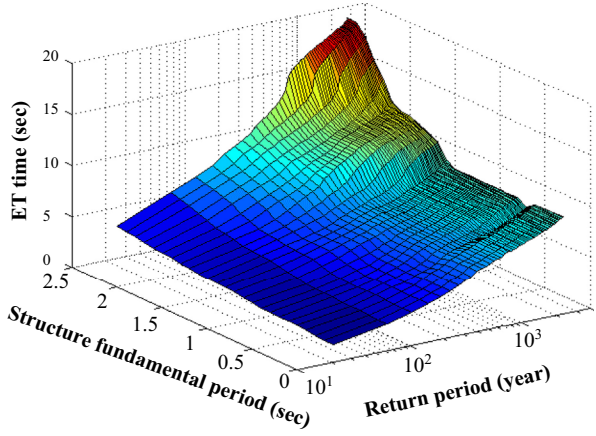

Figure 9.3. Return period vs. structural period and ET analysis time.

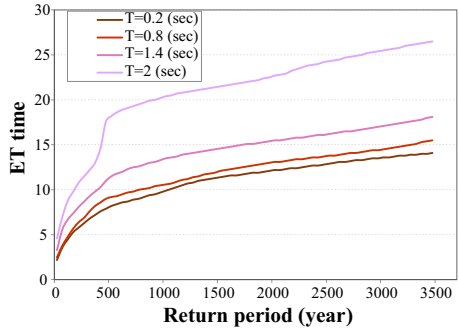

Figure 9.4. Equivalent ET analysis time vs. hazard return period for different structural periods.

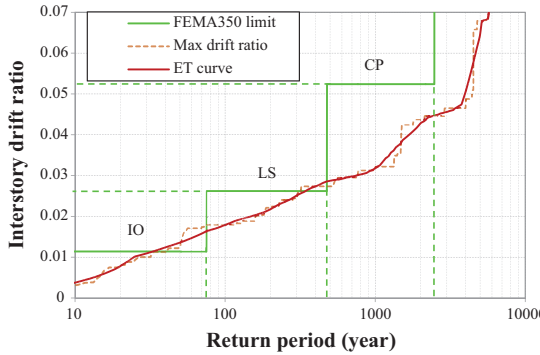

Figure 9.5. A sample performance curve (ET curve) for the steel frame.

variation of the return period with the structural period and time in ET analysis. Using this correlation for a specific structure the corresponding ET time for each hazard level is on hand. The detailed procedure to obtain such a correlation is explained in a work by Mirzaee, Estekanchi, and Vafai (2012).

In Figure 9.5 a sample target curve and performance curve for the five-story structure is depicted where ET analysis time has been mapped into return period on horizontal axis. As it can be seen the structure satisfies the code collapse prevention (CP) level limitations but it has violated the immediate occupancy (IO) and life safety (LS) levels limitations and the frame does not have acceptable performance. Also, moving average is applied to smooth ET results for interstory drift envelope curve. It can be inferred one of advantages of ET method that the performance of the structure in continuous increasing hazard levels can be properly depicted in an easy to read figure.

9.4 PRESCRIPTIVE SEISMIC DESIGN

Commonly in prescriptive seismic design procedures the structure is considered safe if it satisfies a number of checks in one or two deterministically expressed limit states (i.e., ultimate strength and serviceability). Also, the structures are allowed to absorb energy through inelastic deformation by designing them with reduced loading specified by the behavior factor leading to smaller seismic loads.

Prescriptive design of the understudy structure has been accomplished according to the Iranian National Building Code (INBC), which is almost identical to the ANSI/AISC360-10 LRFD design recommendations. The prototype structure is a five-story and one-bay special moment resisting steel frame. All supports are fixed and the joints are all rigid. The beams and columns are selected among seismically compact standard W profiles according to Table 9.1. The geometry of this model can be found in Figure 9.6. Loading is set according to INBC Section 6. The steel material considered has the property as yielding stress of F_y = 235.36 MPa, elastic modulus of E = 200 GPa. The strong column-weak beam design requirement has been considered in design of the structure. According to Iranian seismic design code seismic loading base shear is determined upon design response spectrum of the 475 years return period hazard level and the elastic base shear is reduced by a behavior factor (R) to incorporate the inelastic deformation capacity of the special moment frame. In this section, it has been tried to accomplish the design procedure in the same way as the procedure in common engineering practice. Demand and capacity ratios are depicted in Figure 9.6. As can be seen in this figure in some elements other limitations such as drift limits or strong column-weak beam limitation is dominant.

The seismic performance of the prescriptive design has been investigated according to FEMA-350 limitations on interstory drift ratios. The procedure and recommended limitations are explained in next section. Performance Curve and also Target Curve for this structure is depicted in Figure 9.7. It can be verified that the structure has violated IO level limitation but has a proper performance in LS and CP levels.

9.5 PERFORMANCE-BASED DESIGN

Prescriptive design procedures do not assure reliable performance of the structure in multiple hazard levels during its life span, since these procedures merely intend to keep the ultimate strength of structural members

Table 9.1. List of beams and columns alternative section properties

Beams	W18 × 35	W18 × 40	W18 × 46	W18 × 50	W18 ×55	W18 ×60	W18 ×65	W18 ×71						
Side columns	W10 × 39	W10 × 45	W10 × 54	W10 × 60	W10 ×68	W10 ×77	W10 ×88	W10 ×100	W10 ×112					
Inner columns	W12 × 79	W12 × 87	W12 × 96	W12 × 106	W12 × 120	W12 × 136	W12 × 152	W12 × 170	W12 × 190	W12 × 210	W12 × 230	W12 × 252	W12 × 279	W12 × 305

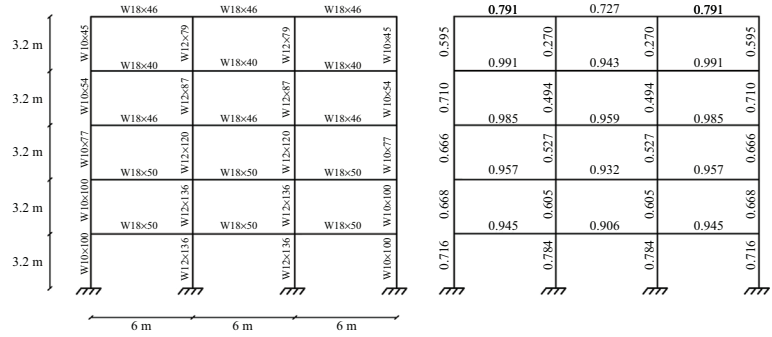

Figure 9.6. Schematics of steel frames under investigation and demand/capacity ratios according to prescriptive design criteria.

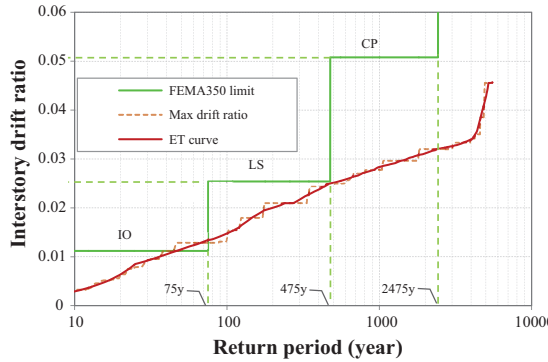

Figure 9.7. Performance curve (ET curve) for the prescriptive design.

at an acceptable level. Compared to these procedures PBD has provided a more general structural design philosophy in which the design criteria are expressed in terms of achieving multiple performance requirements when the structure is subjected to various seismic hazard levels. In most of currant PBD criteria the structural performance of an ordinary building frame is usually defined as: (1) resist a significant accidental earthquake without structural damage, (2) allow repairable structural damage against a rare major earthquake, and (3) resist the maximum credible earthquake without collapse (Pan et al. 2007). The performance measures may include the response stresses, the maximum load carrying capacity, the interstory drift or the plastic rotation at members, and so on. In the most common approaches to PBD, the performances against seismic motions are defined based on the displacements or global deformation. Various methods of structural assessment have been used by researchers and also

engineers. Especially push-over analysis is widely being used in this area; however, time history analysis is so far believed to be the most accurate methodology for evaluating structural performance. In order to satisfy performance-based measures in design procedure and achieve a safe yet economical design, utilizing optimization methods is inevitable. Merits of ET method in optimum PBD and its methodology are introduced in a work by Estekanchi and Basim (2011).

The PBD procedure implemented in this work is based on the method introduced in FEMA-350 (2000). This criterion supplies a probability-based guideline for PBD of new steel moment resisting frames, in which the ground motion variability and the uncertainty in the structural analysis are considered explicitly. FEMA-350 considers two discrete structural performance levels, CP and IO by introducing the limiting damage states for common framing elements related to these performance levels and acceptance criteria are related to the permissible interstory drifts and earthquake-induced forces for the various elements especially in columns. Interstory drift ratio is a commonly used measure of both structural and nonstructural damage because of its close relationship to plastic rotation demands on individual beam-column connection assemblies. As recommended in these criteria other structural performance levels can be determined on a project-specific basis, by interpolation or extrapolation from the criteria provided for the two performance levels. For the purpose of this work LS performance level have been used by interpolating the IO and CP levels. LS level is a damage state in which significant damage has been sustained, although some margin remains against either partial or total collapse. The considered performance objective in this study assuming "seismic use group I" for the prototype special moment frame structure is IO, LS, and CP performance levels corresponding to ground motion levels of 50, 10, and 2 percent probability of being exceeded in 50 years, respectively.

Many uncertain factors exist that affect the behavior and response of a building such as uncertainties in seismic hazard due to the attenuation laws employed, record to record variability or on the other hand uncertainties in structural modeling due to simplifications and assumptions used in the numerical analysis (Liu, Atamturktur, and Juang 2013). Therefore, FEMA-350 adopts a reliability-based probabilistic approach to performance evaluation that explicitly acknowledges these inherent uncertainties. These uncertainties are expressed in terms of a confidence level. A high level of confidence means that the building will very likely be capable of meeting the desired performance. Considering a minimum confidence level of 70 and 90 percent for IO and CP performance levels, respectively, the upper bound limit for calculated interstory drift demand

obtained from structural analysis would be 0.0114 and 0.0524 and interpolation will result in an upper bound of 0.0262 for LS level.

Structural analysis has been performed by OpenSees (Mazzoni et al. 2006) where the nonlinear behavior is represented using the concentrated plasticity concept with zerolength rotational springs and structural elements are modeled using elastic beam-column elements. The rotational behavior of the plastic regions follows a bilinear hysteretic response based on the Modified Ibarra Krawinkler Deterioration Model (Ibarra, Medina, and Krawinkler 2005; Lignos and Krawinkler 2010). Second order effects have been considered using P-Delta Coordinate Transformation object embedded in the platform. To capture panel zone shear deformations, panel zones are modeled using the approach of Gupta and Krawinkler (1999) as a rectangle composed of eight very stiff elastic beam-column elements with one zerolength rotational spring in the corner to represent shear distortions in the panel zone.

In this section, a single objective optimization problem is defined to find a design having the minimum initial steel material weight as optimization objective and according to FEMA-350 recommendations, as PBD criteria, the limitations on interstory drift demand and axial compressive load on columns and also strong column weak beam criterion as optimization constrains. The design variables are the steel section sizes selected among standard W sections. As indicated in FEMA-350, structures should, as a minimum, be designed in accordance with the applicable provisions of the prevailing building code such as specifications of AISC360 (2010) and AISC341 (2010). Thus, the AISC360 requirements and FEMA-350 acceptance criteria are implemented as design constraints. Optimum design sections have been determined using GA algorithm adopted for PBD purposes using ET method introduced in a work by Estekanchi and Basim (2011). The acquired design sections can be found in Figure 9.8. Performance of the structure in various seismic intensities can be investigated using ET curve presented in Figure 9.9. Eventually, an optimum design will meet the constraints (i.e., code requirements) with the least margins.

9.6 VALUE-BASED DESIGN

While value can be defined and considered in its broad sense for design purposes, for the clarity of explanation, in this research we consider the structure that is more economical to construct and maintain, to be the most valued. ET analysis provides a versatile baseline to perform economic

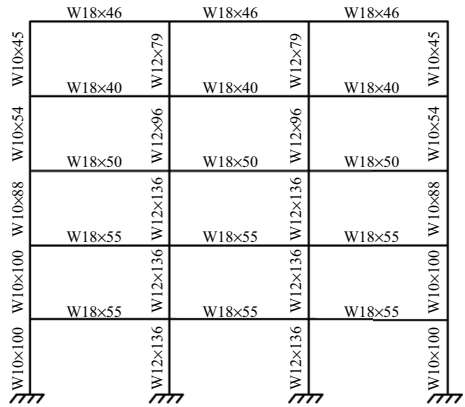

Figure 9.8. Performance-based design sections of the frame.

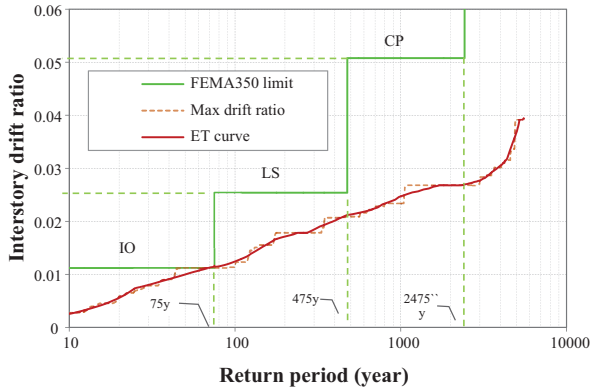

Figure 9.9. Performance curve (ET curve) for the performance-based design.

analyses on design alternatives with acceptable computational cost. Initial construction cost and expected seismic damage cost throughout the life time of the structure are usually the two most important parameters for decision making (Mitropoulou, Lagaros, and Papadrakakis 2011). One of the major obstacles in seismic damage cost assessment of structures is response estimation of structures subject to ground motions in multiple intensities. Various simplified procedures for seismic analyses have been used by researchers in order to overcome huge computational demand involved in assessment of several design alternatives. Nevertheless, cost assessment has been mostly used in comparative study among limited number of design alternatives and incorporation of life-cycle cost directly in design process has attracted the attention of researchers (Mitropoulou, Lagaros, and Papadrakakis 2011; Kaveh, Laknejadi,

and Alinejad 2012; Frangopol, Strauss, and Bergmeister 2009). Push-over analysis has been widely used as seismic assessment tool in this area. However, well-known limitations of this analytical tool besides its disability in properly estimating nonstructural cost components due to floor acceleration have increased the need for more realistic and reliable dynamic analysis procedures with a tolerable computational demand. In this section, ET analysis has been used to estimate seismic response of the structure and the procedure to calculate the required cost components has been formulated.

The total cost C_{TOT} of a structure can be considered as the sum of its initial construction cost C_{IN} which is function of design vector s and the present value of the life-cycle cost C_{LN} which is function of life time t and the design vector s (Mitropoulou, Lagaros, and Papadrakakis 2011):

$$C_{TOT}(t, s) = C_{IN}(s) + C_{LC}(t, s) \tag{1}$$

9.6.1 INITIAL COSTS

Initial cost is the construction cost of a new structure or the rehabilitation cost of an existing facility. In our design example which is a new moment resisting steel frame the initial cost is related to the land price, material, and the labor cost for the construction of the building. As the land price and nonstructural components cost are constant for all design alternatives they can be eliminated from the total cost calculation and the initial steel weight of the structure with a labor overhead can be considered as representor of the initial cost. So, an initial cost equal to \$500 per m^2 over the 700 m^2 total area of the structure for the prescriptive design is considered and for other design alternatives, it will be calculated according to their steel weight difference by a material plus labor cost of 2\$/kg.

9.6.2 LIFE-CYCLE COST

Life-cycle cost in this study refers to the consequent costs resulting from earthquakes that may occur during the life time of the structure. Based on the recent literature, multiple limit states according to interstory drift ratio are considered. These limit states and damages depend on the performance of both structural and nonstructural components. In order to calculate the life-cycle cost of the structure following cost components are involved: the damage repair cost, the cost of loss of contents due to structural damage quantified by the maximum interstory drift and also floor acceleration,

the loss of rental cost, the loss of income cost, the cost of injuries, and the cost of human fatalities (Mitropoulou, Lagaros, and Papadrakakis 2010; Wen and Kang 2001b).

A correlation is required to quantify these losses in economic terms. Several damage indices have been used to quantify seismic performance of structures. Commonly, interstory drift (Δ) has been considered as a measure of both structural and nonstructural damage. In this study, seven limit states according to drift ratios based on ATC-13 (1985) is used to describe structural performance as shown in Table 9.2. On the other hand, maximum floor acceleration is used to quantify the loss of contents. The relation between floor acceleration values and damage states are shown in Table 9.2 based on a work by Elenas and Meskouris (2001). The addition of the maximum floor acceleration component in life-cycle cost calculation is introduced by Mitropoulou, Lagaros, and Papadrakakis (2010). Piecewise linear relation has been assumed in order to establish a continuous relation between damage indices and costs (Mirzaee and Estekanchi 2013).

Expected annual cost is found to be the most proper intermediate parameter to calculate life-cycle cost of structures using ET method. The procedure and formulation whose validity is investigated by Kiureghian (2005) to be used in ET framework is described here in detail.

A common framework for performance-based earthquake engineering, used by researchers at the Pacific Earthquake Engineering Research (PEER) Center, can be summarized by Equation (2) named as PEER framework formula. By the use of this formula the mean annual rate (or annual frequency) of events (e.g., a performance measure) exceeding a specified threshold can be estimated (Kiureghian 2005).

Table 9.2. Drift ratio and floor acceleration limits for damage states

Performance level	Damage states	Drift ratio limit (%) ATC-13 (1985)	Floor acceleration limit (g) (Elenas and Meskouris 2001)
I	None	$\Delta \leq 0.2$	$a_{floor} \leq 0.05$
II	Slight	$0.2 < \Delta \leq 0.5$	$0.05 < a_{floor} \leq 0.10$
III	Light	$0.5 < \Delta \leq 0.7$	$0.10 < a_{floor} \leq 0.20$
IV	Moderate	$0.7 < \Delta \leq 1.5$	$0.20 < a_{floor} \leq 0.80$
V	Heavy	$1.5 < \Delta \leq 2.5$	$0.80 < a_{floor} \leq 0.98$
VI	Major	$2.5 < \Delta \leq 5$	$0.98 < a_{floor} \leq 1.25$
VII	Destroyed	$5.0 < \Delta$	$1.25 < a_{floor}$

$$\lambda(dv) = \int_{dm}\int_{edp}\int_{im} G(dv \mid dm) \mid dG(dm \mid edp) \mid\mid dG(edp \mid im) \mid\mid d\lambda(im) \quad (2)$$

where:

im: an intensity measure (e.g., the peak ground acceleration or spectral intensity)

edp: an engineering demand parameter (e.g., an interstory drift)

dm: a damage measure (e.g., the accumulated plastic rotation at a joint)

dv: a decision variable (e.g., Dollar loss, duration of downtime)

Here $G(x \mid y) = P(x < X \mid Y = y)$ denotes the Conditional Complementary Cumulative Distribution Function (CCDF) of random variable X given $Y = y$, and $\lambda(x)$ is the mean rate of $\{x < X\}$ events per year. All of the aleatory and epistemic uncertainties present in describing the model of the structure and its environment and also stochastic nature of earthquakes can be properly modeled in this formula. It should be noted that the deterioration of the structure has been ignored and it has been assumed that it is instantaneously restored to its original state after each damaging earthquake. Another fundamental assumption made is that, conditioned on *EDP*, *DM* is independent of *IM*, and, conditioned on *DM*, *DV* is independent of *EDP* and *IM*. The later assumption makes it possible to decompose the earthquake engineering task into subtasks presented in Figure 9.10. Note that the ET method is used in response analysis box in this flowchart and will create a proper baseline to calculate the following boxes.

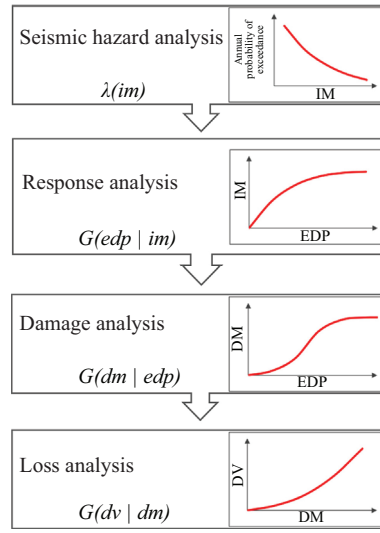

Figure 9.10. Performance-based earthquake engineering framework (Yang, Moehle, and Stojadinovic 2009).

By considering various cost components as decision variable dv and using Equation (2), $\lambda(dv)$ the annual rate that the cost component values (DV) exceeds certain value dv can be obtained. Results can be presented by a curve with cost values dv in horizontal axis and annual rate of exceedance as vertical axis known as "Loss Curve" (Yang, Moehle, and Stojadinovic 2009).

For a variable X, the differential quantity $\left|\lambda(x+dx)-\lambda(x)\right| \cong \left|d\lambda(x)\right|$ describes the mean number of events $\{x < X \leq x + dx\}$ per year. Thus, assuming X is non-negative, its expected cumulative value in one year is

$$E[\Sigma X] = \int_0^\infty x \,|\, d\lambda(x) \,| = \int_0^\infty \lambda(x)\, dx \tag{3}$$

It can be inferred that, the area underneath the $\lambda(x)$ versus x curve gives the mean cumulative value of X for all earthquake events occurring in one year time. Therefore, in our problem where x is the cost component values as decision variable, the area under $\lambda(dv)$ versus dv curve (i.e., Loss Curve) represents the mean cumulative annual considered component cost for all earthquake events in one year.

As a practical procedure, Loss Curve can be acquired from ET curve mentioned previously. Here, the annual probability of exceedance of drift ratios should be determined. By reversing the return period on the x-axis to obtain the mean annual rate of exceedance and using it on the y-axis, the annual rate of exceedance of the interstory drift can be obtained. If the interstory drift is replaced by component cost applying the linear relationship discussed previously using Table 9.2, the annual rate of exceedance for component can be obtained. This curve is the Loss Curve being sought. A Loss Curve due to floor acceleration can be easily obtained similarly. In Figure 9.11 a sample loss curve due to damage cost is depicted. The area under the loss curve represents the mean annual component cost caused by all earthquakes in one year.

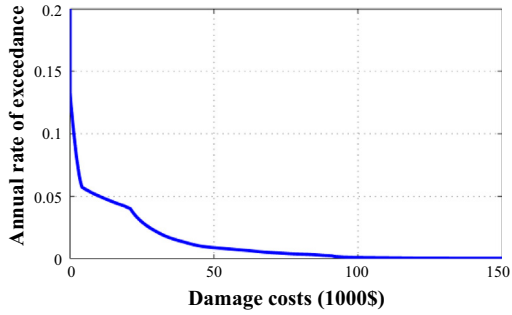

Figure 9.11. A sample loss curve due to damage cost.

As it mentioned life-cycle cost consists of several components and can be calculated as follows:

$$C_{LC} = C_{dam} + C_{con} + C_{ren} + C_{inc} + C_{inj} + C_{fat} \tag{4}$$

$$C_{con} = C_{con}^{\Delta} + C_{con}^{acc} \tag{5}$$

where C_{dam} = the damage repair cost; C_{con}^{Δ} = the loss of contents cost due to structural damage quantified by interstory drift; C_{con}^{acc} = the loss of contents cost due to floor acceleration; C_{ren} = the loss of rental cost; C_{inc} = the cost of income loss; C_{inj} = the cost of injuries and C_{fat} = the cost of human fatality. Formulas to calculate each cost component can be found in Table 9.3. The first term of each formula is presented in the last column of the table as the basic cost. The values of the mean damage index, loss of function, downtime, expected minor injury rate, expected serious injury rate and expected death rate used in this study are based on ATC-13 (1985)

Table 9.3. Formulas for cost components calculation in dollars (Mitropoulou, Lagaros, and Papadrakakis 2011; Wen and Kang 2001a; ATC-13 1985)

Cost component	Formula	Basic cost
Damage repair (C_{dam})	Replacement cost × floor area × mean damage index	400$/m^2
Loss of contents (C_{con})	Unit contents cost × floor area × mean damage index	150$/m^2
Loss of rental (C_{ren})	Rental rate × gross leasable area × loss of function time	10$/month/m^2
Loss of income (C_{inc})	Income rate × gross leasable area × down time	300$/year/m^2
Minor injury ($C_{inj,\,m}$)	Minor injury cost per person × floor area × occupancy rate × expected minor injury rate	2,000$/person
Serious injury ($C_{inj,\,s}$)	Serious injury cost per person × floor area × occupancy rate × expected serious injury rate	20,000$/ person
Human fatality (C_{fat})	Human fatality cost per person × floor area × occupancy rate × expected death rate	300,000$/ person

restated in FEMA-227 (1992). Table 9.4 provides these parameters for each damage state. Loss of function time and down time are considered as the time required to recover the full functionality of the building based on a table from ATC-13 (1985) for earthquake engineering facility classification 16 and medium rise moment resisting steel frame. Also, occupancy rate is taken 2 persons per 100 m^2. Note that these are an estimation of cost components and a detailed assessment is necessary to evaluate the expected cost. The method, with no limitation, has the capability of incorporating detailed calculation on cost components.

According to Equation (1) the total life-cycle cost is considered as the sum of the initial construction costs and the present value of the annual damage costs summed up through the life time of the structure. A discount rate equal to 3 percent over a 50 years life of the building has been considered to transform the damage costs to the present value and calculate the expected damage cost of the structure in its life time. This total cost is used as the objective function in optimization algorithm and a design with the lowest total cost is being sought. Due to capabilities of genetic algorithm this design is the global optimum alternative with a high chance.

As the previous sections, genetic algorithm (GA) has been used to find the optimum design. Alternative designs should meet some initial constraints. One of the constraints is strong column and weak beam criterion which should be checked and the other constraint that should be considered before the analysis phase is that the selected sections for columns in each story should not be weaker than the upper story. Beside these constraints, all AISC360 checks must be satisfied for the gravity loads. Once the expressed constraints are satisfied, the LCC (Life Cycle Cost) analysis is performed. It is important to note that each of these feasible organisms is acceptable design according to the code ignoring seismic actions. But, in order to reach the optimum solution, algorithm will reproduce new design alternatives based on the initial population and mutate until the stop criteria is met. The flowchart of the applied methodology is presented in Figure 9.12.

Genetic algorithm with an initial population size of 200 leads to an optimum design after about 2,600 ET response history analyses. Total costs for feasible design alternatives in optimization procedure are depicted in Figure 9.13. The optimum design sections are presented in Figure 9.14 and its performance in various seismic intensities (i.e., ET curve) is presented in Figure 9.15. It can be seen that the structure satisfies performance limitations of FEMA-350 with a margin that is justified by economic concerns.

Table 9.4. Damage state parameters for cost calculations (ATC-13 1985; FEMA-227 1992)

Damage states	Mean damage index (%)	Expected minor injury rate	Expected serious injury rate	Expected death rate	Loss of function time (days)	Down time (days)
(I)-None	0	0	0	0	0	0
(II)-Slight	0.5	0.00003	0.000004	0.000001	1.1	1.1
(III)-Light	5	0.0003	0.00004	0.00001	16.5	16.5
(IV)-Moderate	20	0.003	0.0004	0.0001	111.8	111.8
(V)-Heavy	45	0.03	0.004	0.001	258.2	258.2
(VI)-Major	80	0.3	0.04	0.01	429.1	429.1
(VII)-Destroyed	100	0.4	0.4	0.2	612	612

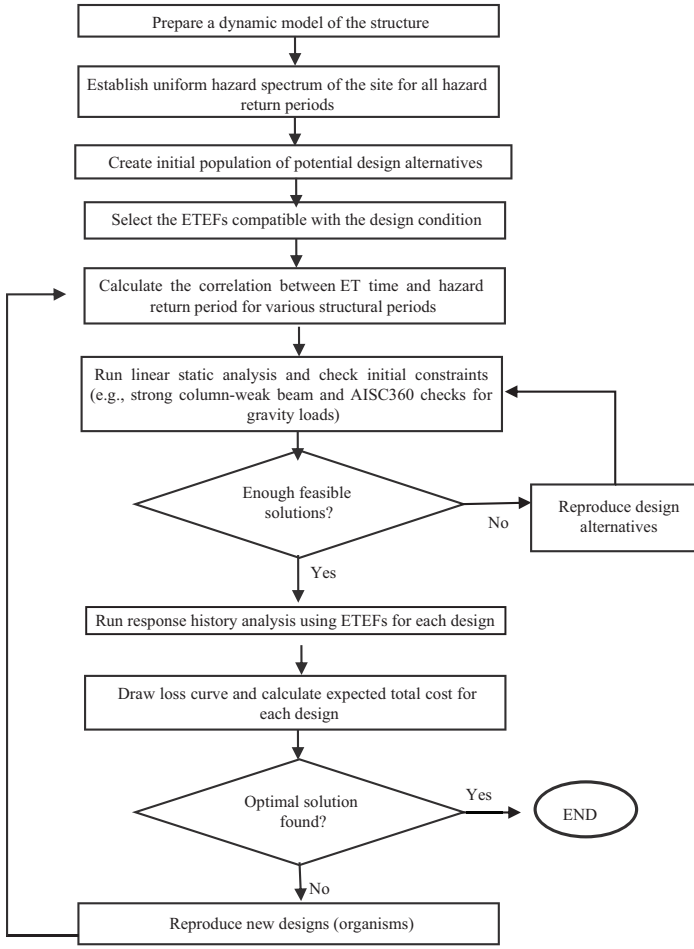

Figure 9.12. Flowchart of the value-based design by the ET method.

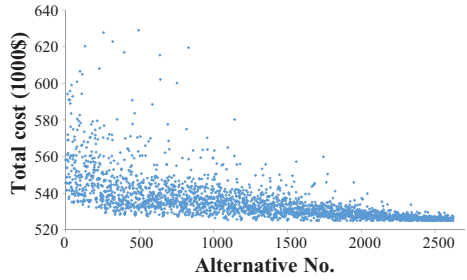

Figure 9.13. Total costs for feasible design alternatives in optimization procedure.

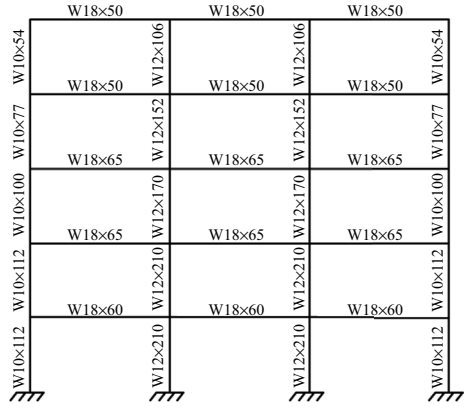

Figure 9.14. Value-based design sections of the frame.

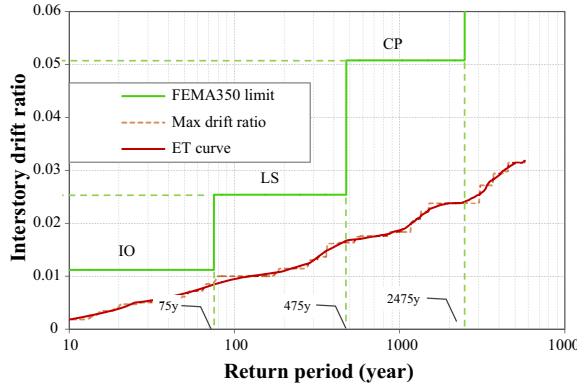

Figure 9.15. Performance curve (ET curve) for the value-based design.

9.7 COMPARATIVE STUDY

In this section, components of life-cycle cost for the three structures (i.e., prescriptive, performance-based, and value-based designs) are compared. These structures are design optimally based on various design philosophies. In Figure 9.16 cost components for the three structures are provided in $1,000. Each bar presents contribution of various cost components and the value of total cost for each design can be found above the bars. Components in bars are in the same order as the legend. As it can be seen, the prescriptive design has the least initial cost but the largest total cost among three and the value-based design having a larger initial cost has the

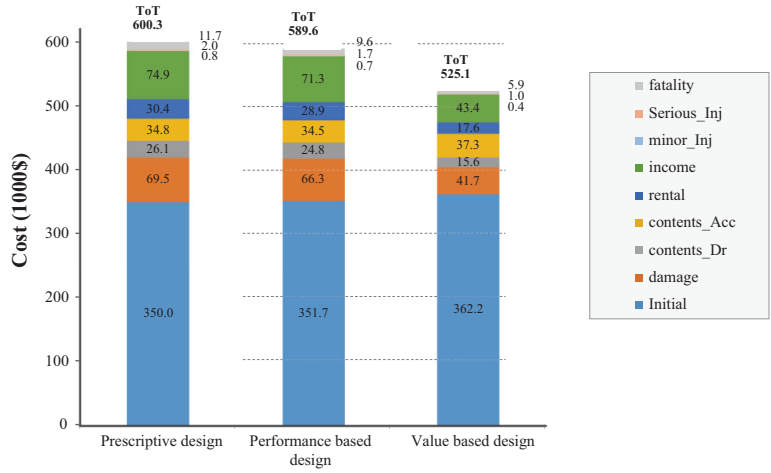

Figure 9.16. Cost components and total cost for the three designs ($1,000).

Table 9.5. Values of life-cycle cost terms for the three designs ($1,000)

Design type	Initial cost	Life-cycle cost	Total cost
Prescriptive	350	250.3	600.3
Performance based	351.7	237.9	589.6
Value based	362.2	162.9	525.1

least total cost in long term. Also, the value-based design has a larger cost of content loss due to floor acceleration. It may reaffirm the sophistications involved in selecting a desired design alternative. In Table 9.5 initial costs based on used initial material, present value of life-cycle costs due to seismic hazards with various exceedance probabilities and the determinative part that is, total cost of three structures are presented. It can be verified that a value-based design has the least total cost and would be an economical alternative in long term. An increase of $12,200 in initial material cost over the prescriptive design will lead to a decrease of $87,400 in expected life-cycle cost having totally $75,200 profit. Although PBD has a minor expected total cost in comparison with the prescriptive design, neither the prescriptive design criteria nor the performance based one will necessarily lead to an economical design in long term.

9.8 SUMMARY AND CONCLUSIONS

A framework for direct use of the concept of value in the structural design procedure incorporating the benefits of ET method has been established. Application of the ET analysis in LCCA has been formulated. ET method

and resultant performance curve has provided a proper baseline to calculate expected damage cost, while the required computational effort is in an acceptable range to be used in conventional optimization techniques. To demonstrate the method and compare it with prescriptive and PBD criteria, a five-story moment frame has been optimally designed according to three distinct design philosophies: a prescriptive design code, a PBD guideline and also the introduced methodology namely value-based design of structures. Structural performance and life-cycle cost components for the three structures have been compared. The resultant prescriptive, performance-based and value-based designs of the frame are different due to their distinct basic design philosophies. Results show that the code-based design of the structure will not necessarily result in an economical design with lower total cost in life time of the structure. PBD in this case turns out to require higher initial material cost in comparison with the prescriptive design due to its more restricting limitations, and as expected, better performance in various hazard intensities. The value-based design, however, demands the highest initial material cost, yet the least total cost among three, justifying the increased initial cost. The proposed methodology provides a pathway toward practical value-based seismic design. It also shows that conventional design procedures based on compliance to design code requirements or performance objectives do not assure achievement of the best final design regarding the overall applicable design values.

NOMENCLATURE

a_{floor}	Floor acceleration
ATC	Applied technology council
CCDF	Conditional complementary cumulative distribution function
CP	Collapse prevention
C_{con}	Loss of contents cost
C_{con}^{acc}	Loss of contents cost due to floor acceleration
C_{con}^{Δ}	Loss of contents cost due to interstory drift
C_{dam}	Damage repair cost
C_{fat}	Cost of human fatality
C_{inc}	Loss of income cost
C_{inj}	Cost of injuries
$C_{inj,\,m}$	Cost of minor injuries
$C_{inj,\,s}$	Cost of serious injuries
C_{ren}	Loss of rental cost
C_{IN}	Initial cost

C_{LC}	Life-cycle cost
C_{TOT}	Total cost
dm	A damage measure threshold
dv	A decision variable threshold
DM	Damage measure
DV	Decision variable
edp	An engineering demand parameter threshold
E	Elastic modulus
EDP	Engineering demand parameter
ET	Endurance time
ETEF	Endurance time excitation function
FEMA	Federal emergency management agency
F_y	Yielding stress
g	Acceleration of gravity
GA	Genetic algorithm
im	An intensity measure threshold
IDA	Incremental dynamic analysis
IM	Intensity measure
IO	Immediate occupancy
INBC	Iranian National Building Code
LCCA	life-cycle cost analysis
LRFD	load resistance factor design
LS	life safety
PBD	Performance-based design
PEER	Pacific earthquake engineering research center
R	Pehavior factor
s	Design vector
t	Life time of structure
t_{ET}	ET excitation time
VBD	value-based design
Δ	Interstory drift ratio

REFERENCES

AISC 341. 2010. *Seismic Provisions for Structural Steel Buildings (ANSI/AISC 341-10)*. Chicago, IL: American Institute of Steel Construction.

AISC 360. 2010. *Specification for Structural Steel Buildings (ANSI/AISC 360-10*). Chicago, IL: American Institute of Steel Construction.

ATC-13. 1985. *Earthquake Damage Evaluation Data for California*. Applied Technology Council.

Elenas, A., and K. Meskouris. 2001. "Correlation Study Between Seismic Acceleration Parameters and Damage Indices of Structures." *Engineering Structures* 23, no. 6, pp. 698–704.

Endurance Time Method Website. 2014. online. https://sites.google.com/site/etmethod/

Estekanchi, H., A. Vafai, and M. Sadeghazar. 2004. "Endurance Time Method for Seismic Analysis and Design of Structures." *Scientia Iranica* 11, no. 4, pp. 361–70.

Estekanchi, H.E., and M.C. Basim. 2011. "Optimal Damper Placement in Steel Frames by the Endurance Time Method." *The Structural Design of Tall and Special Buildings* 20, no. 5, pp. 612–30.

FEMA-227. 1992. *A Benefit–Cost Model for the Seismic Rehabilitation of Buildings.* Washington, DC: Federal Emergency Management Agency, Building Seismic Safety Council.

FEMA-350. 2000. *Recommended Seismic Design Criteria for New Steel Moment-Frame Buildings*. Washington, DC: Federal Emergency Management Agency.

Fragiadakis, M., N.D. Lagaros, and M. Papadrakakis. 2006. "Performance-Based Multiobjective Optimum Design of Steel Structures Considering Life-Cycle Cost." *Structural and Multidisciplinary Optimization* 32, no. 1, pp. 1–11.

Frangopol, D.M., A. Strauss, and K. Bergmeister. 2009. "Lifetime Cost Optimization of Structures by a Combined Condition–Reliability Approach." *Engineering Structures* 31, no. 7, pp. 1572–80.

Ganzerli, S., C. Pantelides, and L. Reaveley. 2000. "Performance-Based Design Using Structural Optimization." *Earthquake Engineering and Structural Dynamics* 29, no. 11, pp. 1677–90.

Gupta, A., and H. Krawinkler. 1999. "Seismic Demands for Performance Evaluation of Steel Moment Resisting Frame Structures." Technical Report 132. The John A. Blume Earthquake Engineering Research Center, Department of Civil Engineering, Stanford University.

Hariri-Ardebili, M., S. Sattar, and H. Estekanchi. 2014. "Performance-Based Seismic Assessment of Steel Frames Using Endurance Time Analysis." *Engineering Structures* 69, pp. 216–34.

Ibarra, L.F., R.A. Medina, and H. Krawinkler. 2005. "Hysteretic Models that Incorporate Strength and Stiffness Deterioration." *Earthquake Engineering and Structural Dynamics* 34, no. 12, pp. 1489–511.

Kappos, A.J., and E. Dimitrakopoulos. 2008. "Feasibility of Pre-Earthquake Strengthening of Buildings Based on Cost-Benefit and Life-Cycle Cost Analysis, with the Aid of Fragility Curves." *Natural Hazards* 45, no. 1, pp. 33–54.

Kaveh, A., K. Laknejadi, and B. Alinejad. 2012. "Performance-Based Multi-Objective Optimization of Large Steel Structures." *Acta Mechanica* 223, no. 2, pp. 355–69.

Kiureghian, A.D. 2005. "Non-ergodicity and PEER's Framework Formula." *Earthquake Engineering and Structural Dynamics* 34, no. 13, pp. 1643–52.

Lignos, D.G., and H. Krawinkler. 2010. "Deterioration Modeling of Steel Components in Support of Collapse Prediction of Steel Moment Frames Under Earthquake Loading." *Journal of Structural Engineering* 137, no. 11, pp. 1291–302.

Liu, M., S.A. Burns, and Y. Wen. 2003. "Optimal Seismic Design of Steel Frame Buildings Based on Life Cycle Cost Considerations." *Earthquake Engineering and Structural Dynamics* 32, no. 9, pp. 1313–32.

Liu, M., S.A. Burns, and Y. Wen. 2005. "Multiobjective Optimization for Performance-Based Seismic Design of Steel Moment Frame Structures." *Earthquake Engineering and Structural Dynamics* 34, no. 3, pp. 289–306.

Liu, Z., S. Atamturktur, and C.H. Juang. 2013. "Performance Based Robust Design Optimization of Steel Moment Resisting Frames." *Journal of Constructional Steel Research* 89, pp. 165–74.

Mazzoni, S., F. McKenna, M.H. Scott, G.L. Fenves, and B. Jeremic. 2006. *Open System for Earthquake Engineering Simulation (OpenSees)*. Berkeley, California.

Mirzaee, A., H. Estekanchi, and A. Vafai. 2010. "Application of Endurance Time Method in Performance-Based Design of Steel Moment Frames." *Scientia Iranica* 17, pp. 361–70.

Mirzaee, A., H. Estekanchi, and A. Vafai. 2012. "Improved Methodology for Endurance Time Analysis: from Time to Seismic Hazard Return Period." *Scientia Iranica* 19, no. 5, pp. 1180–7.

Mirzaee, A., and H.E. Estekanchi. 2013. "Performance-Based Seismic Retrofitting of Steel Frames by Endurance Time Method." *Earthquake Spectra*. online. http://dx.doi.org/10.1193/081312EQS262M

Mitropoulou, C.C., N.D. Lagaros, and M. Papadrakakis. 2010. "Building Design Based on Energy Dissipation: A Critical Assessment." *Bulletin of Earthquake Engineering* 8, no. 6, pp. 1375–96.

Mitropoulou, C.C., N.D. Lagaros, and M. Papadrakakis. 2011. "Life-Cycle Cost Assessment of Optimally Designed Reinforced Concrete Buildings Under Seismic Actions." *Reliability Engineering & System Safety* 96, no. 10, pp. 1311–31.

Nozari, A., and H. Estekanchi. 2011. "Optimization of Endurance Time Acceleration Functions for Seismic Assessment of Structures." *International Journal of Optimization in Civil Engineering* 1, no. 2, pp. 257–77.

Pan, P., M. Ohsaki, and T. Kinoshita. 2007. "Constraint Approach to Performance-Based Design of Steel Moment-Resisting Frames." *Engineering Structures* 29, no. 2, pp. 186–94.

Takahashi, Y., A.D. Kiureghian, and A.H.S. Ang. 2004. "Life-Cycle Cost Analysis Based on a Renewal Model of Earthquake Occurrences." *Earthquake Engineering and Structural Dynamics* 33, no. 7, pp. 859–80.

Wen, Y., and Y. Kang. 2001a. "Minimum Building Life-Cycle Cost Design Criteria. I: Methodology." *Journal of Structural Engineering* 127, no. 3, pp. 330–7.

Wen, Y., and Y. Kang. 2001b. "Minimum Building Life-Cycle Cost Design Criteria. II: Applications." *Journal of Structural Engineering* 127, no. 3, pp. 338–46.

Yang, T.Y., J.P. Moehle, and B. Stojadinovic. 2009. *Performance Evaluation of Innovative Steel Braced Frames*. Berkeley, CA: University of California.

CHAPTER 10

SEISMIC RESILIENT DESIGN BY ET

10.1 INTRODUCTION

The resilience in cities and meanwhile optimum allocation of public resources necessitates structures with predictable and reliable performance in the case of natural hazards.[1] Earthquakes are considered to be one of the most destructive and costly natural hazards that threaten cities in seismically active regions. So, assessment of seismic safety and performance of buildings and structural components is one of the major challenges in Earthquake Engineering. Reliability and accuracy of seismic analysis procedure is a key concern in almost all seismic assessment procedures for both new and existing structures especially in modern approaches of seismic design. Various limitations of simplified seismic analyses have increased the need for more realistic and reliable dynamic analysis procedures. Endurance Time (ET) method is a response-history-based seismic assessment procedure where structures are subjected to gradually intensifying dynamic excitations and their performance is evaluated based on their response at different excitation levels correlated to specific ground motion intensities (Estekanchi, Valamanesh, and Vafai 2007). This procedure considerably reduces the required huge computational demand of a complete response history analysis while maintaining the major benefits of it, that is, accuracy and insensitivity to model complexity. This viable advantage provides the prerequisites to directly incorporate the new age design concerns such as life-cycle cost of the structure

[1] Chapter Source: Estekanchi, H.E., A. Vafai, and C.B. Mohammad. 2016. "Design and Assessment of Seismic Resilient Structures by the Endurance Time Method." *Scientica Iranica* 23, no. 4, pp. 1648–57.

or resiliency measures in design procedure (Basim and Estekanchi 2015). The main objective of this research is to explore the use of ET method in evaluating resiliency of a construction in quantitative terms.

The concept of disaster resilience in communities has been introduced in recent years. The need to emphasize on the preparedness of communities to recover from disasters has been confirmed in the 2005 World Conference on Disaster Reduction (WCDR). The aim is to be prepared and to be able to recover in an acceptable time from an unexpected shock in the community and meanwhile reduce its vulnerability. The overview of intuitive definitions of resiliency can be found on a work by Manyena (2006). Some frameworks are introduced to provide quantitative evaluation of resilience. These methods can be considered as complementary analysis beyond estimating losses. Resilience measures should take into account technical, social, and economic impacts of a disaster to cover the vast definition of resilience (Cimellaro, Reinhorn, and Bruneau 2010). A general framework for evaluating community resilience has been introduced by Bruneau et al. (2003). They used complementary measures of resilience as reduced failure probabilities, reduced consequences from failures and reduced time to recovery. They used four dimensions of resiliency for a system as robustness, rapidity, resourcefulness, and redundancy. Chang and Shinozuka (2004) also introduced a measure of resilience that relate expected losses in future disasters to a community's seismic performance objectives and implemented the method in a case study of the Memphis water delivery system.

Many uncertain parameters are involved in resilience of a construction in the case of a natural or man-made hazard. Bruneau and Reinhorn (2007) tried to relate probability functions, fragilities and resilience in a single integrated approach for acute care facilities. Cimellaro, Reinhorn, and Bruneau (2010) proposed a framework to evaluate disaster resilience based on dimensionless analytical functions related to the variation of functionality during a period of interest, including the losses in the disaster and the recovery path. Losses are described as functions of fragility of systems that are determined using multidimensional performance limit thresholds accounting for uncertainties. They implemented the method for a typical Californian Hospital building and also a hospital network considering direct and indirect losses. Their proposed framework with some modifications is used as the underlying basis of the present study.

Value-based seismic design of structures using the ET method has been introduced in a work by Basim and Estekanchi (2014). In this methodology Life-Cycle Cost Analysis (LCCA) has been used in order to evaluate the performance of the structure during its life span in economic

terms. This analysis can provide a baseline to incorporate technical, economic, and social or any other intended measures thought to be impressive in resilience of cities in design procedure. The broad concept of resilience demands a flexible design framework to employ these several criteria from various fields of expertise in design stage. LCCA demands performance assessment of the structure in multiple hazard levels. Considering the required repetitive and massive analyses in this procedure, application of ET method in combination with the concept of LCCA can provide the means to use economic concerns directly in design stage.

In order to demonstrate the proposed method of quantitative evaluation of the resilience by the ET method, a prototype structure of a hospital building located in Tehran is considered. It is first optimally designed according to Iranian National Building Code (INBC). Then, FEMA-350 (2000) limitations as a performance-based design criteria are applied, and finally, new design sections are acquired through the value-based design method. In the third design approach, it is tried to design a structure having the minimum total cost during its life time. The resilience of the three different designs of the structure is evaluated using the proposed method and results are compared and discussed. Reduced computational demand in ET analysis method provides the prerequisites to use optimization algorithms in design procedure. Although resiliency measures are not directly incorporated in optimization procedure here, this work is intended to pave the way toward the practical design of construction with the highest resiliency.

10.2 EARTHQUAKES AND RESILIENCY

Cities cannot be considered resilient if they are not protected against the dangers and potential damages that may be imposed by natural hazards. Earthquakes are considered to be one of the most destructive and costly natural hazards that threaten cities. So, stability of community during and after seismic hazards thought to have a determinative impact on the resilience of cities in seismically active regions.

On this issue, resilience may have broad measures in the whole city as a body or submeasures in individual buildings. Also, the impact of seismic hazards on a community may be studied from various points of view and also various concepts may be defined as resilience such as time to recovery, life safety, or damage reduction. For example, “downtime” seems to be an impressive resilience measure for a hospital building or a fire station besides life safety and it is wise to consider these measures

with reasonable portion in design stage. Some limitations may be required for such critical facilities too.

Incorporation of seismic resilience factors in design procedure requires mitigation from common design procedures intended to focus on a limited number of objectives such as structural performance or loss prevention to a broader one with the capability to incorporate any desired and advancing terms in priority measures among design alternatives. Codes for building design, commonly, set some minimum compliance-based standards and in performance terms, we can be confident that they will provide safe buildings, but they promise little in terms of recovery. Readily introduced methodology can provide a wider description of design target by defining the earthquake consequences such as structural damages, loss of contents, losses due to downtime, human injuries and fatalities in the form of quantifiable parameters. In this way, it is expected that the resultant design will perform with desired postearthquake capabilities with manageable disruption.

10.3 CONCEPTS OF ENDURANCE TIME METHOD

A reliable estimation of the damage to various structures and their compartments requires realistic evaluation of seismic response of structures when subjected to strong ground motions. This in turn requires the development and utilization of advanced numerical techniques using reasonably realistic dynamic modeling. While any serious development in the area of seismic resistant design has to be backed up with decent real world experimental investigation, the type and number of decision variables (DVs) are usually so diverse that numerical investigations remain to be the only practical alternative in order to seek good solutions regarding performance and safety.

In the ET method, structures are subjected to a predesigned intensifying dynamic excitation and their performance is monitored continuously as the level of excitation is increased (Estekanchi, Vafai, and Sadeghazar 2004). A typical ET Excitation Function (ETEF) is shown in Figure 10.1. Level of excitation or excitation intensity can be assumed to be any relevant parameter considering the nature of the structure or component being investigated.

Classically, parameters such as peak ground acceleration (PGA) or spectral intensity have been considered most relevant parameters in structural design. More recently, parameters based on input energy,

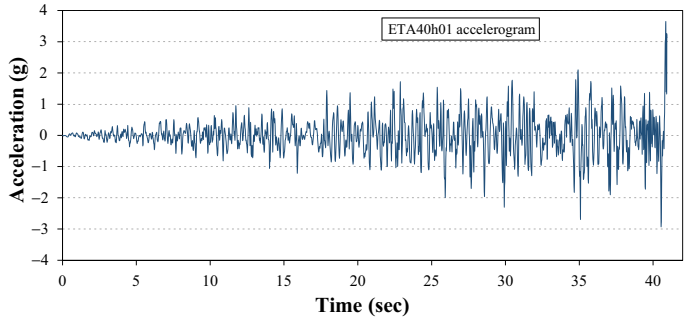

Figure 10.1. Typical ET record incorporating intensifying dynamic excitation.

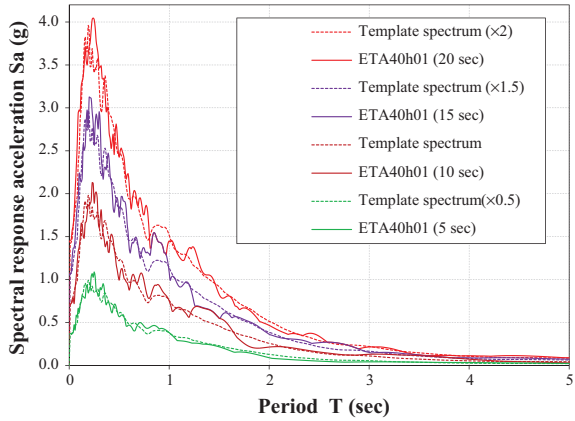

Figure 10.2. Typical response spectra of ET records at various times (ETA40h01).

displacement, and damage spectra are also being proposed as a better representative of the dynamic excitation intensity considering structural response. Figure 10.2 shows the response spectra produced by a typical ETEF at various times. Various ETEFs are publicly available through ET method website (Estekanchi 2014).

While response spectra have been considered to be a standard measure of intensity in producing currently available ETEFs, other intensity measures can also be considered as well. As can be expected, most of these intensity measures are correlated to each other and the problem is to choose a best combination of various parameters to achieve better intensifying excitations that can produce better output. Here, the response spectra

have been considered as the intensity parameter and ETEF has been produced in such a way that the response spectra produced by each window from time 0 to t is proportional to a spectrum.

The application of the ET method in performance-based design was studied by Mirzaee, Estekanchi, and Vafai (2010) introducing "ET curve" and the "Target Curve," which expresses respectively the seismic performance of a structure along various seismic intensities and their limiting values according to code recommendations. Substituting return period or annual probability of exceedance for time in the expression of the performance will make the presentation of the results more explicit and their convenience for calculate probabilistic cost will be increased (Mirzaee, Estekanchi, and Vafai 2012). Also, damage levels had been introduced to express the desired damage states in quantifiable terms.

Hazard return period corresponding to a particular time in ET analysis can be calculated by matching the response spectra at effective periods, for example, from 0.2 to 1.5 times of structure's fundamental period of vibration. The procedure is based on the coincidence of response spectra obtained from the ET accelerogram at different times and response spectra defined for Tehran at different hazard levels. In Figure 10.3 a sample target curve and ET curve considering various performance criteria are depicted where ET analysis time has been mapped into return period on horizontal axis. As it can be seen the structure satisfies the code IO (Immediate Occupancy) level limitations but it has violated the LS (Life Safety) and CP (Collapse Prevention) levels limitations and the frame does not have acceptable performance. It can be inferred one of advantages of ET method that the performance of the structure in continuous increasing hazard levels can be properly depicted in an easy to read figure.

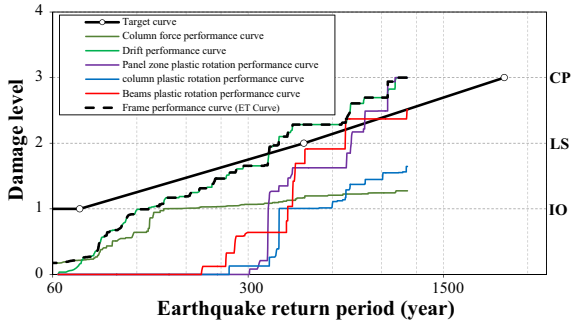

Figure 10.3. Performance assessment by ET method.

10.4 VALUE-BASED SEISMIC DESIGN BY THE ET METHOD

Life-cycle cost analysis (LCCA) has become an important part of structural engineering to assess the structural comeback and evaluate the performance of the structure in economic terms. It has gained considerable attention of decision-making centers to decide on the most cost-effective solution related to the construction of structures in seismic regions. LCCA has provided a reliable tool for estimating damage cost due to future earthquakes during the design life of a structure. Instead of "cost" in dollars, in decision-making process, any other measure can be used to compare and evaluate design alternatives' expected operation. In this section, total expected cost imposed by earthquake occurrences during structure's life span is selected as an evaluation measure since engineers might be more familiar with this concept. A correlation will be required to express other measures mentioned earlier such as downtime or social impacts in economic terms and dollars. By the use of this method the expected total cost of a structure including the initial cost and also losses resulting from earthquakes during its life span can be considered as the main indicator of the priority of design alternatives. This analysis in companion with an optimization algorithm can result in a design with the least total cost. LCCA demands the calculation of the cost components that are related to the performance of the structure in multiple earthquake hazard levels. However, these calculations require repetitive and massive analyses of performance assessment and huge computational demand and sophistications involved may make optimization algorithms impractical or the simplifications used decrease the reliability of the outcome. Application of ET method in combination with the concept of LCCA has led to development of a framework for practical Value-Based Seismic Design of structures.

ET analysis provides a proper baseline to perform economic analyses on design alternatives with acceptable computational cost. While value can be defied and considered in its broad sense for design purposes, for the clarity of explanation, the structure that is more economical to construct and maintain, is considered to be the most valued. Initial construction cost and expected seismic damage cost throughout the life time of the structure are usually the two most important parameters for decision making (Mitropoulou, Lagaros, and Papadrakakis 2011). The cost model used in this study can be found in detail in a work by Basim and Estekanchi (2014). In this model the total cost C_{TOT} of a structure can be considered as the sum

of its initial construction cost C_{IN} which is function of design vector s and the present value of the life-cycle cost C_{LC} which is function of life time t and the design vector s (Mitropoulou, Lagaros, and Papadrakakis 2011).

Initial cost is the construction and equipping cost of a structure. In our hospital building design example which is a new moment resisting steel frame the initial cost is related to the land price, material and the labor cost for the construction of the structure and equipping costs for health care facilities. The land price and nonstructural components cost are constant for all design alternatives.

To calculate the life-cycle cost of the structure following cost components are involved: the damage repair cost, the cost of loss of contents due to structural damage quantified by the maximum interstory drift and also floor acceleration, the loss of rental cost, the loss of income cost, the cost of injuries, and the cost of human fatalities (Wen and Kang 2001; Mitropoulou, Lagaros, and Papadrakakis 2010). Interstory drift (Δ) has been considered as a measure of both structural and nonstructural damage and maximum floor acceleration is used to quantify the loss of contents. In this study, seven limit states according to drift ratios based on ATC-13 (1985) is used to describe structural performance as shown in Table 10.1. The relation between floor acceleration values and damage states are shown in Table 10.1 based on a work by Elenas and Meskouris (2001). The addition of the maximum floor acceleration component in life-cycle cost calculation is introduced by Mitropoulou, Lagaros, and Papadrakakis (2010). Piecewise linear relation has been assumed between damage indices and costs (Mirzaee and Estekanchi 2015).

Table 10.1. Drift ratio and floor acceleration limits for damage states

Performance level	Damage states	Drift ratio limit (%) ATC-13 (1985)	Floor acceleration limit (g) Elenas and Meskouris (2001)
I	None	$\Delta \leq 0.2$	$a_{floor} \leq 0.05$
II	Slight	$0.2 < \Delta \leq 0.5$	$0.05 < a_{floor} \leq 0.10$
III	Light	$0.5 < \Delta \leq 0.7$	$0.10 < a_{floor} \leq 0.20$
IV	Moderate	$0.7 < \Delta \leq 1.5$	$0.20 < a_{floor} \leq 0.80$
V	Heavy	$1.5 < \Delta \leq 2.5$	$0.80 < a_{floor} \leq 0.98$
VI	Major	$2.5 < \Delta \leq 5$	$0.98 < a_{floor} \leq 1.25$
VII	Destroyed	$5.0 < \Delta$	$1.25 < a_{floor}$

Life-cycle cost of the structure is calculated by summing the cost components as follows:

$$C_{LC} = C_{dam} + C_{con} + C_{ren} + C_{inc} + C_{inj} + C_{fat} \quad (1)$$

$$C_{con} = C_{con}^{\Delta} + C_{con}^{acc} \quad (2)$$

where C_{dam} = the damage repair cost; C_{con}^{Δ} = the loss of contents cost due to structural damage quantified by interstory drift; C_{con}^{acc} = the loss of contents cost due to floor acceleration; C_{ren} = the loss of rental cost; C_{inc} = the cost of income loss; C_{inj} = the cost of injuries; and C_{fat} = the cost of human fatality. Formulas to calculate each cost component are depicted in Table 10.2. The values of the mean damage index, loss of function, downtime, expected minor injury rate, expected serious injury rate and expected death rate used in this study are based on ATC-13 (1985) restated in FEMA-227 (1992). Table 10.3 provides these parameters for each damage state.

Table 10.2. Formulas for cost components calculation in Dollars (ATC-13 1985; Wen and Kang 2001; Mitropoulou, Lagaros, and Papadrakakis 2011)

Cost component	Formula	Basic cost
Damage repair (C_{dam})	Replacement cost × floor area × mean damage index	500\$/m^2
Loss of contents (C_{con})	Unit contents cost × floor area × mean damage index	250\$/m^2
Loss of rental (C_{ren})	Rental rate × gross leasable area × loss of function time	20\$/month/m^2
Loss of income (C_{inc})	Income rate × gross leasable area × down time	300\$/year/m^2
Minor injury ($C_{inj,\,m}$)	Minor injury cost per person × floor area × occupancy rate × expected minor injury rate	2,000\$/person
Serious injury ($C_{inj,\,s}$)	Serious injury cost per person × floor area × occupancy rate × expected serious injury rate	20,000\$/person
Human fatality (C_{fat})	Human fatality cost per person × floor area × occupancy rate × expected death rate	300,000\$/ person

Table 10.3. Damage state parameters for cost calculations (ATC-13 1985; FEMA-227 1992)

Damage states	Mean damage index (%)	Expected minor injury rate	Expected serious injury rate	Expected death rate	Loss of function time (days)	Down time (days)
(I)-None	0	0	0	0	0	0
(II)-Slight	0.5	0.00003	0.000004	0.000001	1.1	1.1
(III)-Light	5	0.0003	0.00004	0.00001	16.5	16.5
(IV)-Moderate	20	0.003	0.0004	0.0001	111.8	111.8
(V)-Heavy	45	0.03	0.004	0.001	258.2	258.2
(VI)-Major	80	0.3	0.04	0.01	429.1	429.1
(VII)-Destroyed	100	0.4	0.4	0.2	612	612

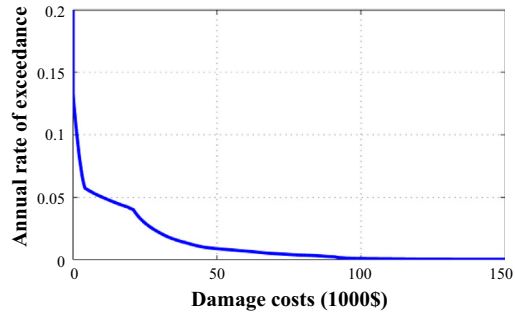

Figure 10.4. A typical loss curve for the three-story frame.

As described in (Basim and Estekanchi 2014) the annual rate that any cost component exceeds a threshold value is calculated using the PEER framework. This will result in a curve with cost values in horizontal axis and annual rate of exceedance in vertical axis known as Loss Curve (Yang, Moehle, and Stojadinovic 2009). In Figure 10.4 a sample loss curve due to damage cost is depicted. The area under the loss curve represents the mean annual component cost caused by all earthquakes in one year. Life-cycle cost of the building is the present value of the annual damage costs summed up through the life time of the structure. A discount rate equal to 3 percent over a 50 years life of the building has been considered to transform the damage costs to the present value. The total cost of the structure is calculated by summing the initial cost and the life-cycle cost and is used as the objective function in optimization algorithm seeking a design with the least total cost.

10.5 CASE STUDY: THREE-STORY STEEL MOMENT FRAME

In order to demonstrate the method a three-story and one-bay steel special moment frame used as a hospital building is optimally designed according to Iranian National Building Code (INBC), which is almost identical to the ANSI/AISC360 (2010) LRFD design recommendations. Also, the frame is designed optimally to conform to FEMA-350 (2000) limitations as a performance-based design criteria and as a third step a new design sections has been acquired through the value-based design method to have the minimum total cost during its life time that is assumed 50 years. The performance of the designed frames is investigated by the ET method. For the value-based design the total cost of the structure is selected as the

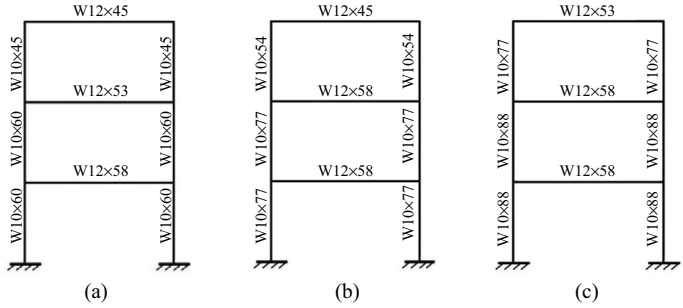

Figure 10.5. Frame design results after optimization: (a) codified design (b) performance-based design (c) value-based design (least LCC).

optimization objective to be minimized. An initial cost equal to \$500 per m^2 over the 300 m^2 total area of the structure for the prescriptive design is considered and for other design alternatives, it will be calculated according to their steel weight difference by a material plus labor cost of 2\$/kg. Occupancy rate is taken 10 persons per 100 m^2.

Structural response history analyses were performed in OpenSees (Mazzoni et al. 2006). Genetic algorithm (GA) has been used to find the optimum design. Alternative designs should meet some initial constraints. One of the constraints is strong column and weak beam criterion which should be checked and the other constraint that should be considered before the analysis phase is that the selected sections for columns in each story should not be weaker than the upper story. Beside these constraints, all AISC 360 checks must be satisfied for the gravity loads. Once the expressed constraints are satisfied, the LCC (Life Cycle Cost) analysis is performed. Genetic algorithm with an initial population size of 100 leads to an optimum design after about 1,800 ET response history analyses.

The resultant prescriptive, performance-based and value-based designs of the frame are different due to their distinct basic design philosophies. Design sections for each method are depicted in Figure 10.5. Seismic performance of each design of the frame is shown in Figure 10.6. It can be seen that for the value-based design the structure satisfies performance limitations of FEMA350 with a margin that is justified by economic concerns.

10.6 QUANTIFICATION OF RESILIENCE

Resilience can be quantified using a function which presents the ability of the system to sustain its functionality over a period of time. Such a function for a system which has exposed an external shock is presented

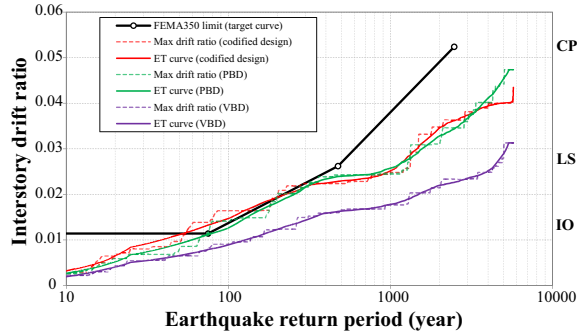

Figure 10.6. Comparison of the frames response at various hazard levels.

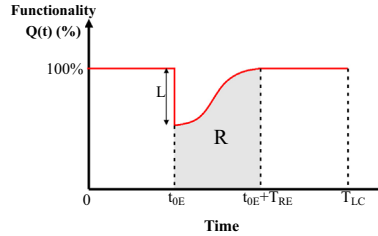

Figure 10.7. Schematics of a functionality function for a system.

in Figure 10.7. The system can be a building, infrastructure, lifeline networks, or a whole community. In this figure, the normalized functionality $Q(t)$ of the system is traced during a control time T_{LC} which may be the life time of a construction. It is assumed that a disastrous event occurs in a time t_{0E} and it takes a period of time T_{RE} as recovery time in which the system regains its full functionality. Although the final functionality of the system may differ from the initial, it is assumed here that the recovery process restores the under study building to its initial condition. For a construction under seismic hazards T_{RE} depends on many external parameters such as hazard intensities, induced damages, management quality, and resources to repair damages. Many uncertainties are involved in the required recovery time and also the amount of loss of functionality in the case of an event. The recovery time is known to be the most difficult quantity to predict in this function.

A resilience measure should represent the all dimensions of resilience which includes the amount of direct and indirect losses and also the rapidity of recovery process. According to MCEER (Multidisciplinary Center of Earthquake Engineering to Extreme Event) terminology, resilience

is quantified as the area under the functionality curve $Q(t)$ of a system. This measure can be considered as a somehow comprehensive DV to evaluate the performance of a construction (Bruneau and Reinhorn 2007; Cimellaro, Reinhorn, and Bruneau 2010). Resilience R can be formulated by the following formula as a dimensionless parameter in percentage (Cimellaro, Reinhorn, and Bruneau 2010):

$$R = \int_{t_{0E}}^{t_{0E}+T_{RE}} Q(t) / T_{RE} dt \tag{3}$$

$$Q(t) = 1 - L(1, T_{RE}) \left[H\left(t - t_{0E}\right) - H\left(t - \left(t_{0E} + T_{RE}\right)\right) \right] \times f_{\mathrm{Rec}}\left(t, t_{0E}, T_{RE}\right) \tag{4}$$

$L(1, T_{RE})$ is the loss function and $f_{Rec}(t, t_{0E}, T_{RE})$ is the recovery function. H is the Heaviside step function. Other used parameters have been defined previously. Rapidity in the recovery process can be represented by the slope of the functionality curve ($dQ(t)/dt$). The amount of resources and the quality of management and many other parameters will affect the shape and the slope of the recovery curve and the recovery time T_{RE}. The other dimension of resilience thought to be important in recover capacity of a system is robustness. It is usually taken as the residual functionality after a disastrous event and in the framework discussed by Cimellaro, Reinhorn, and Bruneau (2010) is considered as $1\text{-}\overline{L}(m_L, \alpha\sigma_L$ where $\overline{L}$ is a random variable with the mean m_L and the standard deviation σ_L and α is a multiplier of the standard deviation corresponding to a specific level of losses. Here, for simplicity of the representation, the estimation of the resilience R is based on the mean values of L. Uncertainties can be modeled considered using a Monte Carlo approach or reliability methods.

The loss model used in this section is similar to that of the previous section. Of course, many uncertainties are involved in these losses and various probabilistic loss-estimation methods are proposed in the literature. For simplicity of presentation a somehow simple loss model with limited uncertainty calculations is used here. The method has the capability to use more detailed loss-estimation techniques. Total loss L in this framework can be considered as a function of earthquake intensity I and recovery time T_{RE} as it contains both direct losses (L_D) and indirect losses (L_I). The later losses can be directly affected by the recovery time. Each of direct and indirect losses has two subcategories as economic losses and casualties' losses. Therefore, total loss $L(I, T_{RE})$ consists of four contributions: direct economic losses L_{DE}, direct casualties losses L_{DC}, indirect economic losses L_{IE}, and indirect casualties' losses L_{IC}. In this context, direct economic losses L_{DE} is considered as sum of damage repair cost and loss of contents cost as a ratio of the total building replacement cost. So, L_{DE} is a function of intensity I. More detailed loss models using fragilities can

be used by the formulation presented in the work by Cimellaro, Reinhorn, and Bruneau (2010).

Direct casualties' losses L_{DC} are calculated as a ratio of the instantaneous number of injured or dead people N_{in} to the total number of occupants N_{tot}. This parameter can also be calculated using the model defined in previous section:

$$L_{DC}(I) = \frac{N_{in}}{N_{tot}} \tag{5}$$

The indirect economic losses may be significant for lifeline systems or any critical facilities such as health care centers. The indirect economic losses $L_{IE}(I, T_{RE})$ are related to hazard intensity and also the recovery time. More comprehensive models are required to estimate the postearthquake losses. Loss of rental and loss of income costs in the used cost model can be considered as components of L_{IE}. Some other components may be involved in lifeline systems such as water or gas delivery networks that may be much more than direct economic losses.

The indirect casualties' losses $L_{IC}(I, T_{RE})$ may be significant for a health care center. These losses are caused by the hospital dysfunction in recovery time after an earthquake. In this framework L_{IC} can be calculated as the ratio of the number of injured persons N_{in} to the total population N_{tot} served or supposed to be served.

$$L_{IC}(I, T_{RE}) = \frac{N_{in}}{N_{tot}} \tag{6}$$

Casualties' losses will affect the total loss as a penalty function using weighting factors according to the following formulas:

$$L_D = L_{DE}\left(1 + \alpha_{DC} L_{DC}\right) \tag{7}$$

$$L_I = L_{IE}\left(1 + \alpha_{IC} L_{IC}\right)$$

α_{DC}, α_{IC} are the weighting factors representative for the importance of the occupancy that are determined based on social concerns. The total losses L are a combination of direct losses L_D and indirect losses L_I:

$$L(I, T_{RE}) = L_D(I) + \alpha_I L_I\left(I, T_{RE}\right) \tag{8}$$

α_I is used as a weighting factor to represent the importance of indirect losses to other facilities in community. It is obvious that the more recovery time T_{RE} results in more total loss values. The next step to calculate

resilience of the construction is to estimate a recovery path through which the building regains its functionality. This process is complex and is influenced by many environmental conditions such as quality of management and amount of resources and may be affected by the amount of disaster consequences in other sectors of the community. The recovery model used in this section is based on the simplified model introduced by Cimellaro, Reinhorn, and Bruneau (2010) with some modifications. Trigonometric function is selected according to the experienced condition in Iran.

$$f_{rec}(t) = a/2\left\{1+\cos\left[\pi b\left(t-t_{0E}\right)/T_{RE}\right]\right\} \tag{9}$$

where a, b are constant values which it is assumed here $a = b = 1$. This function is used when the process of recovery starts with considerable delay due to lack of resource or proper management. It is assumed that the structural response to a specific intensity level does not vary in the life time of the structure. In other words, deterioration of structural system is ignored for the sake of simplicity. As noted, the structural responses for any hazard intensity are provided through ET analysis. The results are represented via ET curve. The resilience of the understudy building in case of hazards with any intensity can be calculated using the presented method.

The resilience R of each structure conditional on the occurrence of earthquakes with any intensity is depicted in Figure 10.8. In this figure vertical axis shows the expected resilience of the structure conditional on the occurrence of an earthquake with the annual probability of exceedance presented in horizontal axis. Using the ET method, the resilience

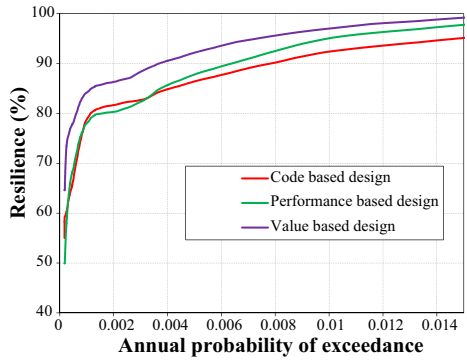

Figure 10.8. Resilience curve for the three structures.

of the structure can be explored in a continuous range of intensities. It is obvious that the value-based design is the most resilient structure among the three alternatives. The reduced computational cost in this framework provides the means to incorporate reliability analyses and account for uncertainties.

10.7 SUMMARY AND CONCLUSIONS

A framework to calculate a resilience measure using the ET method in proposed. A simplified cost and recovery model for a prototype hospital building was developed. Three optimum design alternatives for the structure were considered according to a prescriptive design code, performance-based design guideline and a value-based approach. Application of the ET analysis in LCCA has been briefly explained. ET method and resultant performance curve has provided a proper baseline to calculate expected damage cost, while the required computational effort is in an acceptable range to be used in conventional optimization techniques. Structural performance for the three structures has been compared using ET curve. A resilience measure according to the current literature was defined and a method to calculate the resilience of the structure conditional on the occurrence of hazard with any intensity was developed. Results were depicted in an easy to read figure introducing "Resilience Curve." Results show that the value-based design will have a better performance regarding to the resilience measures. Although the involved uncertainties were not highlighted in this study, the method has the capability to account for them requiring acceptable amount of computational effort.

REFERENCES

AISC 360. 2010. *Specification for Structural Steel Buildings (ANSI/AISC 360-10)*. Chicago, IL: American Institute of Steel Construction.

ATC-13. 1985. *Earthquake Damage Evaluation Data for California*. Applied Technology Council.

Basim, M.C., and H.E. Estekanchi. 2014. "Value Based Seismic Design of Structures by the Endurance Time Method." (submitted).

Basim, M.C., and H.E. Estekanchi. 2015. "Application of Endurance Time Method in Performance-Based Optimum Design of Structures." *Structural Safety* 56, pp. 52–67.

Bruneau, M., S.E. Chang, R.T. Eguchi, G.C. Lee, T.D. O'Rourke, A.M. Reinhorn, M. Shinozuka, K. Tierney, W.A. Wallace, and D. von Winterfeldt. 2003. "A Framework to Quantitatively Assess and Enhance the Seismic Resilience of Communities." *Earthquake Spectra* 19, no. 4, pp. 733–52.

Bruneau, M., and A. Reinhorn. 2007. "Exploring the Concept of Seismic Resilience for Acute Care Facilities." *Earthquake Spectra* 23, no. 1, pp. 41–62.

Chang, S.E., and M. Shinozuka. 2004. "Measuring Improvements in the Disaster Resilience of Communities." *Earthquake Spectra* 20, no. 3, pp. 739–55.

Cimellaro, G.P., A.M. Reinhorn, and M. Bruneau. 2010. "Framework for Analytical Quantification of Disaster Resilience." *Engineering Structures* 32, no. 11, pp. 3639–49.

Elenas, A., and K. Meskouris. 2001. "Correlation Study Between Seismic Acceleration Parameters and Damage Indices of Structures." *Engineering Structures* 23, no. 6, pp. 698–704.

Estekanchi, H.E., A. Vafai, and M. Sadeghazar. 2004. "Endurance Time Method for Seismic Analysis and Design of Structures." *Scientia Iranica* 11, no. 4, pp. 361–70.

Estekanchi, H., V. Valamanesh, and A. Vafai. 2007. "Application of Endurance Time Method in Linear Seismic Analysis." *Engineering Structures* 29, no. 10, pp. 2551–62.

Estekanchi, H.E. 2014. *Endurance Time Method Website*. https://sites.google.com/site/etmethod/

FEMA-227. 1992. *A Benefit–Cost Model for the Seismic Rehabilitation of Buildings*. Washington, DC: Federal Emergency Management Agency, Building Seismic Safety Council.

FEMA-350. 2000. *Recommended Seismic Design Criteria for New Steel Moment-Frame Buildings.* Washington, DC: Federal Emergency Management Agency.

Manyena, S.B. 2006. "The Concept of Resilience Revisited." *Disasters* 30, no. 4, pp. 434–50.

Mazzoni, S., F. McKenna, M.H. Scott, G.L. Fenves, and B. Jeremic. 2006. *Open System for Earthquake Engineering Simulation (OpenSees)*. Berkeley, California.

Mirzaee, A., H.E. Estekanchi, and A. Vafai. 2010. "Application of Endurance Time Method in Performance-Based Design of Steel Moment Frames." *Scientia Iranica* 17, no. 6, pp. 361–70.

Mirzaee, A., H.E. Estekanchi, and A. Vafai. 2012. "Improved Methodology for Endurance Time Analysis: From Time to Seismic Hazard Return Period." *Scientia Iranica* 19, no. 5, pp. 1180–87.

Mirzaee, A., and H.E. Estekanchi. 2015. "Performance-Based Seismic Retrofitting of Steel Frames by Endurance Time Method." *Earthquake Spectra* 31, no. 1, pp. 383–402. http://dx.doi.org/10.1193/081312EQS262M

Mitropoulou, C.C., N.D. Lagaros, and M. Papadrakakis. 2010. "Building Design Based on Energy Dissipation: A Critical Assessment." *Bulletin of Earthquake Engineering* 8, no. 6, pp. 1375–96.

Mitropoulou, C.C., N.D. Lagaros, and M. Papadrakakis. 2011. "Life-Cycle Cost Assessment of Optimally Designed Reinforced Concrete Buildings Under Seismic Actions." *Reliability Engineering & System Safety* 96, no. 10, pp. 1311–31.

Wen, Y., and Y. Kang. 2001. "Minimum Building Life-Cycle Cost Design Criteria. II: Applications." *Journal of Structural Engineering* 127, no. 3, pp. 338–46.

Yang, T.Y., J.P. Moehle, and B. Stojadinovic. 2009. *Performance Evaluation of Innovative Steel Braced Frames.* Berkeley, CA: University of California.

CHAPTER 11

SAMPLE ENGINEERING APPLICATION: EDR SEISMIC PERFORMANCE

11.1 INTRODUCTION

While the "smart structure" concept has been applied in aerospace and mechanical industries since a relatively long time, application of this concept for wind and seismic response reduction of civil engineering structures is still a cutting-edge technology under research and development (Cheng, Jiang, and Lou 2008).[1] A smart structure can be designed by applying various types of structural control devices. The four well-known types of these devices are seismic isolation, passive, semiactive and active, as well as hybrid control systems. Passive devices have the virtue of being more economical and less complicated compared to other types of control devices.

Friction dampers are among typical passive energy dissipating systems. Friction is an efficient, reliable, and economical mechanism which can dissipate kinetic energy by converting it to heat, so it can be used to slow down the motion of buildings. The function of friction devices in a building is analogous to the function of the braking system in an automobile (Soong and Dargush 1997). Based primarily on this analogy, Pall, Marsh, and Fazio (1980) began the development of friction dampers to improve the seismic response of civil engineering structures. Some of the most conventional types of these devices are the X-braced friction damper (Pall and Marsh 1982), Sumitomo friction damper (Aiken and Kelly

[1] Chapter Source: Foyuzat, M.A., and H.E. Estekanchi. 2016. "Evaluation of the EDR Performance in Seismic Control of Steel Structures Using Endurance Time Method." *Scientica Iranica* 23, no. 3, pp. 827–41.

1990), Energy Dissipating Restraint (EDR) (Nims et al. 1993), and Slotted Bolted Connection (SBC) (FitzGerald et al. 1989), to name but a few.

The focus of the paper in hand is on the performance of the EDR. EDR is a uniaxial friction damper which has been designed by Richter et al. (1990). The mechanics of this device are described in detail in (Nims et al. 1993) and (Inaudi and Kelly 1996). The principal components of the device are internal spring, compression wedges, friction wedges, stops, and cylinder (Figure 11.1). The variable parameters are the number of wedges, spring constant, gap, and spring precompression. The role of the compression and friction wedges is to transmit and convert the axial force of the internal spring to a normal force on the cylinder wall.

The length of the spring can be variable through the operation of the device, which leads to a variable sliding friction. By adjusting the initial slip force and gap size, different hysteresis loops can be produced. With zero gaps and an initial slip force, the double flag-shaped loops, as is indicated in Figure 11.2, result. The parameters of the device are displayed in this figure. These double flag-shaped loops manifest the self-centering characteristic, that is, while unloading to zero, the device will return to its initial position without any residual deformations.

Several experimental studies have been carried out on the device, the results of which indicate the effectiveness of the EDR in reducing the seismic response of structures (e.g., Richter et al. 1990; Aiken et al. 1993). The remarkable results are that the flag-shaped loops prove to be well-defined and quite consistent. Moreover, investigating cumulative energy

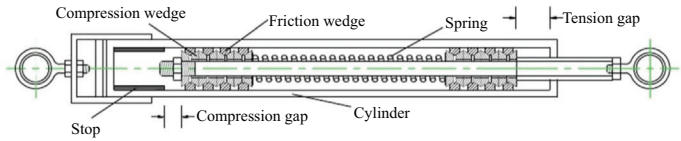

Figure 11.1. Configuration of the EDR.

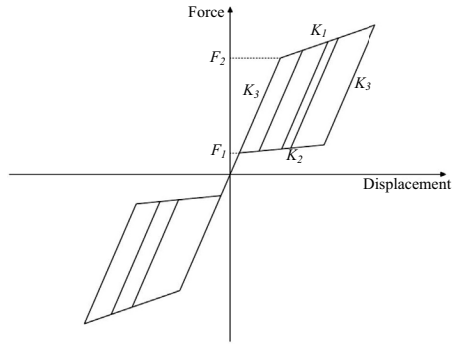

Figure 11.2. Double flag-shaped hysteretic loops of the EDR.

time histories under earthquake signals implies that the frictional devices dissipate a significant portion of the total input energy.

The adequacy of the EDR has also been verified through manifold analytical studies (e.g., Inaudi and Kelly 1996; Inaudi and Nicos 1996; and Zhou and Peng 2009). However, as noted by the researchers, hysteretic mechanisms do not respond quickly to sudden impulses. Additionally, higher modes were sometimes excited due to sudden stiffness changes associated with the frictional devices. These limitations showed that the EDR device consistently provided reductions in displacements and inter-story drifts, and increased the effective damping ratio of the test structure.

One of the most outstanding properties of the EDR, when the device is adjusted to have zero gaps, is that it is self-centering. As mentioned earlier, in this case, the EDR demonstrates double flag-shaped hysteresis loops. This property has the merit of reducing the permanent deformations in buildings after severe earthquakes. No other friction damper enjoys this characteristic (Nims, Richter, and Bachman 1993). In fact, for the conventional friction dampers, which lack the self-centering property, significant permanent displacements could remain in the structure after the completion of the ground motion. This, in turn, brings about remarkable damage repair costs. From now on, wherever the EDR is mentioned in this paper, it refers to the device with double flag-shaped loops.

As a result of the absolutely nonlinear behavior of friction dampers, the use of the demanding nonlinear time-history method is inevitable for their analysis and design. In fact, the alternate simplified methods which have been authorized by existing codes (e.g., nonlinear static and response spectrum procedures) are not reliable enough, on account of manifold simplifying postulations made in their development. Time history has the advantage of potentially being capable of directly including almost all sources of nonlinear and time-dependent material and geometric effects. Nevertheless, its traditional pitfall is being the most complex and time-consuming procedure.

As is apparent from Figure 11.2, the hysteretic behavior of the EDR device exhibits high nonlinearity. Therefore, it is necessary to apply the nonlinear time-history method for the performance-based analysis and design of the EDR-controlled structures. In the next section, a novel seismic analysis procedure, which is called the "Endurance Time (ET)" method, will be introduced. The ET method is not as much complicated and computationally demanding as the conventional time-history analysis. At the same time, it is not as much unreliable and approximate as simplified methods. In fact, this method offers a more practical procedure for performance-based design of structures.

In this study, the application of the ET method in the performance-based seismic rehabilitation of the steel frames by using the EDR

devices is investigated. Three steel moment-resisting frames with different story numbers are considered as case studies. By applying the ET method, the performance of the frames before and after installing the EDR devices is compared with each other. Several engineering demand parameters (including interstory drift, plastic rotation of beams and columns, and absolute acceleration) are employed to this end. Furthermore, the maximum interstory drift responses are calculated once more through the nonlinear time-history analysis, using real ground motions, and the results are compared with those from ET method.

11.2 BASIC CONCEPTS OF THE ENDURANCE TIME METHOD

Among various standard methods for the analysis of structures subjected to earthquake loadings, the nonlinear time-history analysis procedure is expected to produce the most realistic prediction of structural behavior. However, the complexity and high computational effort associated with this procedure have encouraged researchers to develop alternate analysis methods. These methods are much less complicated and can estimate the seismic demands to an acceptable degree of accuracy.

ET method is one of the significant types of these new methods, which is introduced by Estekanchi, Vafai, and Sadeghazar (2004). This method is a time-history-based pushover procedure, in which the structure is subjected to a set of predesigned accelerograms that intensify with time—referred to as Endurance Time Excitation Functions (ETEFs). The ETEFs are generated in such a way that their response spectra increase by the time; hence, the response of the structure under this kind of excitation gradually increases with time (Estekanchi, Valamanesh, and Vafai 2007). In other words, each time in an ETEF is a representative of a record with a certain level of intensity (Figure 11.3). In the process of generating excitation functions, the ETEFs have been optimized to fit a specific target spectrum, which could be a codified spectrum or the average spectrum of an ensemble of ground motions. In that process, the linear spectral acceleration of an ETEF is adjusted to satisfy Equations (1) and (2):

$$S_a(T,t) = \frac{t}{t_{target}} S_{aC}(T) \tag{1}$$

$$S_u(T,t) = \frac{t}{t_{target}} S_{uC}(T) \times \frac{T^2}{4\pi^2} \tag{2}$$

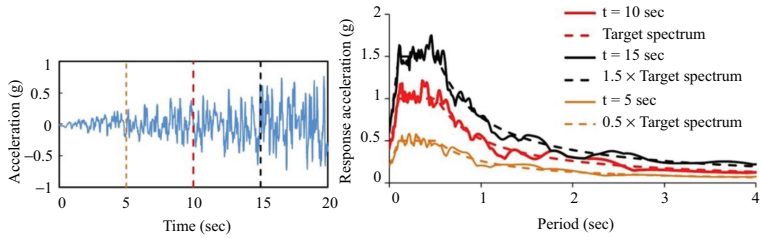

Figure 11.3. A typical ETEF and its response spectra at different times along with the target spectra.

where T is the free vibration period of the Single-Degree-Of-Freedom (SDOF) system; t is the time in the ETEF; S_a and are the ETEFs' spectral acceleration and displacement spectra, respectively; S_{aC} and S_{uC} are the codified acceleration and displacement spectra, respectively; and t_{target} is a predefined time (equals 10 seconds) at which S_a and S_u coincide with S_{aC} and S_{uC}, respectively (Estekanchi, Valamanesh, and Vafai 2007). The performance of the structure is estimated based on the length of time, during which it can endure the imposed ETEF. By using a properly designed excitation function, this endurance can be correlated to the intensity level of ground motions that the intended structure can be expected to endure. More description on the concept of the ET method as well as the characteristics of the ET excitation functions can be found in literature (e.g., Estekanchi, Vafai, and Sadeghazar 2004; Estekanchi, Valamanesh, and Vafai 2007; and Nozari and Estekanchi 2011).

The main advantage of the ET method over the regular time-history method, using ground motions, is that it needs a small number of analyses. In the ET method, the structural responses at different excitation levels are obtained in a single time-history analysis, thereby significantly reducing the computational demand. Accordingly, by using the ET method and regarding the concepts of performance-based design, the performance of a structure at various seismic hazard levels can be predicted in a single time-history analysis. The application of the ET method in the seismic performance assessment of steel frames has been studied by Mirzaee and Estekanchi (2015).

The results of ET analysis are usually presented by increasing ET response curves. The ordinate at each time value, t, corresponds to the maximum absolute value of the required engineering demand parameter in the time interval [0, t], as is expressed in Equation (3):

$$\Omega\big(P(t)\big) \equiv \max\Big(\big|P(\tau)\big|\Big) \qquad \tau \in [0, t] \tag{3}$$

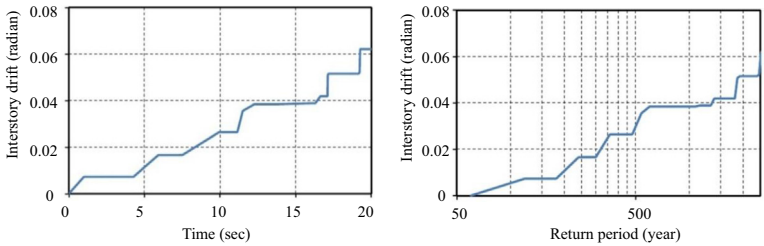

Figure 11.4. Sample ET response curve with horizontal axis in (a) time, (b) return period.

In this equation, Ω is the *Max-Abs* operator as was defined previously, and $P(t)$ is the desired response history such as interstory drift ratio, base shear, or other parameters of interest. The abscissa of an ET response curve is time, which is an indicator of the intensity in ET analysis. Figure 11.4(a) shows a typical ET response curve in which the maximum interstory drift is utilized as the demand parameter. ET curves are usually serrated, because of the statistical characteristics and dispersion of the results of the ET analysis in the nonlinear range. Sometimes the response value does not pass the maximum value experienced before in a time interval, and therefore the resulting ET curve has a constant value in that interval. In order to get more accurate and consistent ET curves, Estekanchi et al. recommended using the average of the results from three ET excitation functions (Estekanchi, Valamanesh, and Vafai 2007).

Mirzaee, Estekanchi, and Vafai (2012) originally investigated the correlation between time—as an indicator of the intensity in ET analysis—and seismic hazard return period. Substituting a common parameter, like the return period for time, increases the readability and efficiency of response curves and can considerably improve the presentation of ET analysis results. They utilized the elastic response spectrum defined in ASCE (2006) as an intermediate criterion to establish this correlation.

Further investigations suggested that utilizing the elastic spectrum as the intermediate intensity measure to correlate the time and return period is not reliable in the cases which the structures experience large nonlinear deformations (Estekanchi, Riahi, and Vafai 2011; Riahi, Estekanchi, and Vafai 2009). Actually, in the structures which experience large nonlinear deformations, the difference between the results obtained by this procedure and the nonlinear time-history analysis, using ground motions, can be significant.

Foyouzat and Estekanchi (2014) proposed using nonlinear Rigid-Perfectly Plastic (RPP) spectra in lieu of elastic response spectra to correlate the time in ET analysis and return period. The results suggested that the application of RPP spectra significantly improves the accuracy and

reliability of the response curves resulted from ET analysis in nonlinear range compared with the procedures based on linear elastic spectra. As a result, regarding the high nonlinearity associated with the EDR device, as is discussed in the previous section, the RPP spectra are more appropriate intensity measures than the elastic spectra for the ET analysis of the structures outfitted with EDR devices. In what follows, a brief explanation of this approach, which is discussed in detail in (Foyouzat and Estekanchi 2014), is presented. An RPP system is a system possessing a force-displacement relationship, as is indicated in Figure 11.5. No deformation occurs until reaches the yield force, F_y, and the force cannot exceed the yield force, that is, $|F| \leq F_y$. The RPP model can be simulated by a Coulomb friction block with a sliding friction force equal to F_y.

For a given earthquake excitation, the response of an RPP SDOF system depends only on the ratio $A_y = F_y/m$, where m is the mass of the SDOF system. For a given ground motion, if maximum absolute displacements of RPP SDOF systems are calculated for a range of A_ys, the RPP spectrum of that ground motion will be provided. Furthermore, if the ground motion is scaled to a seismic hazard level corresponding to a specific return period, the resulted spectrum is the RPP spectrum corresponding to that return period. Besides this, one could obtain the RPP spectra of an ensemble of ground motions that are scaled to a specific return period and then use the average of those spectra as the RPP spectrum corresponding to that return period.

As is clear from the previous discussion, the RPP spectrum is a function of two variables, namely the return period (R) and A_y/g, that is to say $S_{RPP} = S_{RPP}(A_y/g, R)$. Apart from this, the RPP spectrum for an ETEF is defined as is indicated in Equation (4):

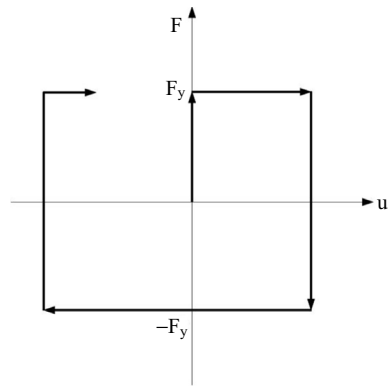

Figure 11.5. Force-displacement behavior of an RPP model.

$$S_{RPP}\left(A_y / g, t\right) = \max\left(\left|\Delta(\tau)\right|\right) \qquad \tau \in [0, t] \tag{4}$$

where t is time, and $\Delta(\tau)$ is the displacement of the RPP system at time due to an ETEF. If more than one ETEF is desired to be used (usually three, as pointed out earlier), the average spectra of those ETEFs can be applied. By acquiring the inverse of the function S_{RPP} with respect to R, return period can be written as $R = f\,(S_{RPP}, A_y/g)$, where f is a function that relates the return period to S_{RPP} and A_y/g. From Equation (4), $S_{RPP} = S_{RPP}(A_y/g, t)$, the result of which would be Equation (5):

$$R = f\left(S_{RPP}(A_y / g, t), A_y / g\right) = h\left(A_y / g, t\right) \tag{5}$$

where h is a function that relates the return period to A_y/g and t. Since expressing function h via a closed form formulation is difficult, this function is evaluated numerically in a range of A_y/gs and ts, and the values of R can be stored in a matrix format as done by Foyouzat and Estekanchi (2014). The ET time at which Equation (5) holds is referred to as the *equivalent time* corresponding to return period R and A_y/g.

In order to calculate the parameter A_y/g of a structure, it is proposed to use the pushover curve resulted from a load pattern that is based on the first elastic mode shape. The effective yield force that is obtained from the pushover curve is divided by the mass of the structure to give parameter A_y. Having the return period and parameter A_y/g of the structure, one can, using Equation (5), readily get the ET equivalent time sought. After imposing an ETEF to the structure, the maximum absolute value of a desired response up to the equivalent time is calculated. If a set of ETEFs is considered, the average value is recorded as the response demand corresponding to the considered return period. This process is renewed for several return periods until the response curve of the structure is acquired. A typical response curve which is produced in this way is shown in Figure 11.4(b). The return period axis is plotted in a logarithmic scale.

11.3 MODELING THE EDR DEVICE IN OPENSEES

OpenSees is one of the best software to model highly nonlinear macromodeling problems. Thus, in this research, all nonlinear analyses are performed in OpenSees (PEERC 2013). Unfortunately, there are no predefined materials in OpenSees which behave like EDR in loading and unloading phases. However, by assembling a few uniaxial materials, the EDR behavior can be modeled easily.

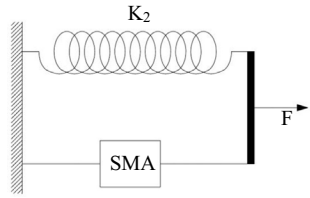

Figure 11.6. Modeling the EDR behavior in OpenSees.

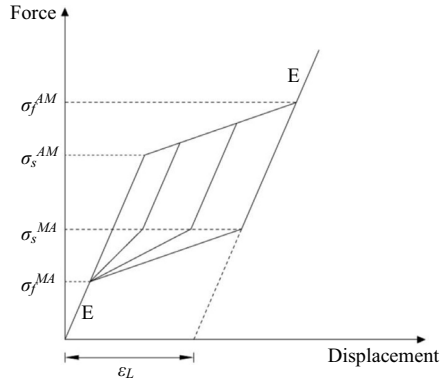

Figure 11.7. The hysteretic behavior of an SMA uniaxial element in OpenSees.

Let us consider the flag-shaped loops whose parameters are indicated in Figure 11.2. In order to model the flag-shaped behavior in OpenSees, one can combine a uniaxial element with linear elastic behavior and a uniaxial element with Shape Memory Alloy (SMA) behavior in parallel (Figure 11.6). The hysteretic behavior of an SMA uniaxial element in OpenSees together with the required parameters is displayed in Figure 11.7. If the stiffness of the linear elastic element is set equal to K_2, the parameters of the SMA are given by Equations (6) through (9):

$$E = K_3 - K_2 \tag{6}$$

$$\sigma_s^{AM} = \frac{(K_3 - K_2)F_2}{K_3} \tag{7}$$

$$\sigma_s^{MA} = \sigma_f^{MA} = \frac{(K_3 - K_2)F_1}{K_3} \tag{8}$$

$$\sigma_f^{AM} = \frac{(K_3 - K_2)F_2}{K_3} + \frac{(K_1 - K_2)(K_3 - K_2)\varepsilon_L}{K_3 - K_1} \tag{9}$$

Since the hardening part of the SMA is not present in the EDR loops, the magnitude of ε_L can be taken a very large value so that, actually, this point can never be reached in the numerical analyses. It has been observed that F_1 is not independent of other four parameters (Inaudi and Kelly 1996). In fact, it can be shown that Equation (10) holds between these five parameters of the EDR:

$$F_1 = \frac{K_2\left(K_3 - K_1\right)}{K_1\left(K_3 - K_2\right)} F_2 \tag{10}$$

As a result, only four parameters are needed so as to completely model the EDR device.

11.4 PERFORMANCE ASSESSMENT OF EDR DEVICES

In this section, the effectiveness of the EDR devices in controlling the seismic response of structures is investigated by applying the ET analysis method. Three steel Moment Resisting Frames (MRFs) with different numbers of stories are addressed as the case studies. The set under investigation consists of two-dimensional frames with 3, 6, and 10 stories and 3 bays which are built on a site in Los Angeles region with Soil Class C, as is defined in ASCE (American Society of Civil Engineers 2006). The height of all stories is 3.2 m and the bay width is 5.0 m. Some basic properties of these frames are summarized in Table 11.1. In this table, parameter A_y/g is calculated according to the procedure that is explained in Section 2.

The supports of 3st3bINITIAL and 6st3bINITIAL frames are assumed to be fixed, while hinged supports are considered for 10st3bINITIAL frame. The first story of frame 6st3bINITIAL is assumed to be surrounded

Table 11.1. Properties of the initial frames in summary

Property	3st3bINITIAL	6st3bINITIAL	10st3bINITIAL
Mass participation (mode 1)	81%	77%	78%
Fundamental period, T_1 (sec)	0.97	1.24	1.6
A_y/g	0.24	0.17	0.23

by a concrete retaining wall, which binds it to have similar lateral displacements to the ground at any time. As a result, the base level of this frame is transferred to the level of the first story. These structures are designed by applying only a fraction of the codified design base shear per INBC code (Iranian National Building Code 2005)—which is quite consistent with AISC-ASD building code (American Institute of Steel Construction 1989)—so that the structures will require rehabilitation by using EDR devices. Additionally, it is assumed that, for practical reasons, the owner has constrained the installation of the EDRs to only one bay in each story.

Table 11.2 describes the ground motions employed in the current study. All of these ground motions are recorded on Soil Type C. The scale factor for each ground motion, corresponding to return period, R, is selected so that the 5 percent damping linear elastic spectrum of the ground motion between $0.2T$ and $1.5T$ will not fall below the codified spectrum (corresponding to return period, R) in the same range, where T is the fundamental period of the structure being analyzed. The codified spectrum corresponding to any return period is formulated in ASCE41. After the calculation of the scale factors, the average RPP spectrum corresponding to each return period can be obtained. For example, the RPP spectra for these ensemble of ground motions scaled to the return period of 475-yr for $T = 1$ sec together with their average are represented in Figure 11.8 (g is the acceleration of gravity).

The ETA20inx01-3 series, generated with the duration of 20 seconds, is used as ETEFs. More information on different ETEF series is publicly available on ET method website (Endurance Time Method website 2016). The RPP spectrum for each ETEF can be acquired by applying Equation (4). Equivalent times can now be calculated through using Equation (5), and

Table 11.2. Description of the ground motions used in this study

ID No.	Year	Earthquake name	Station	Component (deg)	PGA (m/s^2)
1	1999	Kocaeli, Turkey	Arcelik	0	2.15
2	1976	Friuli, Italy	Tolmezzo	0	3.45
3	1995	Kobe, Japan	Nishi-Akashi	0	5.00
4	1999	Hector Mine	Hector	90	3.30
5	1986	Palmsprings	Fun Valley	45	1.29
6	1979	Imperial Valley	El Centro, Parachute Test	315	2.00
7	1984	Morgan Hill	Gilroy #6, San Ysidro	90	2.80

at last, by pursuing the procedure explained in Section 2, the ET response curves can be achieved. The provisions of ASCE41-06 are applied for performance-based design and check of the structures. The rehabilitation objective is selected as Enhanced Objectives–k and p and b, as is defined in ASCE41-06.

Before getting down to the analysis of the three aforementioned frames, it is worth introducing two useful definitions, which were originally proposed by Mirzaee and Estekanchi (2015). These definitions can facilitate the evaluation of the seismic performance of the structures using the ET method. The first definition is referred to as the *Damage Level* (DL) index, which is a normalized continuous numerical value as is defined by Equation (11). The DL is a dimensionless index which creates a numerical presentation for performance levels (values of 1, 2, and 3 for IO (Immediate Occupancy), LS (Life Safe), and CP (Collapse Prevention) levels, respectively).

$$DL = \sum_{i=1}^{n} \frac{\max\left\{\theta_{i-1}, \min\left(\theta, \theta_i\right)\right\} - \theta_{i-1}}{\theta_i - \theta_{i-1}} \tag{11}$$

In this equation, θ is the parameter that should be computed from the analyses and checked as per codes in order to evaluate the seismic behavior of the structure. The parameter θ can be a representative of the plastic rotation in beams, the plastic rotation in columns, or any other significant response parameter for which limiting values as per codes have been adopted. Additionally, n is the number of performance levels considered in the design ($n = 3$ in this study). The parameters θ_i is the ASCE41-06 limiting values at each performance level, and θ_0 is always set equal to zero. It should be noted that the DL index is not a new response parameter in addition to those addressed in ASCE41 for the evaluation of the structures. It is only a new form of representing the responses on a normalized continuous numerical scale. Moreover, utilizing the DL index facilitates the combination of different parameters that are involved in assessing the seismic performance of a structure. The second definition is referred to as the *target curve*. The target curve specifies maximum acceptable responses at various DLs as a continuous curve (Mirzaee and Estekanchi 2015). By comparing the ET performance curve with the target curve, the seismic performance of the structure at different seismic intensities can be evaluated.

Figures 11.9 through 11.12 illustrate the interstory drift, plastic rotation of columns, plastic rotation of beams, and absolute acceleration response curves for the foregoing frames, respectively. According to the ASCE41 provisions, the limiting values for the plastic rotation of beams depend on the section properties, while for the plastic rotation of columns, they depend on both the section properties and the axial force

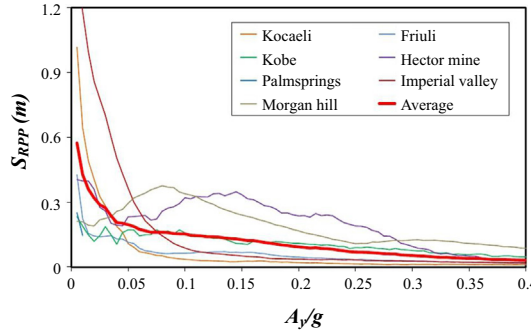

Figure 11.8. The RPP spectra of an ensemble of scaled ground motions together with their average.

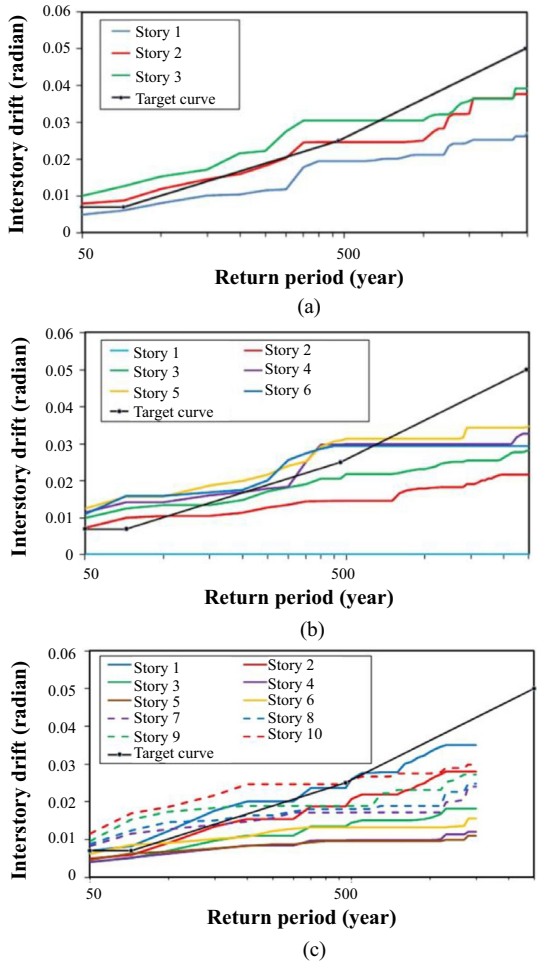

Figure 11.9. Interstory drift response curves for (a) 3st3bINITIAL, (b) 6st3bINITIAL, and (c) 10st3bINITIAL frames.

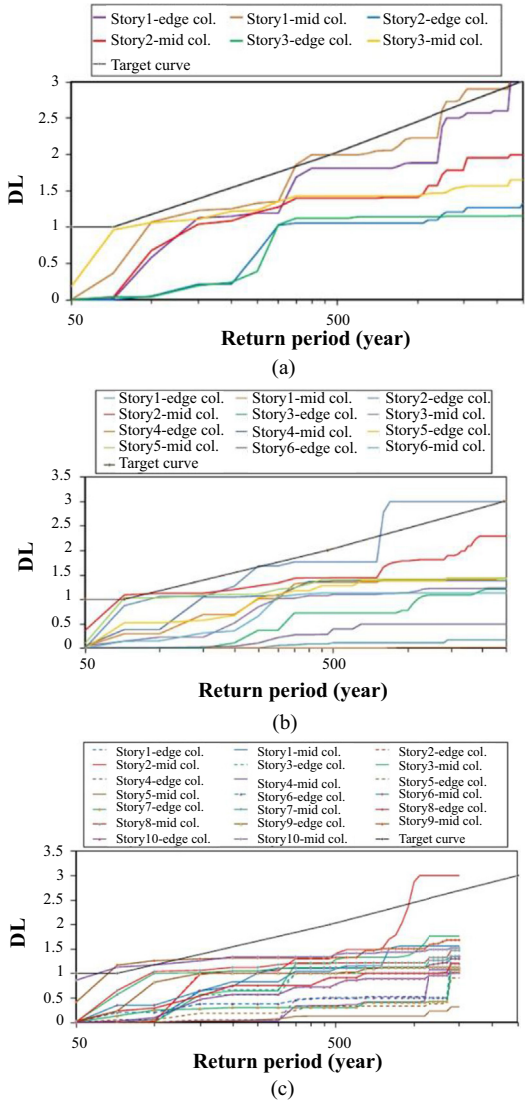

Figure 11.10. Column rotation response curves for (a) 3st3bINITIAL, (b) 6st3bINITIAL, and (c) 10st3bINITIAL frames.

of the columns. Hence, the plastic rotations are represented in terms of the DL index in order to avoid multiple target curves and streamline the presentation of the diagrams. Since no acceptance criterion for the absolute acceleration has yet been established in ASCE41, the target curve is absent from the absolute acceleration diagrams. For the 10-story frame, the response curves are shown up to the return period of 1,500 year. The

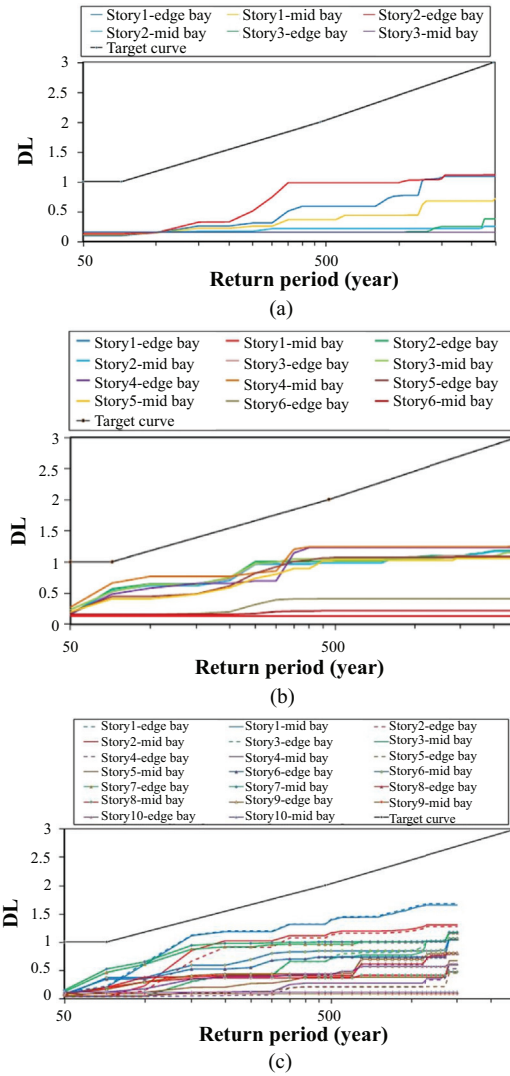

Figure 11.11. Beam rotation response curves for (a) 3st3bINITIAL, (b) 6st3bINITIAL, and (c) 10st3bINITIAL frames.

reason is that the duration of ETA20inx01-3 series (20 seconds) is not sufficient to cover all the return periods of interest. Generating ETEFs with longer durations can resolve this shortcoming.

According to ASCE41-06, if the axial force to P_{CL} (the lower bound axial column strength) ratio of a column falls below 0.5, only the column rotation needs to be checked, and there is no need to check the axial force-bending moment interaction equation. As was observed in all the

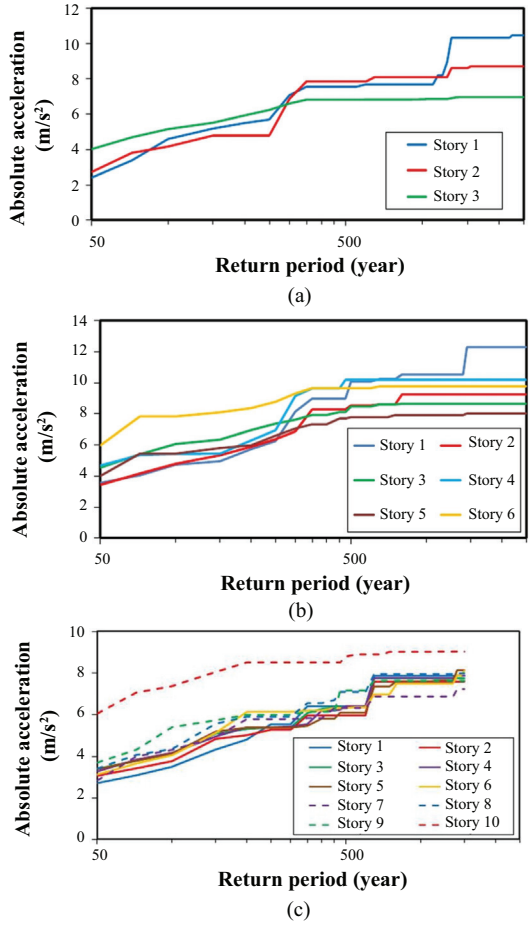

Figure 11.12. Absolute acceleration response curves for (a) 3st3bINITIAL, (b) 6st3bINITIAL, and (c) 10st3bINITIAL frames.

results of this study, in no column did this ratio exceed 0.5; thus, checking the interaction equation is no longer necessary. It is discernible from the response curves that the drifts and column rotations exceed the target curve in some cases and the structures need to be rehabilitated. To this end, EDR dampers are to be employed to control the seismic response of the structures. In the middle bay of each story, two identical EDR devices are installed in the form of cross bracings. The properties of each device are selected by trial and error until an acceptable response is achieved.

At each stage of the trial and error process, the fundamental period and parameter A_y/g of the rehabilitated structure are calculated. By doing so, the equivalent times are obtained, which must be employed to acquire

the ET response curves, as was previously explained. The A_y/g parameter does not significantly vary through stages, thanks to the relatively small stiffness of EDR devices. Therefore, the equivalent times undergo trivial changes at each stage, as compared to the preceding stages. As a result, one can use the same A_y/g of the initial structure for the ensuing stages to avoid performing a separate pushover analysis for each stage. After reaching an acceptable response, a pushover analysis can be performed to obtain the exact A_y/g of the last stage and reproduce the response curves. This procedure effectively reduces the designing time.

The characteristics of each device at the end of the trial and error process together with the parameters of the rehabilitated frames—referred to as 3st3bEDR, 6st3bEDR, and 10st3bEDR—are summarized in Table 11.3. The resulted response curves of the rehabilitated frames are shown in Figures 11.13 through 11.16. As can be inferred from these

Table 11.3. Properties of the rehabilitated frames in summary

Frame name	EDR location	K_1 (kN/m)	K_2 (kN/m)	K_3 (kN/m)	F_2 (kN)
3st3bEDR T_1 = 0.85 sec A_y/g = 0.26	1st story	1338.8	17.8	13388.2	60.0
	2nd story	1338.8	17.8	13388.2	60.0
	3rd story	964.0	17.8	9639.6	40.1
6st3bEDR T_1 = 1.13 sec A_y/g = 0.19	2nd story	1606.6	17.8	16065.9	60.0
	3rd story	1338.8	17.8	13388.2	60.0
	4th story	1606.6	17.8	16065.9	60.0
	5th story	1071.0	17.8	10710.6	60.0
	6th story	428.4	17.8	4284.2	40.1
10st3bEDR T_1 = 1.51 sec A_y/g = 0.24	1st story	4819.8	17.8	48197.6	50.0
	2nd story	2142.1	17.8	21421.2	50.0
	3rd story	2409.9	17.8	24098.8	50.0
	4th story	1499.5	17.8	14994.8	40.0
	5th story	1071.1	17.8	10710.6	40.0
	6th story	1071.1	17.8	10710.6	40.0
	7th story	1285.3	17.8	12852.7	50.0
	8th story	1285.3	17.8	12852.7	50.0
	9th story	1285.3	17.8	12852.7	50.0
	10th story	1285.3	17.8	12852.7	50.0

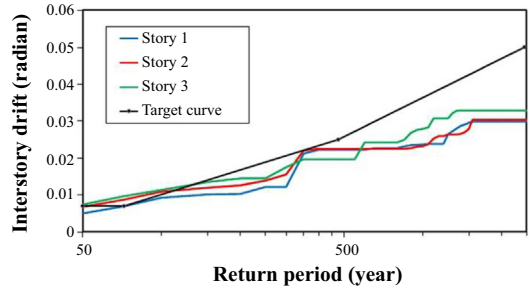

(a)

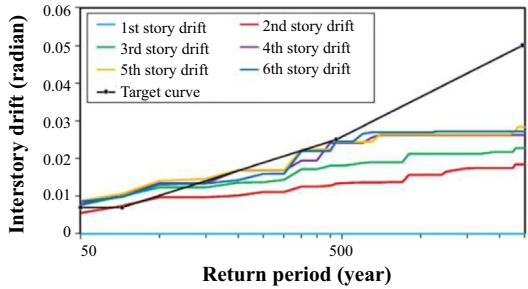

(b)

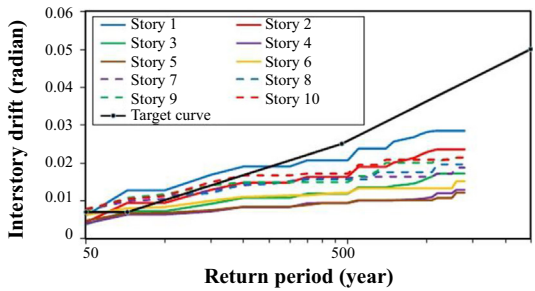

(c)

Figure 11.13. Interstory drift response curves for (a) 3st3bEDR, (b) 6st3bEDR, and (c) 10st3bEDR frames.

figures, EDR devices have significantly reduced the drifts and column rotations of the structures in large and medium return periods, which correspond to moderate and strong ground motions, respectively.

Despite this, there is only a slight reduction in small return periods, and the interstory drift response curves do not completely fall below the target curve in this range. The main reason is that, in small events, few hysteresis loops develop, and a small amount of energy is dissipated. However, in medium and large return periods, the formation of quite a few loops dissipates a large amount of energy, which causes the responses to be considerably mitigated.

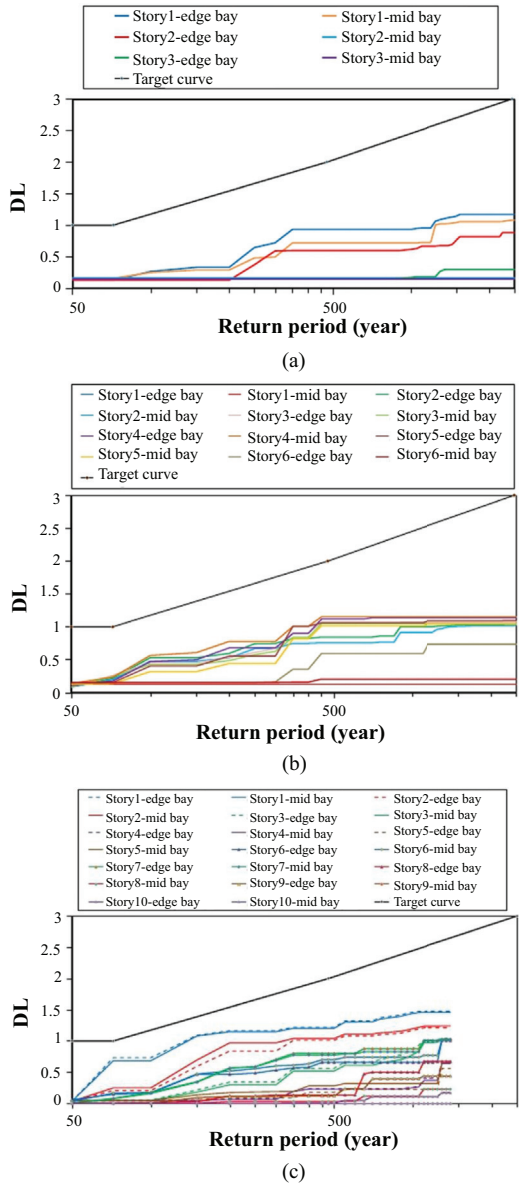

Figure 11.14. Column rotation response curves for (a) 3st3bEDR, (b) 6st3bEDR, and (c) 10st3bEDR frames.

Even by increasing the slip forces (F_2s) of the devices, the responses do not improve effectively in small return periods. Similarly, the use of a higher initial stiffness is not useful, since this will increase the axial force demand of the damper, which causes the device to fail.

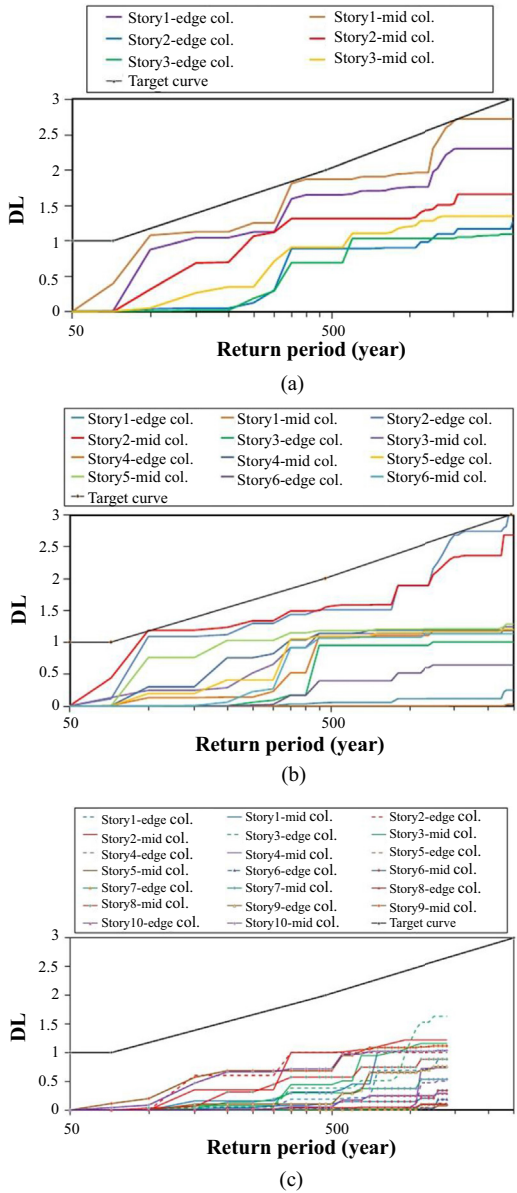

Figure 11.15. Beam rotation response curves for (a) 3st3bEDR, (b) 6st3bEDR, and (c) 10st3bEDR frames.

It is worth noting that the interstory drift acceptance criteria stipulated in ASCE41-06, are only recommended values, and it is not imperative for a structure to satisfy them. In fact, if a design can meet the beam and column plastic rotation acceptance criteria (and, if necessary, the axial

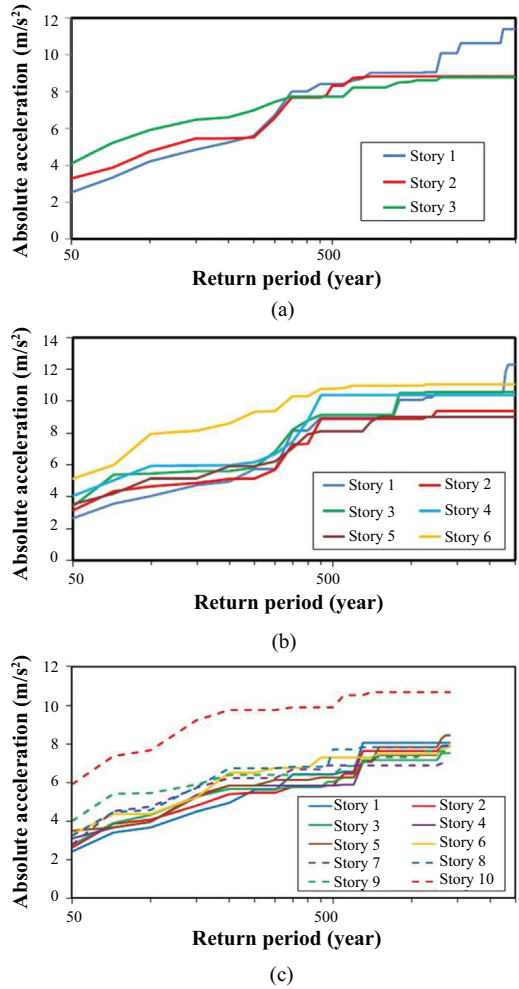

Figure 11.16. Absolute acceleration response curves for (a) 3st3bEDR, (b) 6st3bEDR, and (c) 10st3bEDR frames.

force-bending moment interaction effect), it is rated as an acceptable design. Accordingly, the designs of the rehabilitated frames are quite acceptable, regarding the performance objectives.

Referring to the foregoing results, it could be concluded that if it is desired to provide additional damping for a range of moderate and large earthquakes, the EDR device is an apt choice. This would be the case, provided that the building performance for small events is satisfactory, and also limiting the device force is important. Through applying the time-history analysis method on a range of SDOF structures, Nims et al. (1993)

drew a similar conclusion for SDOF systems. By using a more affordable ET method, the current study has verified this result for real multistory frames.

Figures 11.12 and 11.16 display the absolute acceleration response curves of the foregoing frames, before and after the rehabilitation, respectively. The absolute acceleration is among those parameters which play an important role in the nonstructural damage, the life-cycle cost due to the loss of contents (Elenas and Meskouris 2001), and the occupants' comfort (Connor 2002). Generally, moment-resisting frames have acceptable values for absolute acceleration, while the absolute accelerations in braced frames are large. As can be observed from Figures 11.12 and 11.16, the installation of the EDR devices have not significantly increased the absolute accelerations compared to that of the initial structures. This result reveals one of the advantages of these devices. The reason for this behavior lies in the relatively small stiffness of the EDRs as well as the energy absorption due to their operation during the earthquake.

As stated previously, as far as the absolute acceleration is concerned, no acceptance criterion has been stipulated in ASCE41-06. However, several researchers have proposed limiting values for the absolute acceleration at different performance levels. For example, according to Elenas and Meskouris (2001), for the IO, LS, and CP levels, the corresponding limiting values are 2.0, 9.8, and 12.5 m/s^2, respectively. Figure 11.16 suggests that, except for the small return periods, the absolute accelerations satisfy the above limitations.

11.5 COMPARATIVE STUDY

In this section, a comparative study is carried out between three different methods of analysis, namely time-history analysis, ET method based on RPP spectra, and ET method based on elastic spectra. The results of the second method were obtained in the previous section. The last method, as was discussed in the preceding sections, utilizes the elastic spectra as the intermediate intensity measure to correlate the time and return period. A detailed description of this method can be found in the study accomplished by Mirzaee, Estekanchi, and Vafai (2012). Apart from this, the time-history analysis is performed by using the ground motions described in Table 11.2. The maximum interstory drift responses of the aforementioned frames are calculated via these three methods in a number of return periods, some results of which are displayed in Figure 11.17. Note that the time-history responses in Figure 11.17 are based on the average of the

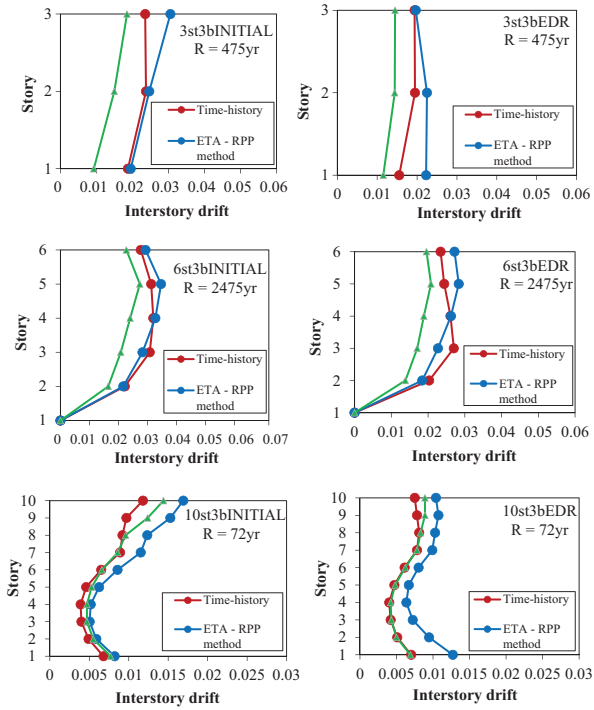

Figure 11.17. Comparison of the maximum interstory drift responses of the frames under study for a number of return periods calculated via time-history analysis, ET method based on RPP spectra, and ET method based on elastic spectra.

maximum absolute values resulted from the analyses over the considered ground motions.

Figure 11.17 suggests that in medium and large return periods (i.e., return periods greater than 475 year), the results of the ET method based on RPP spectra show a good concordance with the results of the time-history analysis. In addition, the trends of the diagrams are well predicted by the ET method. This stems from the fact that the frames experience significant inelastic displacements at these return periods. However, in small return periods, the frames experience slight plastic deformations. Therefore, in small return periods, the ET method that is based on elastic. spectra yield a better result, although the RPP spectra-based method is still a good approximate. Basically, these observations are in line with the results reported in (Foyouzat and Estekanchi 2014).

It must be noted that the RPP model has zero plastic phase slope, while the slope of the second portion of the EDR devices is a nonzero value (see Figure 11.2). Additionally, the hysteresis loops of the EDR

devices are completely different from the loops of the RPP materials. Apart from this, the inherent dispersion of the results of the ET method can be another important source of error. In spite of these important differences, the results of the ET method based on RPP spectra, as previously observed, show an acceptable degree of accuracy. Moreover, the ET results are conservative in quite a few cases.

Another important point is that, in the time-history method, the structural responses were generated by using seven ground motions at three return periods, requiring 21 time-history analyses. On the other hand, generating the responses by the ET method required only 3 time-history analyses. Furthermore, if it is needed to calculate the responses in more return periods, the required number of the analyses increases proportionally in the time-history method, whereas it remains the same (i.e., three analyses) when the ET method is utilized.

11.6 SUMMARY AND CONCLUSIONS

In this study, the application of the ET method in the performance assessment of EDR friction devices for the seismic rehabilitation of steel frames is investigated. Three steel MRFs with different numbers of stories are considered as the case studies. Double flag-shaped EDR devices are employed in order to improve the seismic response of the initial frames. The behavior of these dampers is highly nonlinear in comparison with other friction dampers. Accordingly, the improved ET method, which is based on nonlinear RPP spectra, is applied in order to satisfactorily estimate the responses in nonlinear range. From the results of this study, the following conclusions can be drawn:

1. In medium and large return periods, double flag-shaped EDR devices effectively improve the seismic responses of the initial frames and reduce the demand parameters to acceptable codified values.
2. In small return periods, the seismic responses of the frames are not considerably improved. Therefore, if the initial frame significantly fails to satisfy performance limits corresponding to small return periods (for instance, the 72-year return period), double flag-shaped EDRs cannot effectively mitigate the responses to reach the allowable limits.
3. As a result of the relatively small stiffness of the EDRs as well as the energy absorption due to their operation during the earthquake, the installation of the EDR devices does not significantly increase

the absolute acceleration of stories compared to that of the initial structures.

4. The application of the RPP spectra improves the accuracy and reliability of the response curves resulted from ET analysis in nonlinear range compared with the procedures based on linear elastic spectra. The results of the RPP spectra-based method show a good concordance with the results of the time-history analysis.

As far as the computational cost is concerned, the ET method is far more economical in comparison with the conventional time-history method. Moreover, this method enjoys high reliability and accuracy compared to the alternate simplified methods and enables the evaluation of the seismic performance as a continuous function of seismic hazard return period. As a result, the ET method can be effectively employed for the multilevel performance-based seismic rehabilitation of structures.

Since friction is an effective, reliable, and economical mechanism which can dissipate the energy introduced to structures by seismic events, the use of this mechanism can be highly desirable in the seismic rehabilitation. The EDR is a self-centering friction device; thus, it can alleviate the permanent deformations of structures after the completion of the earthquake, leading to decreased damage repair costs. The hysteretic behavior of this device is highly nonlinear, so the use of the demanding nonlinear time-history analysis is requisite for the frames whose responses have been controlled through EDR devices. Applying the ET method can surmount the intricacy of the time-consuming nonlinear time-history analysis and place a more practical and favorable way at the disposal of structural designers in order to exploit the EDR friction mechanism for seismic hazard mitigation.

REFERENCES

Aiken, I.D., and J.M. Kelly. 1990. *Earthquake Simulator Testing and Analytical Studies of Two Energy-absorbing Systems for Multistory Structures* (Report No. UCB/EERC-90/03). Berkeley, CA: Earthquake Engineering Research Center, College of Engineering, University of California.

Aiken, I.D., D.K. Nims, A.S. Whittaker, and J.M. Kelly. 1993. "Testing of Passive Energy Dissipation Systems." *Earthquake Spectr* 9, no. 3, pp. 335–70.

American Institute of Steel Construction (AISC). 1989. *Manual of Steel Construction: Allowable Stress Design*, 9th ed. Chicago, IL.

American Society of Civil Engineers (ASCE). 2006. *Seismic Rehabilitation of Existing Buildings*, *ASCE/SEI 41-06*. Reston, VA.

Cheng, F.Y., H. Jiang, and K. Lou. 2008. *Smart Structures: Innovative Systems for Seismic Response Control*. Boca Raton, FL: CRC Press.

Connor, J.J. 2002. *Introduction to Structural Motion Control*. Upper Saddle River, NJ: MIT/Prentice Hall.

Elenas, A., and K. Meskouris. 2001. "Correlation Study Between Seismic Acceleration Parameters and Damage Indices of Structures." *Engineering Structures* 23, pp. 698–704.

Endurance Time Method website. 2016. https://sites.google.com/site/etmethod/

Estekanchi, H.E., A. Vafai, and M. Sadeghazar. 2004. "Endurance Time Method for Seismic Analysis and Design of Structures." *Scientia Iranica* 11, no. 4, pp. 361–70.

Estekanchi, H.E., V. Valamanesh, and A. Vafai. 2007. "Application of Endurance Time Method in Linear Seismic Analysis." *Engineering Structures* 29, no. 10, pp. 2551–62.

Estekanchi, H.E., H.T. Riahi, and A. Vafai. 2011. "Application of Endurance Time Method in Seismic Assessment of Steel Frames." *Engineering Structures* 33, pp. 2535–46.

FitzGerald, T.F., T. Anagnos, M. Goodson, and T. Zsutty. 1989. "Slotted Bolted Connections in Aseismic Design for Concentrically Braced Connections." *Earthquake Spectra* 5, no. 2, pp. 383–91.

Foyouzat, M.A., and H.E. Estekanchi. 2014. "Application of Rigid-perfectly Plastic Spectra in Improved Seismic Response Assessment by Endurance Time Method." *Engineering Structures* 111, pp. 24–35.

Inaudi, J.A., and J.M. Kelly. 1996. "Dynamics of Homogeneous Frictional Systems." *Dynamics with Friction: Modeling, Analysis, and Experiments* 7, pp. 93–136.

Inaudi, J.A., and M. Nicos. 1996. "Time-domain Analysis of Linear Hysteretic Damping." *Earthquake Engineering and Structural Dynamics* 25, pp. 529−45.

Iranian National Building Code (INBC). 2005. *Design and Construction of Steel Structures*. Tehran, Iran: Office of Collection and Extension of National Building Code, Ministry of Housing and Urban Development.

Mirzaee, A., H.E. Estekanchi, and A. Vafai. 2012. "Improved Methodology for Endurance Time Analysis: From Time to Seismic Hazard Return Period." *Scientia Iranica* 19, no. 5, pp. 1180–87.

Mirzaee, A., and H.E. Estekanchi. 2015. "Performance-based Seismic Retrofitting of Steel Frames by Endurance Time Method." *Earthquake Spectra* 31, no. 1, pp. 383–402.

Nims, D.K., J.A. Inaudi, P.J. Richter, and J.M. Kelly. 1993. "Application of the Energy Dissipating Restraint to Buildings." *Proceedings of ATC 17-1 on Seismic Isolation, Passive Energy Dissipation, and Active Control* 2, pp. 627–38.

Nims, D.K., P.J. Richter, and R.E. Bachman. 1993. "The Use of the Energy Dissipating Restraint for Seismic Hazard Mitigation." *Earthquake Spectra* 9, no. 3, pp. 467–89.

Nozari, A., and H.E. Estekanchi. 2011. "Optimization of Endurance Time Acceleration Functions for Seismic Assessment of Structures." *International Journal of Optimization in Civil Engineering* 1, no. 2, pp. 257–77.

Pacific Earthquake Engineering Research Center (PEERC). 2013. *Open System for Earthquake Engineering Simulation (OpenSees)*. Berkeley, CA: University of California, Berkeley. Available online http://opensees.berkeley.edu/

Pall, A.S., C. Marsh, and P. Fazio. 1980. "Friction Joints for Seismic Control of Large Panel Structures." *Journal of Prestressed Concrete Institute* 25, no. 6, pp. 38–6l.

Pall, A.S., and C. Marsh. 1982. "Response of Friction Damped Braced Frames." *Journal of Structural Division, ASCE* 108, no. 9, pp. 1313–23.

Riahi, H.T., H.E. Estekanchi, and A. Vafai. 2009. "Estimates of Average Inelastic Deformation Demands for Regular Steel Frames by the Endurance Time Method." *Scientia Iranica* 16, no. 5, pp. 388–402.

Richter, P.J., D.K. Nims, J.M. Kelly, and R.M. Kallenbach. 1990. "The EDR-energy Dissipating Restraint, a New Device for Mitigating Seismic Effects." *Proceedings of the 1990 SEAOC Convention* 1, Lake Tahoe, pp. 377–401.

Soong, T.T., and G.F. Dargush. 1997. *Passive Energy Dissipation Systems in Structural Engineering*. New York, NY: John Wiley and Sons.

Zhou, X., and L. Peng. 2009. "A New Type of Damper with Friction-variable Characteristics." *Earthquake Engineering and Engineering Vibration* 8, no. 4, pp. 507–20.

INDEX

OTHER TITLES IN OUR SUSTAINABLE STRUCTURAL SYSTEMS COLLECTION

Mohammad Noori, *Editor*

Numerical Structural Analysis
by Steven O'Hara and Carisa H. Ramming

A Systems Approach to Modeling Community Development Projects
by Bernard Amadei

Momentum Press is one of the leading book publishers in the field of engineering, mathematics, health, and applied sciences. Momentum Press offers over 30 collections, including Aerospace, Biomedical, Civil, Environmental, Nanomaterials, Geotechnical, and many others.

Momentum Press is actively seeking collection editors as well as authors. For more information about becoming an MP author or collection editor, please visit http://www.momentumpress.net/contact

---

Seismic Analysis and Design Using the Endurance Time Method

Volume II: Advanced Topics and Application

H.E. Estekanchi • H.A. Vafai

A new approach to seismic assessment of structures called endurance time method (ETM) is developed. ETM is a dynamic analysis procedure in which intensifying dynamic excitations are used as the loading function. ETM provides many unique benefits in seismic assessment and design of structures and is a response history-based procedure. ETM considerably reduces the computational effort needed in typical response history analyses.

Conceptual simplicity makes ETM a great tool for preliminary response history analysis of almost any dynamic structural system. Most important areas of application of ETM are in the fields of seismic design optimization, value-based seismic design, and experimental studies. This book is aimed to serve as a coherent source of information for students, engineers, and researchers who want to familiarize themselves with the concepts and put the concepts into practice.

Homayoon Estekanchi is a professor of civil engineering at Sharif University of Technology. He received his PhD in civil engineering from SUT in 1997 and has been a faculty member at SUT since then. He is a member of Iranian Construction Engineers Organization, ASCE, Iranian Inventors Association and several other professional associations. His research interests include a broad area of topics in structural and earthquake engineering with a special focus on the development of the endurance time method and the value based seismic design.

Hassan Vafai has held position of professorship in civil engineering at different Universities including: Sharif University of Technology, Washington State University and University of Arizona. He was founder and editor-in-chief of *Scientia*, a peer-reviewed international journal of science and technology. Through out his professional career, he has received numerous awards and distinctions including: emeritus distinguished engineer by the National Academy of Sciences, Iran; an honorary doctorate by the Senatus Academicus of Moscow Region State Institution of Higher Education and the "Order of Palm Academiques", awarded by the Ministry of Education, Research and Technology of France.

MOMENTUM PRESS ENGINEERING

ISBN: 978-1-94708-326-4
90000
9 781947 083264